# Continuum-based Modeling and Analysis of Lipid Membranes induced by Cellular Function

**by**

**Tsegay Debalkew Belay**

A thesis submitted in partial fulfillment of the requirements for the degree of

*Doctor of Philosophy*

Department of Mechanical Engineering

University of Alberta

# Abstract

Lipid membranes represent a critically important interface in biological cells and cellular organelles and mediate all interactions between cells and their surrounding environment. Although quite fragile and negligibly thin, they can be homogeneous down to molecular dimension. Consequently, their mechanical properties can be described by idealizing their structure as a thin-walled continuum approximated by a two-dimensional surface. In this context, theoretical approaches based on continuum mechanics are becoming powerful tools to examine lipid bilayer membrane models to explain various aspects of the mechanical deformability of the membrane. However, the corresponding analysis most often involves heavy numerical treatments due to the highly nonlinear nature of the resulting systems of equations. For example, some analytical description of lipid membranes assembled into non-axisymmetric shapes such as rectangular and elliptical shapes remains largely absent from the literature. In addition, most bilayer membrane studies have been conducted using the classical elastic model of lipid membranes which cannot account for simultaneous changes in membrane shape and membrane tension arising from certain biological phenomena such as protein absorption or surface diffusion of proteins on the membrane surface.

To address these issues, in the present work we employ the theory of continuum mechanics to develop a comprehensive model for predicting the deformation behavior of both uniform and non-uniform lipid bilayer membranes. For the uniform lipid membrane, our emphasis is to develop an analytical description for the membrane morphology when different membrane shapes are subjected to various types of boundary forces or membrane

lipid-protein interactions. In this regard, we supply a complete analytical solution predicting the deformation profile of rectangular lipid membranes resulting from boundary forces acting on the perimeter of the membrane. We also give a complete semi-analytic analysis for the deformation profiles of lipid membranes induced by their interactions with solid elliptical cylinder substrates (e.g. proteins). In both problems, the theoretical framework for the mechanics of lipid membranes is described in terms of the classical Helfrich model. A linearized version of the shape equation describing the membrane morphology is obtained via a limit of superposed incremental deformations for the respective problems. Thus, complete analytical solutions are obtained by reducing the corresponding problem to a single partial differential equation and formulating the resulting shape equations with suitable coordinate systems to accommodate the shapes of the membrane. Each of the analytical results successfully predict smooth morphological transitions over the respective domain of interest.

Membrane proteins play a vital role in various cellular activities (such as endocytosis, vesiculation and tubulation) yet the study of the contribution of membrane proteins presents a major challenge with one of the main difficulties being the lack of a full understanding of the mechanics of membrane-protein interaction. Therefore, a portion of this work is devoted to the study of the mechanics of vesicle formation on a non-uniform flat bilayer membrane where the vesicle formation process is assumed to be induced by surface diffusion of transmembrane proteins and acting line tension energy on the membrane. Much attention is also given to the discussion of the role of thickness deformation (distension) in the vesicle formation of the bilayer membrane. Since the classical elastic model of lipid membranes cannot account for simultaneous changes in membrane shape and membrane tension due to surface diffusion proteins, we propose a modified Helfrich-type model for non-homogeneous membranes. The proposed model is based on the free energy functional accounting for the bending energy of the membrane including the spontaneous curvature, thickness distension and the acting line tension energy on the boundary of the protein concentrated domain and

the surrounding bulk lipid. In the analysis, the protein concentration level is coupled to the deformation of the membrane through the spontaneous curvature term appearing in the resulting shape equation.

Our emphasis in this research is the rigorous mathematical treatment of this model, in particular to find the numerical solution of the membrane shape equation with associated boundary conditions. Accordingly, we supply numerical solutions by reducing the corresponding problem to a coupled two-point boundary value problem by the use of collocation method. These results successfully predict the vesicle formation phenomenon on a flat lipid membrane surface with a smooth transition of membrane thickness variation inside the boundary layer where the protein-free membrane and the protein-coated domain is observed.

# Preface

Four journal papers were combined to compose the main body of this thesis.

Chapters 2 of this thesis has been published as: Belay T., Kim C.I, and Schiavone P., Analytical Solution of Lipid Membrane Morphology Subjected to Boundary Forces on the Edges of Rectangular Membranes, Continuum Mechanics and Thermodynamics, 2016 (28), 305–315; Chapter 3 as: Belay T., Kim C.I, and Schiavone P., Interaction Induced Morphological Transitions of Lipid Membranes in Contact with an Elliptical Cross Section of a Rigid Substrate, Journal of Applied Mechanics (ASME), 2016 83(1), 011001-011001-12; Chapters 4 as: Belay T., Kim C.I, and Schiavone P., Bud formation of lipid membranes in response to the surface diffusion of transmembrane proteins and line tension. Mathematics and Mechanics of Solids, 2016, doi: 10.1177/108128516657684; Chapter 5 as: Belay T., Kim C.I, and Schiavone P., Mechanics of lipid bilayer membrane budding subjected to thickness distension, Mathematics and Mechanics of Solids, 2016, doi: 10.1177/1081286516666136. I was responsible for the development of the models, derivation of the solutions, analysis and was principal author on all of the papers. Kim C.I. is the supervisory author who suggested the problems. Kim C.I. and Schiavone P. are the supervisory authors who contributed on the concept development of the problems, checked all the analysis and corresponding results, and revised the manuscripts.

I would like to dedicate this thesis to my parents, my wife Meaza A. Desta and in memory of my daughter Abigel Tsegay Belay who died during childbirth on July 19, 2014.

# Acknowledgements

I would like to express my deepest appreciation to my supervisor Dr. Kim. Thank you for encouraging my research and for supporting me to grow into this research area. Without his guidance and persistent help this thesis would not have been possible. I would also like to express special appreciation and thanks to my co-supervisor Professor Dr. Schiavone. Words can not express how grateful I am for his tremendous help not only academically but also emotionally through the rough road since the days I began working on this research to finishing this thesis. He has also been a tremendous mentor for me and his advice on both research as well as on my career have been invaluable.

I am extremely grateful to Kassa Michael W. Yohannes and Tsega Birhan Gebru who have given me unconditional mentorship and encouragement during my educational journey thus far. I am also indebted to Professor Dr. Ichiro Hagiwara for the inspiration he instilled in me to pursue graduate studies in the field of Mechanical Engineering.

Besides, I wish to thank many of my colleagues, friends and family who have supported me. A special thanks to my father, Debalkew Belay, and mother, Meaza Mesfin, for all the sacrifices they have made on my behalf and prayer for me which sustained me thus far. I would like to express how grateful I am to my brothers, sisters and father-in-law, Abraham G. Desta and Abdirashid Dulane (Ambassador) for their continuous help and encouragement. I would also like to thank to my beautiful and beloved wife, Meaza A. Desta. Thank you for supporting me for everything, and especially I can't thank you enough for your continued patience and encouraging me throughout this journey. To my beloved daughter

Eliora Tsegay Belay, I would like to express my thanks for being such a good baby girl who always makes my heart smile, my face light up and made me laugh every time I saw her.

Finally, thank you God, for letting me through all the difficult times and allowing me to finish my degree. I always keep on trusting You in my life.

# Table of contents

# List of figures

# Chapter 1

# Introduction and Background

*Lipid bilayer membranes represent a critically important interface in biological cells and cellular organelles and mediate all interactions between cells and their surrounding environment. They are also home to a variety of proteins, which perform the majority of biological functions. Although, bilayer membranes are quite fragile and negligibly thin, they can be homogeneous down to molecular dimension. Therefore, their mechanical properties can be described by idealizing their structure as a thin-walled continuum approximated by a two-dimensional surface.*

## 1.1 Introduction

### 1.1.1 Biological membranes

Biological cells are surrounded by membranes which have distinct functions. The extracellular (plasma) membrane of the cell serves as a physical barrier, forming the boundary of every cell, while the internal-limited membranes compartimentalize functions into the organelles of animal and plant cells. The outer membrane can also play a vital role in transmitting information to the cell in the form of chemical or electrical signals assisted by signalling molecules, which may initiate various cellular activities within the cell, such as cell division and protein production. In most cases, the signal transmitting molecules are bound to specific receptors in the plasma membrane which generate a secondary signal inside the cell, but they are sometimes able to cross the plasma membrane into the cell [30]. Membranes also help to control the flow and exchange of many substances in and out of the cell. These

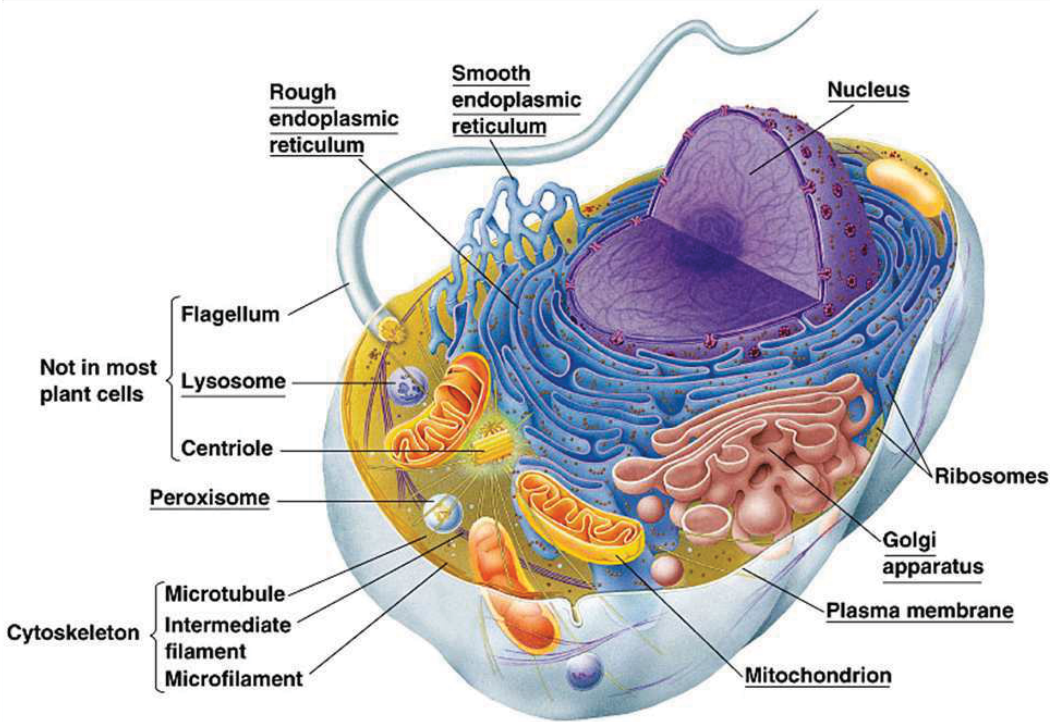


Fig. 1.1 Schematics of a biological cell. (*Picture taken from: © 2003 Pearson Education, Inc., Publishing as Benjamin Cummings*).

substances include water, ions, gases, and other useful nutrients. In addition, various waste products are removed from the cell with the help of the membrane.

From the above discussion, we observe that membranes are critically important components of cellular structures. Besides that, due to the interaction with the surrounding environment, every living cell can experience bending, compression, stretching and shear deformations. Therefore, to cope with applied external forces, the different tasks mentioned above and execute many other crucial cellular activities, cell membranes need to be flexible and elastic in order to allow variation of shape and motion.

Figure 1.1 shows a schematic structure of a biological cell. Different organelles play different roles in the cell, for instance, the mitochondria is responsible for the cell's metabolism, the nucleus contains the genetic materials, the endoplasmic reticulum is responsible for protein molecules synthesis, and Golgi apparatus is involved in sorting and packaging of proteins [56]. Despite their differing functions, these organelles have certain structure in com-

mon: a lipid bilayer membrane which is a thin sheet like structure that consists of mainly thin film of lipids and protein molecules (Figure 1.4).

### 1.1.2 Lipid bilayers

Lipid molecules are biologically important molecules that contain hydrocarbon chains and make up the structural and functional building blocks for all living cells. Lipid molecules are amphiphilic in that they have hydrophilic polar (i.e., "water-loving") head groups and a hydrophobic nonpolar (i.e., "water-hating") tail end (see Fig. 1.2). The polarity of the hydrophilic head is due to the presence of a negatively charged phosphate group linked to a positively charged amine. The hydrophilic molecules dissolve readily in water and have the tendency to interact or form hydrogen bonds with water molecules. The hydrophobic molecules, however, disturb the hydrogen bonds that exist between the water molecules close to it and hence don't dissolve in water [98]. When dispersed in water, the difference in solvation preference of these two parts of the lipid molecules forces them to assemble spontaneously into a condensed structure, such that their polar heads are facing out toward the aqueous environment, shielding their hydrophobic tails from the water. The morphology of the assembled structures depends on the specific size and shape of the hydrophobic and hydrophilic parts and as a result the lipid molecules can form typical structures such as bilayers, miceles and vesicles (see Fig. 1.3). Besides, other forms of structures such as circular, cylindrical and elliptical shapes can be formed from lipid molecules ( see, e.g., Fig. 3.1, in Chap. 3).

In fact, it is known that a lipid bilayer structure is characteristic of all biomembranes [33, 73]. For example, in plasma membranes, lipid bilayer structues provide a physical barrier to separate the extracellular environment from the interior part of the cell. Furthermore, the organelles (internal membrane-limited subcompartments) of animal and plant cells, the endoplasmic reticulum which is the powerhouse where protein molecules are synthesized [56] all

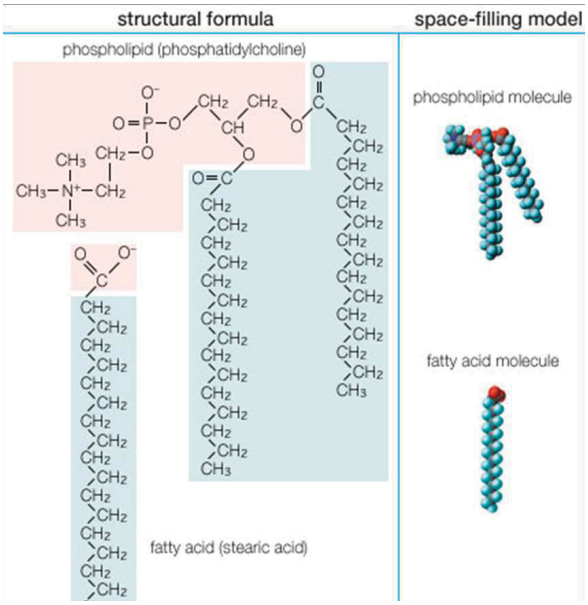


Fig. 1.2 Chemical structure and schematics of amphiphilic lipid molecule. (*Picture taken from: © 2009 Encyclopedia Britannica, Inc.*)

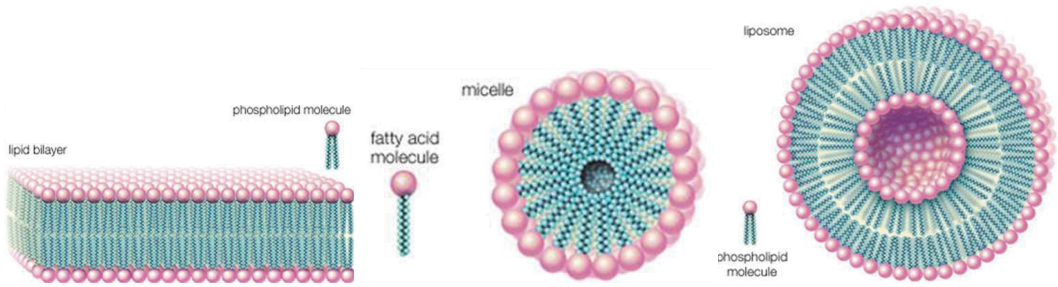


(a) planar bilayer (b) spherical micelles (c) bilayer vesicle

Fig. 1.3 Schematics of self-assembled structures of lipid molecules. (*Picture taken from: © 2009 Encyclopedia Britannica, Inc.*)

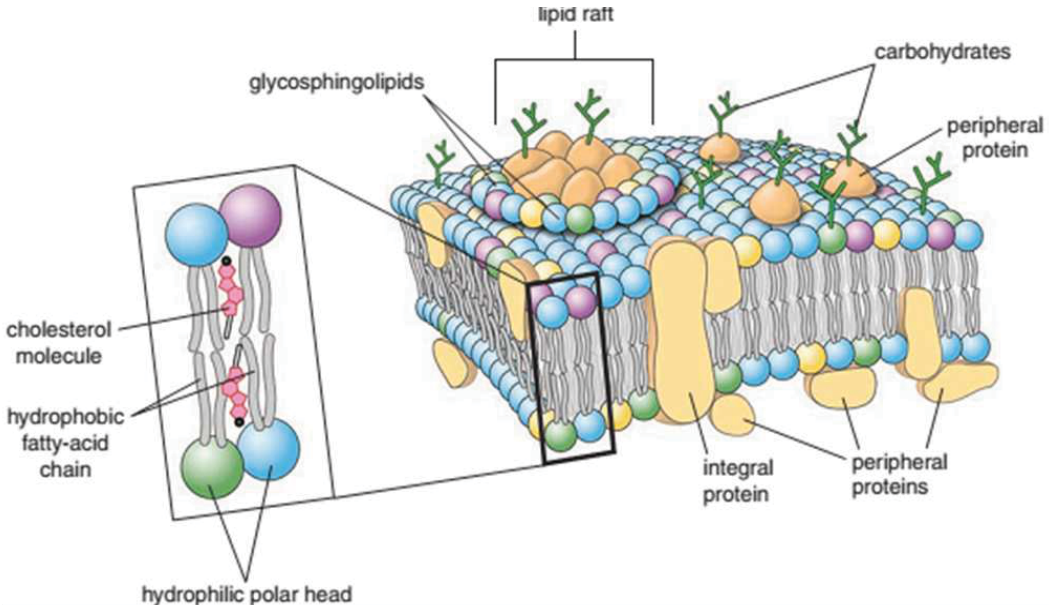


Fig. 1.4 Schematic diagram of membrane proteins in a biological membrane. (*Picture taken from: Michael H. Ross et al. 2005*).

contain the lipid bilayer structures. The bilayer of a biological membrane is approximately (5-10 nm) thick and the membrane's molecular composition is highly inhomogeneous which typically contains many different types of lipids. The lipid fractions vary between cells, the many different organelles within the cell, and between the two sides of the bilayer (see Ref. [56] for the biological details).

### 1.1.3 Membrane proteins

Biological membranes consist of various proteins interacting with or embedded within lipid bilayer membranes (see Fig. 1.4). In general, membrane proteins are amphiphatic and hence, they orient and fold themselves in the lipid bilayer accordingly. The hydrophobic part of the protein associate with the interior of the membrane, whereas hydrophilic regions protrude into the aqueous environment at the surface of the membrane.

An array of protein families can be bound to the bilayer membranes in different ways: (i) transmembrane (integral) proteins, which span the lipid bilayer; (ii) Peripheral membrane

proteins which are either bound through interaction with the transmembrane proteins or the lipid hydrophilic head group. These proteins do not interact with the hydrophobic tail groups of the lipid molecules. (iii) Lipid-anchored membrane proteins which are bound covalently to one or more lipid molecules. The hydrophobic tail of the attached lipid is embedded in one leaflet of the membrane. All types of proteins can interact with one another, interact with the membrane and can also diffuse laterally in the bilayer membrane. In general, membrane proteins perform most cellular activities such as transport of molecules, ion pumps, signal transduction, endocytosis, vesiculation, tubulation, fission and fusion (for example, see [7, 10, 15, 53, 71] and the references therein). These various cellular tasks may rely heavily on mechanical membrane properties and can be studied by developing appropriate mathematical models. In this thesis, since our focus is the study of the mechanical response of lipid membranes subjected to various boundary interactions, the interested reader is referred to [56] for biological details of membranes. Further detailed and related literature reviews will accompany subsequent chapters.

## 1.2 Background and motivation

From the above discussions, we observe that lipid bilayer membranes are critically important components of cellular structures. Besides that, they rely heavily on mechanical membrane properties to execute many crucial cellular activities and hence, can be studied within the framework of applied mathematics and theoretical physics. On the other hand, interest in artificially produced lipid membranes with different shapes is also gaining momentum in various commercial applications most notably in drug delivery and other potential applications such as in the field of biosensors and in the development of bilayer-based devices (see e.g., [40, 43, 68, 99]). Therefore, due to the rise of important practical applications in medical and biological sectors, the need to develop comprehensive models able to adequately describe the behavior of lipid membranes is crucial.

Several recent studies on the mechanics of lipid membranes have identified various conformational states of the membranes such as scaffolding by proteins [71] and the aggregation of transmembrane proteins [11, 13, 63]. Further examples can be found in Harvey et al. [60] and the references contained therein. In each of these cases, the interactions of intermembrane proteins provide necessary mechanical forces to regulate the membrane's shape. The generated membrane deformation profiles are also dependent on the mechanical responses of lipid bilayers. Therefore, most of the protein-induced deformations of lipid membranes can be examined through the "compatible deformations" assimilated by resultant tensions, bending moments and intra-bilayer pressures on the boundaries and/or some parts of lipid membranes.

Many of the aforementioned studies indicate that the bilayer of biological membranes are quite fragile and negligibly thin (typically 5nm-10nm) but they can be homogeneous down to molecular dimension and therefore, the mechanical response and associated morphological transitions of the lipid membranes can be described by quantitative theoretical models arising from the classical bilayer mechanics theory [14, 25, 37]. In this context, the mechanical properties of a lipid membrane can be described by idealizing its structure as a thin-walled continuum approximated by a two-dimensional surface embedded in three-dimensional Euclidean space. Besides, in the process of membrane modeling, the shape of the proteins can be analogized to a cone, a cylinder or an inverted cone. With these idealizations, in the theory of classical bilayer mechanics, the mechanical surface response of the membrane can be described by the deformation and geometry of the membrane surface and the equilibrium configurations of the membrane corresponds to the local minimum of an areal free-energy density. It should be noted that the free energy density associated with the lipid membrane is often completely described by a surface parametrization-invariant such as the mean and Gaussian curvatures which depends only on the surface geometry and this energy is mainly dominated by bending. This is because the bending mode of deformation

of a membrane is weak and therefore costs much less energy than, for example, stretching. The resulting predictive models (which are highly nonlinear), and the admissible boundary forces and moments transmitted through the membrane can also be expressed in terms of the membrane surface geometry invariants such as the mean and Gaussian curvatures of the surface. Unfortunately, the resulting equilibrium equation is a highly nonlinear partial differential equation of fourth order and the corresponding analyses most often involve heavy numerical treatments. This suggests that obtaining these nonlinear systems of equations is not a substitute for solving the relevant field equation if one wants to determine the actual shape of the membrane. On the other hand, exact analytical approaches have been proposed under the assumption of superposed incremental deformations of lipid membranes, yet scarify the complexity of the associate boundary forces and domains of interest [1] and thus far, in many of the existing analytical and numerical analysis of lipid membranes in the literature, one of the main challenges that one faces is breaking the assumption of axisymmetry.

Lipid bilayer membranes with different shapes, for example, such as (circular, rectangular, elliptical) are powerful tools for studying various cellular activities such as functional analysis of proteins in cells [87]. Moreover, membranes with these shapes are artificially engineered in order to mimic the fundamental properties of natural cells and can be used in biosensors development, biotechnology applications [40, 43, 68, 99]. As a result, there is an imperative demand for the thorough understanding of the mechanical response of the membrane morphology with these shapes when they are subjected to some specified boundary conditions or interacting with other substrates; there is also demand for a generation of reliable mathematical models to predict the interaction induced smooth morphological transition of the lipid membranes with these shapes. To the author's knowledge, analytical solutions which predict the deformation profile of rectangular or elliptical membrane shapes subjected to boundary interactions are absent from the literature. The lack of sufficient studies may be due to the mathematical complexity of the governing equations and

admissible boundary conditions corresponding to these problems. Indeed, the analytical solution predicting the deformation of membrane morphology with elliptical shape subjected to boundary interactions and protein substrate, for example, requires to break the assumption of axisymmetry, which is the main challenge in the analytical and numerical analysis of lipid membranes. To this end, in Chapters 2 and 3, the contents of which can be found in the author's publications [9, 10], we develop complete analytical solutions which are able to serve as a predictive model for the the deformation behaviour of membranes with rectangular and elliptical shapes subjected to various boundary force/substrate interactions.

Most of the studies of the mechanical response of lipid membranes are within the framework of the classical elastic model of lipid membranes. However, the classical mechanics of a membrane model fails to explain numerous phenomena occurring in the deformation of nonuniform lipid membranes which experience simultaneous changes in membrane shape and membrane tension, for example, due to protein absorption on the membrane [70] or other protein-mediated morphology changes in biomembranes [2, 90]. The work by Steigmann [90] has addressed this issue to remedy the shortcomings of classical elasticity and some important papers have been published since then (for example, see [2, 70] and the references therein). In general, the deformation of nonuniform lipid membranes can experience the simultaneous changes in membrane shape and membrane tension during the deformation or morphological transition.

One reason for the inhomogeneity of lipid membranes is the existence of non-uniformly distributed proteins over the composite membrane surface. As reported above, since membrane proteins play a vital role in various cellular activities (such as endocytosis, vesiculation and tubulation ) and studying membrane proteins still represents a major challenge, with one of the major difficulties being the problems encountered when interacting with the membrane, a portion of this work is devoted to the study of lipid membrane deformation behaviour subjected to surface diffusion of transmembrane proteins. In this regard, we will

discuss nonuniform membrane remodeling, particularly, the mechanics of bud formation on a membrane as an example where protein diffusion on the membrane surface acts to change the membrane curvature locally which is an important step in cellular vesicular transport such as exocytosis and endocytosis processes [50, 75]. This intracellular vesicle transport is promoted by vesicle transport proteins which are required to move molecules between cellular organelles. Unfortunately, to the best of the author's knowledge, the mechanics of bud formation on a nonuniform membrane subjected to surface diffusion of proteins over a membrane surface (which also undergoes inhomogeneous thickness deformation) remains absent from the literature. This again may be due to the mathematical complexity of the resulting systems of equations and boundary conditions. Therefore, a rigorous numerical analysis of the corresponding systems of equation and boundary conditions is needed to obtain the required solution of this challenging problem. Furthermore, despite tremendous progress in the theory of continuum-based modeling of lipid membranes and several studies on the influence of proteins on membrane bud formation (for example, see [3, 26, 42, 60, 72] and the references therein), the mechanics of membrane budding is not yet fully understood [79]. Regarding this situation, researchers have faced challenges in their attempts to fully understand the mechanics of protein interaction with the membranes and its effect in membrane budding. Therefore, we propose a comprehensive continuum-based model which will be able to serve as a predictive model for the formation of vesicles on a nonuniform lipid membrane. To this end, in Chapter 4 and 5, the contents of which can be found in the author's publications [7, 8], we discuss the mechanics of bud formation of lipid membranes in response to the surface diffusion of transmembrane proteins. We also discuss the mechanics of lipid bilayer subjected to thickness deformation (distension) and membrane budding.

## 1.3 Aims and scope

The ultimate goal of this study is therefore, to develop analytical and numerical descriptions for the lipid membrane morphology when different membrane shapes (eg. rectangular, elliptic patches) are subjected to various types of boundary forces (e.g clamping, applied moments etc...) on their edges or membrane lipid-protein interactions. The analytical description presented in this thesis will overcome one of the main challenges that one faces when simulating membrane response: breaking the assumption of axisymmetry.

It is also the focus of this study to develop theoretical model and numerical solutions which are able to describe the mechanical response of lipid membranes which undergo inhomogeneous thickness deformation in which inhomogeneity of the membrane is assumed to arise from a non-uniform spatial distribution and diffusion of transmembrane proteins. Specifically, this model will predict one particular phenomenana of membrane deformation which is membrane budding.

Overall, a framework is established in the thesis to predict the mechanical response (deformation profile) of membrane morphology with rectangular and elliptical membrane shapes when they are subjected to some specified boundary forces or boundary interactions with substrates (e.g., proteins). In addition, a comprehensive theoretical framework is also established to predict membrane budding subjected to surface diffusion of transmembrane proteins and line tension energy on the membrane. In addition, a mechanistic model which enables to assess the role of thickness deformation (distension) in membrane budding will be developed.

## 1.4 Structure of the thesis

Part I of this thesis is concerned with the analysis of uniform lipid membrane morphology subjected to boundary interactions, comprising of

- Chapter 2, discussing the analytical approaches to prediction of the deformation of lipid membrane morphology with rectangular shape subjected to boundary forces acting on the perimeter of the membrane;

- Chapter 3, introducing analytical methods to predict interaction-induced morphological transition of lipid membranes in contact with an elliptical cross-section of a rigid substrate.

Part II of this thesis is concerned with the simulation of a bud formation process on a nonuniform lipid membrane, which consists of

- Chapter 4, introducing a new proposed continuum-based model describing the mechanics of bud formation on lipid membranes induced by the surface diffusion of transmembrane proteins and acting line tension on the membrane. This chapter also presents the results of numerical simulations of the proposed theoretical model which predicts the vesicle formation phenomenon on an initially flat lipid membrane surface;

- Chapter 5, presenting a new proposed continuum-based model describing the mechanics of lipid bilayer membrane subjected to thickness distension and membrane budding based on the work in chapter 4 and can be used to study the phenomena of membrane budding in the scenarios where there exists an inhomogeneous deformation along the thickness of the membrane.

Each of Chapters 2 to 5 also contains an independent abstract, introduction and literature review regarding the main topic of that chapter.

The last chapter summarizes the entire work and identifies potential research that could be addressed in the future work.

# Chapter 2

# Analytical Solution of Lipid Membrane Morphology Subjected to Boundary Forces on the Edges of Rectangular Membranes

*We develop a complete analytical solution predicting the deformation of rectangular lipid membranes resulting from boundary forces acting on the perimeter of the membrane. The shape equation describing the equilibrium state of a lipid membrane is taken from the classical Helfrich model. A linearized version of the shape equation describing membrane morphology (within the Monge representation) is obtained via a limit of superposed incremental deformations. We obtain a complete analytical solution by reducing the corresponding problem to a single partial differential equation and by using Fourier series representations for various types of boundary forces. The solution obtained predicts smooth morphological transition over the domain of interest. Finally, we note that the methods used in our analysis are not restricted to the particular type of boundary conditions considered here and can accommodate a wide class of practical and important edge conditions.*

## 2.1 Introduction

Biological membranes are the basic elements of cell and cellular organelles which may include the mitochondria, chloroplast, the endoplasmic reticulum (**ER**) , the Golgi apparatus, and lysosomes. It was found (Gorter and Grendel [33]; Robertson [73]) that a lipid bilayer structure is, in fact, characteristic of all biological membranes (biomembranes). Lipid membranes are quite fragile and negligibly thin (typically 5nm – 10nm), yet form a continuous

permeability barrier around cells. In addition, the composition of the lipid bilayer matrix (together with cellular proteins) assist the cell membrane to undergo constant morphological transitions such as invaginations, fusion, fission [15, 53] regulated by membrane forces. This in turn, suggests that the mechanical response of a lipid membrane plays an important role for a wide range of essential cellular functions [60, 84, 96].

Recent studies on the mechanics of lipid membranes have identified various conformational states of the membranes: the aggregation of transmembrane proteins [11, 13, 63], scaffolding by proteins [71], filament assembly and the disassembly process of cytoskeleton [58, 86, 102]. Further examples can be found in Harvey et al. [60], and the references contained therein. In these cases, the interactions of intermembrane proteins provide necessary mechanical forces to regulate the membrane's morphological transitions. The induced morphological profiles are also dependent on the mechanical responses of lipid bilayers. Therefore, most of the protein-induced deformations of lipid membranes can be examined through the "compatible deformations" assimilated by resultant tensions, bending moments and intra-bilayer pressures on the boundaries and/or some parts of lipid membranes. For example, Evans [25] discussed chemically induced bending moments in lipid membranes as a possible mechanism for the crenation of red blood cells (more studies can be found in the references therein).

The aforementioned studies indicate that the mechanical response and associate morphological transitions of lipid membranes can be described by quantitative theoretical models arising from the classical bilayer mechanics theory [14, 25, 37]. In this context, a lipid bilayer can be regarded as a closed membrane, much like a thin film sandwich structure where a fluid-like substance is present between the two films. This further allows for a continuum setting in the modeling of biomembranes, mainly via the couple-stress theory of elastic surfaces [45, 61, 100]. In this context, it also seems useful to consider models belonging to the (two-dimensional) theory of second-gradient fluids, which are able to take into account

capillarity effects in an elastic fluid at small length scales. Relevant developments may be found in [17–20]. The resulting predictive models demonstrate good agreement with experimental data, particularly when the area density of lipids on the membrane is sufficiently high [93]. However, the corresponding analyses most often involve heavy numerical treatments due to the highly nonlinear nature of the resulting systems of equations. On the other hand, exact analytical approaches have been proposed under the assumption of superposed incremental deformations of lipid membranes, yet scarify the complexity of the associate boundary forces and domains of interest [1].

The present study seeks to develop a complete analytical description for lipid membrane morphology when rectangular membranes are subjected to various types of boundary forces (e.g clamping, applied moments etc...) on their edges. Emphasis is placed on the assimilation of the complex nature of boundary forces by means of Fourier series expansions, at the same time, maintaining the rigor and generality in the derivation of compatible shape equations within the prescription of superposed incremental deformations. We obtain an exact analytical solution by reducing the problem to that for a single PDE and by using Fourier series representation for boundary forces. The corresponding boundary problem indicates smooth transition of deformation profiles over the domain of interest and converges to the imposed boundary conditions/forces on the edges of the membrane.

The chapter is organized as follows. Section 2.2 introduces a review of the geometry and kinematics of the surfaces. Sections 2.3 to 2.4 describe the generalized equilibrium-shape equation of the lipid membrane and the corresponding admissible edge conditions. Sections 2.5 and 2.6 present the derivation of the analytical solutions and discuss the results with examples. Finally, Section 2.7 presents our conclusions.

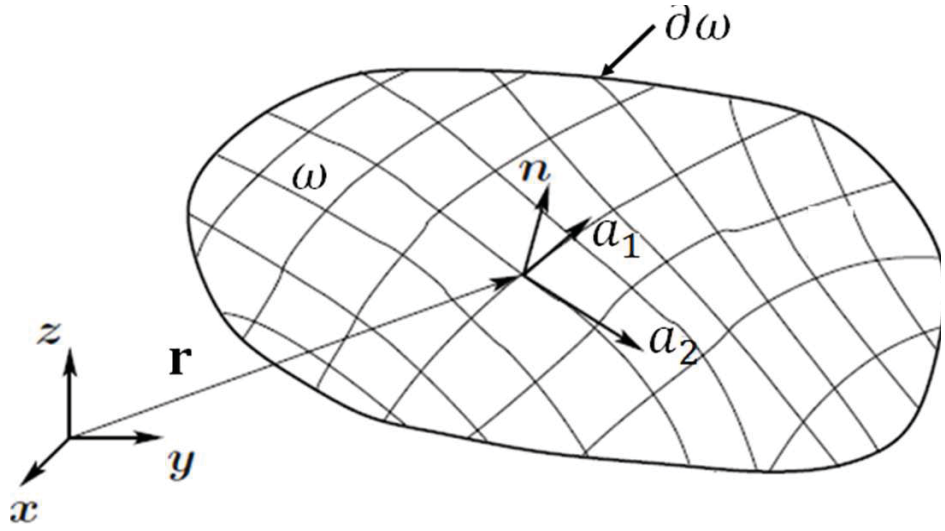


Fig. 2.1 Representation of membrane surface.

## 2.2 Mathematical model

Thus far, it has been noted that the bilayer membrane can be modelled as a continuous elastic two-dimensional geometric surface embedded in Euclidean three-dimensional space. The geometry of the surface can be described by its mean curvature and Gaussian curvature (see, e.g., [95]). Here, some useful formulas and definitions are given making use of the basic notions of differential geometry after which we introduce the bilayer equilibrium equation (shape equation) and admissible edge conditions from the literature.

### 2.2.1 Definitions and basic formulas related to surface geometry

Suppose that $\omega$ represents the membrane surface, parametrized by two internal surface co-ordinates $\{x_1, x_2\}$, such that the position vector of a point on the surface $\mathbf{r} \in \mathbb{R}^3$ is given by the map $\mathbf{r}= \mathbf{r}\{x_1, x_2\}$ (see Fig. 2.1). The following vector and tensor quantities are defined for later use:

$$\mathbf{a}_\alpha = \mathbf{r}_{,\alpha}, \quad a_{\alpha\beta} = \mathbf{a}_\alpha \cdot \mathbf{a}_\beta, \quad a^{\alpha\beta} = (a_{\alpha\beta})^{-1}, \quad a = \det(a_{\alpha\beta}), \quad (\alpha, \beta = 1,2) \tag{2.1}$$

where $\mathbf{a}_\alpha$ are the tangent vectors to $\omega$ induced by the parametrization $\mathbf{r}\ \{\mathrm{x}_1, \mathrm{x}_2\}$, $\mathrm{a}^{\alpha\beta}$ is the matrix of dual metric components (i.e, the contravariant components of the surface metric tensor), $\mathbf{a}_{\alpha\beta}$ is the induced surface metric tensor which is non-negative definite in general, a is the determinant of the metric tensor $\mathrm{a}_{\alpha\beta}$ and the commas are used to denote partial differentiation with respect to the surface coordinates $(i.e., (*)_{,\alpha} = \frac{\partial(*)}{\partial x_\alpha})$

$$\mathbf{n} = \frac{1}{2}\varepsilon^{\alpha\beta}\mathbf{a}_\alpha \times \mathbf{a}_\beta, \quad \mathrm{b}_{\alpha\beta} = \mathbf{n}\cdot\mathbf{a}_{\alpha,\beta}, \quad \mathrm{b}^{\alpha\beta} = \mathrm{a}^{\alpha\lambda}\mathrm{a}^{\beta\mu}\mathrm{b}_{\lambda\mu}, \tag{2.2}$$

where $\mathbf{n}$ is the local surface orientation, $\varepsilon^{\alpha\beta} = \frac{\mathrm{e}^{\alpha\beta}}{\sqrt{a}}$ is the permutation tensor density with $\mathrm{e}^{12} = -\mathrm{e}^{21} = 1$, $\mathrm{e}^{11} = \mathrm{e}^{22} = 0$ and $\mathrm{b}_{\alpha\beta}$ are the symmetric coefficients of the second fundamental form on $\omega$.

The geometry of the bilayer membrane can be described in terms of the mean curvature $H$ and Gaussian curvature $K$ of the membrane surface $\omega$. These are defined by

$$H = \frac{1}{2}\mathrm{a}^{\alpha\beta}\mathrm{b}_{\alpha\beta}, \quad K = \frac{1}{2}\varepsilon^{\alpha\beta}\varepsilon^{\lambda\mu}\mathrm{b}_{\alpha\lambda}\mathrm{b}_{\beta\mu}, \tag{2.3}$$

and the cofactor of the curvature $\tilde{b}^{\alpha\beta}$ is given by [90].

$$\tilde{b}^{\alpha\beta} = 2H\mathrm{a}^{\alpha\beta} - \mathrm{b}^{\alpha\beta}. \tag{2.4}$$

### 2.2.2 Shape equations and edge Conditions

In the theory of classical bilayer mechanics, the response of the membrane can be described by the deformation and geometry of the membrane surface, and the equilibrium configurations of the membrane corresponds to the local minimum of an areal free-energy density $W_f$. For a bilayer membrane with densely distributed lipid molecules on the surface, the area of the lipid membrane can be almost regarded as incompressible, and the equilibrium shape

of the membrane is determined by the local energy minimization of Helfrich's model [37] given by

$$W_f = \frac{k}{2}\oint (2H - H_0)^2 dA + \Delta p \int dV + \lambda \oint dA. \tag{2.5}$$

where $dA$ is the surface area element, $dV$ is the volume element, $k$ is the (positive) bending modulus, $H$ is the surface mean curvature, $H_0$ is the spontaneous curvature, $\Delta p$ serves as the Lagrange multiplier due to constant volume of the system and denotes the osmotic pressure difference between the two leaflets of the lipid bilayer membrane and $\lambda$ is the Lagrange multiplier due to the constraint of constant area and denotes the tensile stress acting on the surface of the membrane. The first part of Eq. (2.5) is the free energy associated with bending deformation on the membrane surface (or the curvature-elastic energy of the membrane). The second and third terms are energy contributions from volume deformations induced by pressure differences and membrane surface tension, respectively.

Much of the literature on bilayer membrane mechanics has revealed that the bending energy $W_b$ in terms of $H$ and $K$ plays a crucial role in the determination of the equilibrium configuration of lipid bilayer membranes, which is given by Helfrich [37] as

$$W_b(H,K) = \frac{k}{2}(2H - H_0)^2 + \bar{k}K. \tag{2.6}$$

Here $k$ and $\bar{k}$ are bending rigidities which pertains to lipid membranes with uniform properties. While $\bar{k}$ is unrestricted, $k$ is found to be positive [1]. In the above, $H_0$ is called the spontaneous curvature which reflects any possible intrinsic curvature of the membrane, due to, for example, either the bilayer asymmetry or the physical constraint [29, 47, 60, 104]. The bilayer asymmetry can be produced by the transbilayer lipid shape asymmetry [104]. Hamai et. al. [36] has analogized the shape of lipids to a cone, a cylinder or an inverted cone, corresponding to negative, zero or positive spontaneous curvature. The physical constraint can arise from the interaction of proteins on the lipid bilayer membrane surfaces without

penetrating into the hydrophobic region of the bilayer [29]. Therefore, the above-mentioned and other chemical factors may cause a nonzero value of the spontaneous curvature. However, as reported in [27], some mechanism of spontaneous curvature, such as the splayed geometry of the individual lipid, can be mitigated by the slow process of transmembrane diffusion of lipids from one layer to the other [84].

Following the works of Agrawal et. al. [1], in this paper, we study a simplified uniform bilayer membrane that has no natural orientation in which the free energy function $W_f$ satisfies the symmetry relation $W_f(H,K)$=$W_f(-H,K)$ [92] and present the governing equations describing the equilibrium configurations of the membrane within the framework of the well-known Helfrich model:

$$W(H,K;x_\alpha) = \; kH^2 + \bar{k}K. \tag{2.7}$$

Minimization of the free energy $\int_\omega W(H,K;x_\alpha)\,da$ with respect to Helfrich's zero spontaneous curvature model in Eq. (2.7) using variational method leads to the shape equation [1] of the lipid bilayer membrane, which furnishes

$$k[\Delta H + 2H(H^2-K)] - 2\lambda H = P. \tag{2.8}$$

The admissible boundary conditions (e.g., boundary forces $\mathbf{f}$ and moments $M$ on $\partial\omega$) of Eq. (2.8) are derived in detail in [1, 70, 90, 91]. These are given by

$$\mathbf{f} = \mathrm{F}_\upsilon \upsilon + F_\tau \tau + F_\mathrm{n}\mathbf{n}, \tag{2.9}$$

$$M = \frac{1}{2} W_H + \kappa_\tau W_K, \tag{2.10}$$

where $\upsilon$ and $\tau = \mathbf{n}\times\upsilon$ correspond to the exterior unit normal and unit tangent to $\partial\omega$, respectively, and

$$\mathrm{F}_\upsilon = W + \lambda - \kappa_\upsilon M, \quad \mathrm{F}_\tau = -\tau M, \quad \mathrm{F}_n = (\tau M)^{'} - (\frac{1}{2} W_H)_{,\upsilon} - (W_K)_{,\beta} \tilde{b}^{\alpha\beta} \upsilon_\alpha, \qquad (2.11)$$

respectively, are the $\upsilon$-,$\tau$- and **n**-components of distributed forces per unit length applied to $\partial\omega$. Here, the subscripts $H$ and $K$ refers to partial derivative with respect to the indicated variables (e.g., $W_H = \frac{\partial W}{\partial H}$ etc...). For example, the force applied to the membrane at the $i$th corner of $\partial\omega$ is

$$\mathbf{f}_i = W_K[\tau]_i \mathbf{n}, \qquad (2.12)$$

where,

$$\tau = \mathrm{b}^{\alpha\beta} \tau_\alpha \upsilon_\beta, \qquad (2.13)$$

is the twist of the membrane surface $\omega$ on the $(\upsilon, \tau)$- axes with $(\upsilon_\alpha = \mathbf{a}_\alpha.\upsilon$ and $\tau_\beta = \mathbf{a}_\beta.\tau)$, and

$$\kappa_\upsilon = \mathrm{b}^{\alpha\beta} \upsilon_\alpha \upsilon_\beta, \quad \kappa_\tau = \mathrm{b}^{\alpha\beta} \tau_\alpha \tau_\beta. \qquad (2.14)$$

are the normal curvatures of $\omega$ in the directions of $\upsilon$ and $\tau$, respectively.

## 2.3 Monge representation

We consider a uniform symmetric bilayer membrane described by a surface $\omega$ embedded in $\mathbb{R}^3$ and written as a function of the parametric variables $(x_1, x_2)$. For convenience, here and henceforth, the subscripts of the surface coordinates are dropped and replaced by $x_1 = x$, $x_2 = y$. In order to analyze the responses of the membrane in the rectangular domain, we use

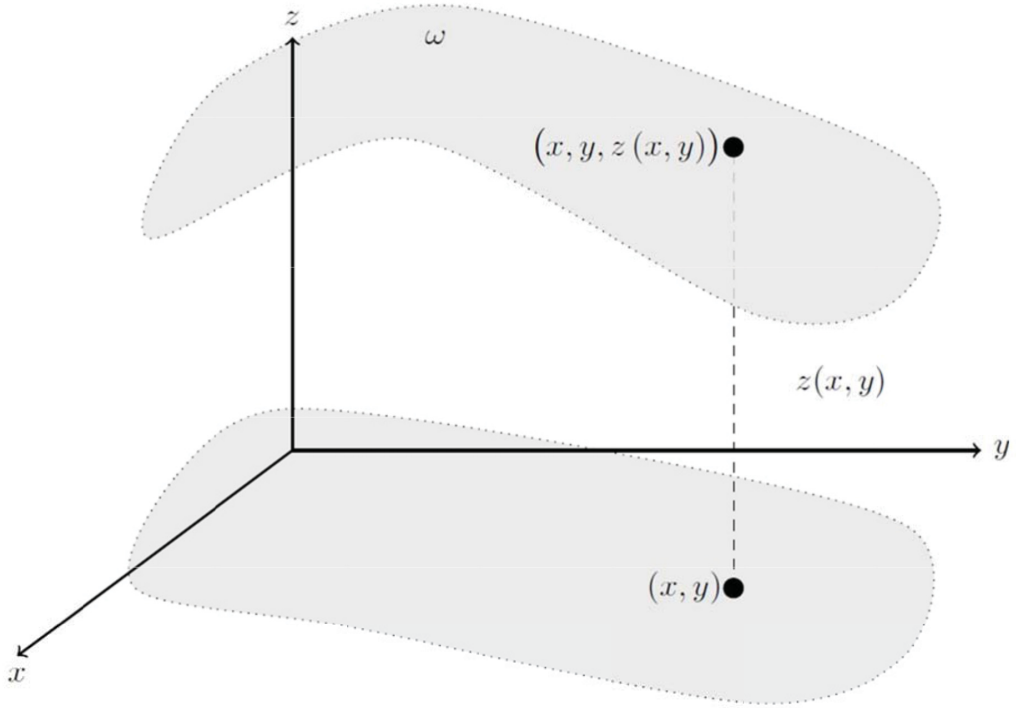


Fig. 2.2 Monge representation of points in a membrane surface using cartesian coordinate system.

the Monge representation with space vector **r** representing material points on the membrane surface which is given by

$$\mathbf{r}(x,y) = x\mathbf{e}_1 + y\mathbf{e}_2 + z(x,y)\mathbf{k}, \tag{2.15}$$

where $x$ and $y$ are positions on a plane, $(\mathbf{e}_1, \mathbf{e}_2, \mathbf{k})$ is the orthonormal Cartesian basis and $z(x,y)$ is height function that describes the bilayer membrane mid-plane shape. Here we note that the thickness of the membrane is assumed to be uniform. The Monge representation is an approximation of out-of-plane deformations in which no folds of the membrane are allowed, and hence, $z(x,y)$ is restricted to a single valued function. This representation is valid for nearly flat membrane surfaces with gradual variation of the height function away

from the xy-plane, leading to relatively simple expressions for the corresponding curvature tensor and other response variables given by:

$$a = [1 + (z_x)^2 + (z_y)^2], \quad \mathbf{n} = \frac{(\mathbf{k} - \nabla z)}{\sqrt{a}}, \quad \mathbf{b} = \frac{(z_{,\alpha\beta}\mathbf{e}_\alpha \otimes \mathbf{e}_\beta)}{\sqrt{a}}, \tag{2.16}$$

$$H = \frac{(1 + (z_y)^2)z_{xx} - 2z_x z_y z_{xy} + (1 + (z_x)^2)z_{yy}}{2[1 + (z_x)^2 + (z_y)^2]^{3/2}}, \quad K = \frac{z_{xx}z_{yy} - (z_{xy})^2}{[1 + (z_x)^2 + (z_y)^2]^{3/2}}. \tag{2.17}$$

However, the evaluation of the corresponding shape equation Eq. (2.8) in terms of Eqs. $(2.17)_1$ *and* $(2.17)_2$ furnishes a highly non-linear PDE system which most often requires heavy computational resources. Instead, a means of "admissible linearization" can be employed to make the system mathematically tractable with minimum loss of generality.

## 2.4 Linearization

Within the description of superposed incremental deformations and nearly flat membranes, we speculate that $z_{,\alpha} \ll 1$ $(\alpha = x, y)$, and therefore, their products can be neglected. Thus, using the notation $\simeq$ to identify equations to the leading order in $z$, Eqs. (2.16 - 2.17) reduce to

$$a \simeq 1, \quad \mathbf{n} \simeq \mathbf{k} - \nabla z, \quad \textit{and} \quad \mathbf{b} \simeq \nabla^2 z, \tag{2.18}$$

$$H \simeq \frac{z_{xx} + z_{yy}}{2} \simeq \frac{1}{2}\Delta z \quad \textit{and} \quad K \simeq 0, \tag{2.19}$$

where $\nabla^2 z = z_{,\alpha\beta}\mathbf{e}_\alpha \otimes \mathbf{e}_\beta$ is the second gradient on the plane and $\Delta z = tr(\nabla^2 z)$ is the corresponding Laplacian on the plane.

Equations (2.18 - 2.19) together with Eq. (2.8) yield the following simplified shape equation in the case of a uniform Helfrich membrane:

$$\frac{1}{2}k\Delta(\Delta z) - \lambda\Delta z \simeq P. \tag{2.20}$$

Now, let $\bar{\mathbf{r}}(S) = \mathbf{r}(\bar{\mathbf{X}}(S))$ where $\bar{\mathbf{X}}(S)$ is the arclength parametrization of the projected curve $\partial\omega$ on the plane. Note that ($\mathbf{X} = x\mathbf{e_1} + y\mathbf{e_2}$) in Eq. (2.15) parametrizes the plane in the global sense. The first derivative can be interpreted as the local tangent vectors $\bar{\mathbf{r}}_{,S} = \bar{\tau} + (\bar{\tau}.\nabla z)\mathbf{k}$, where $\bar{\tau} = \bar{\mathbf{X}}'(S)$ is the unit tangent to the projected curve. Then $\tau$ and $\bar{\tau}$ are related as $\bar{\mathbf{r}}_{,S} = \left|\bar{\mathbf{r}}_{,S}\right| \tau$ where $\left|\bar{\mathbf{r}}_{,S}\right| = \sqrt{1 + (\bar{\tau}.\nabla z)^2}$. Up to leading order, we obtain

$$\tau \simeq \bar{\tau} + (\bar{\tau}.\nabla z)\mathbf{k}, \tag{2.21}$$

and similarly for $\upsilon$ as

$$\upsilon = \tau \times \mathbf{n} \simeq \bar{\upsilon} + \nabla z \times \mathbf{k}, \tag{2.22}$$

where $\bar{\upsilon} = \bar{\tau} \times \mathbf{k}$ is the unit normal to the projected curve. Consequently, Eqs. (2.13) and (2.14) yield,

$$\tau \simeq \bar{\tau}.(\nabla^2 z)\bar{\upsilon}, \quad \kappa_\upsilon \simeq \bar{\upsilon}.(\nabla^2 z)\bar{\upsilon}, \quad \textit{and} \quad \kappa_\tau \simeq \bar{\tau}.(\nabla^2 z)\bar{\tau}. \tag{2.23}$$

Thus, the linearized expansion of the edge conditions ( i.e, forces and bending moments in Eqs. (2.9)-(2.11) in terms of the unit tangents and normals of the projected curve $\partial\omega$ can be obtained as

$$M \simeq \frac{1}{2}k\Delta z + \bar{k}\bar{\tau}.(\nabla^2 z)\bar{\tau}, \tag{2.24}$$

and

$$f_\upsilon \simeq \lambda, \quad f_\tau \simeq 0, \quad \textit{and} \quad f_n \simeq \bar{k}\bar{\tau}.\nabla\tau - k\bar{\upsilon}.\nabla H. \tag{2.25}$$

where $\tau$ and $H$ are given by Eqs. $(2.23)_1$ *and* $(2.19)_1$, respectively.

## 2.5 Analytical series solution to the linearized shape equation

In this work, we consider the deformations of a rectangular lipid membrane, in the case of vanishing lateral pressure and superposed incremental deformations, subjected to various types of boundary forces. Emphasis is placed on the cases where the membrane is subjected to applied boundary moments, since the corresponding deformation profiles are quantitatively equivalent to those induced by the lateral pressure gradient in the membrane conformation. However, we also note here that the methods adopted in the present analyses are sufficient general in that they can accommodate more general types of boundary conditions (e.g., non-uniform tractions, forces and edge clamping etc...).

Consider an isotropic homogeneous bilayer membrane deformation over a rectangular domain $(-\frac{a}{2} \leq x \leq \frac{a}{2}, -\frac{b}{2} \leq y \leq \frac{b}{2})$ with simply supported edges (see Fig. 2.3).

The kinematic edge conditions are $z = 0$ and $\mathbf{n} \simeq \mathbf{k} - \nabla z = \mathbf{k}$. The later implies that $\nabla z = 0$ on the boundary, and thus, the edge moment acting in the boundary (2.24) becomes $M \simeq \frac{1}{2} k \Delta z$. Therefore, the shape equation for the surface deformation of the membrane reduces to

$$\frac{1}{2} k \Delta(\Delta z) - \lambda \Delta z \simeq 0. \tag{2.26}$$

and is subject to the boundary conditions:

$$z = 0, \quad \textit{and} \quad \frac{1}{2} k \Delta z = M, \quad \textit{on} \quad \partial \omega \tag{2.27}$$

where $k$ is the bending modulus and $\lambda$ is a constitutively indeterminate Lagrange-multiplier field associated with the lipid membrane surface area constraint [1, 41, 70]. Note that the

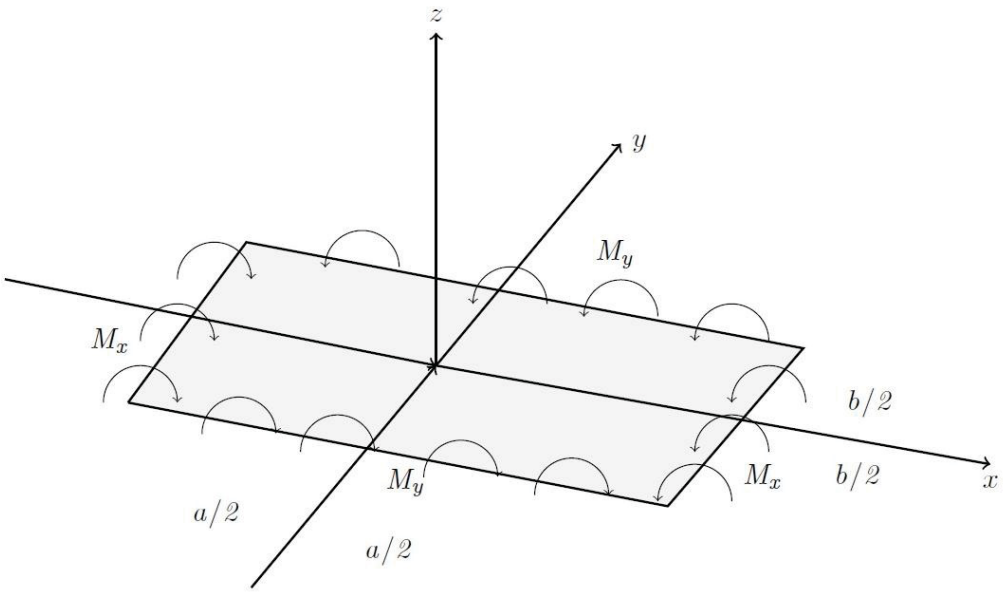


Fig. 2.3 Coordinate systems of lipid bilayer membrane and schematic of applied moment at the edges.

latter is not a material property and hence can be assigned any value in the equation of the equilibrium and any related conditions in a particular problem whenever deemed necessary. For example, if the surface area of the lipid membrane is fixed and prevents local dilation of the area, then $\lambda$ can be physically interpreted as surface pressure, and this may be a spatially varying field [70]. Accordingly, in the case of constant surface pressure, $\lambda$ can be assigned a negative constant, $\lambda < 0$. On the other hand, $\lambda$ can also be mechanically interpreted as the traction acting on the surface of the lipid membrane induced by the bending couple and assuming this stress to be tensile, it can be assigned a positive constant, $\lambda > 0$. Note that although $\lambda > 0$ *and* $\lambda < 0$ have quantitatively different behaviour, both of these cases can be treated analytically in a similar manner. For instance, for the case $\lambda < 0$, the Eq. (2.26) can be recast to the two-dimensional Helmholtz equation which has the form shown in Eq. (2.28) (with $\in = -1$) and the general solution to $z(x,y)$ can be established as sums of trigonometric functions using the methods of separation of variables plus Fourier series. Similarly, for the case $\lambda > 0$ considered in the present work, the general solution to the linearized shape

equation $z(x,y)$ can be obtained by recasting Eq. (2.26) to the following modified Helmholtz equation (with $\in = 1$)

$$\Delta H - \in \mu^2 H = 0, \tag{2.28}$$

where $H = \frac{1}{2}\Delta z$ from Eq. $(2.19)_1$ and

$$\mu^2 = \frac{2\lambda}{k}, \quad where \quad (k > 0). \tag{2.29}$$

Further, combining $(2.19)_1$ *and* (2.28) furnishes $\Delta[z - (\frac{2}{\mu^2})H] = 0$. Therefore, we obtain the general solution of $z(x,y)$ as

$$z(x,y) = \frac{2}{\mu^2}H(x,y) + \phi(x,y), \tag{2.30}$$

where $\phi$ is a plane harmonic function (i.e, $\Delta\phi = 0$).

An analytical series solution to Eq. (2.28) for domains with rectangular boundaries can be obtained through the method of separation of variables and the general solution for $H(x,y)$ becomes:

$$H(x,y) = \sum_{n=0}^{\infty}(C_n \sinh\beta_n y + D_n \cosh\beta_n y)(A_n \sin\alpha_n x + B_n \cos\alpha_n x), \tag{2.31}$$

Here, the arbitrary constants $A_n, B_n, C_n, D_n$ and separation constant $\alpha_n^2$, are to be determined from the admissible boundary conditions. Additionally, $\beta_n$ is defined as $(\beta_n^2 = \mu^2 + \alpha_n^2)$. We can also get another kind of like solutions for $H$ by changing the sign of $\alpha_n^2$. Regarding $\phi$ in Eq. (2.30), we propose the following plane harmonic function which is a product of trigonometric and hyperbolic functions as

$$\phi(x,y) = \sum_{n=0}^{\infty}(E_n \sinh\alpha_n y + F_n \cosh\alpha_n y)\sin\alpha_n x, \tag{2.32}$$

where $E_n$ and $F_n$ are arbitrary constants. Consequently, the solution for the linearized shape equation (2.26) can be formed by the composition of solutions chosen suitably from the given solution of $H$ and the proposed function of $\phi$. In addition, it will be simpler to solve the linearized shape equation if we make use of symmetric conditions. For symmetric surface deformation of the membrane with respect to both axes (see Fig. 2.3):

$$\begin{aligned} z(-\frac{a}{2},y) &= z(\frac{a}{2},y), \\ z(x,-\frac{b}{2}) &= z(x,\frac{b}{2}). \end{aligned} \tag{2.33}$$

Accordingly, the solution for solving the bilayer membrane deformation and for satisfying the above double symmetry and boundary conditions of the four edges can be established in the following form:

$$\begin{aligned} z(x,y) = \sum_{n=1}^{\infty} (\frac{2}{\mu^2} D_n \cosh \beta_n y + F_n \cosh \alpha_n y)(\cos \alpha_n x) + \\ \frac{2}{\mu^2} \sum_{n=1}^{\infty} (G_n \frac{\cosh \theta_n x}{\cosh \theta_n \frac{a}{2}} + L_n \frac{\cosh \gamma_n x}{\cosh \gamma_n \frac{a}{2}}) \cos \gamma_n y, \end{aligned} \tag{2.34}$$

where and $D_n, F_n, G_n$ and $L_n$ are unknown constants, which can be completely determined by imposing admissible boundary conditions, $a$ and $b$ are lengths of the rectangular domain and:

$$\beta_n^2 = \mu^2 + \alpha_n^2, \quad \theta_n^2 = \mu^2 + \gamma_n^2, \quad \alpha_n = \frac{n\pi}{a}, \quad \gamma_n = \frac{n\pi}{b}. \tag{2.35}$$

It should also be noted that by introducing the double symmetry conditions into the expressions for the shape function Eq. (2.33), the solution of the problem is reduced to the determination of four unknown coefficients.

Finally, the procedure for the computation of the analytical solution starts by introducing the applied moment in the form of Fourier series expansions:

$$\begin{aligned} f(y) &= \sum_{n=1}^{\infty} Q_n \cos \gamma_n y, \\ g(x) &= \sum_{n=1}^{\infty} R_n \cos \alpha_n x \end{aligned} \tag{2.36}$$

where $Q_n$ and $R_n$ are coefficients of the Fourier series, which can be determined from the given distribution $f(y)$ and $g(x)$, respectively (see [16]). Thus, by substituting the expressions in (2.34) into Eq. (2.27), we obtain

$$\begin{aligned} z(x,y)|_{x=-\frac{a}{2}} = 0, \quad \Rightarrow \quad & \frac{\partial^2 z}{\partial y^2} = 0, \quad M_x|_{x=-\frac{a}{2}} = \frac{1}{2}k\frac{\partial^2 z}{\partial x^2} = f(y) \\ z(x,y)|_{x=\frac{a}{2}} = 0, \quad \Rightarrow \quad & \frac{\partial^2 z}{\partial y^2} = 0, \quad M_x|_{x=\frac{a}{2}} = \frac{1}{2}k\frac{\partial^2 z}{\partial x^2} = f(y) \\ z(x,y)|_{y=-\frac{b}{2}} = 0, \quad \Rightarrow \quad & \frac{\partial^2 z}{\partial x^2} = 0, \quad M_y|_{y=-\frac{b}{2}} = \frac{1}{2}k\frac{\partial^2 z}{\partial y^2} = g(x) \\ z(x,y)|_{y=\frac{b}{2}} = 0, \quad \Rightarrow \quad & \frac{\partial^2 z}{\partial x^2} = 0, \quad M_y|_{y=\frac{b}{2}} = \frac{1}{2}k\frac{\partial^2 z}{\partial y^2} = g(x) \end{aligned} \tag{2.37}$$

In general, eight boundary conditions (two on each side) are necessary to completely determine the unknowns, but due to the introduction of the double symmetry condition, the solution of the linearized shape equation of the membrane is reduced to the determination of four unknown $D_n, F_n, G_n$ and $L_n$ from the above specified boundary conditions. The boundary conditions also follow most easily from an analysis of the symmetry at $(x,y)$-axes (see Fig. 2.3). Thus, solving procedure for the unknown constants continues with selection of two boundary conditions through which the direct dependence between appropriate groups of unknown coefficients is defined. Applying the boundary conditions along the edges $y = \pm\frac{b}{2}$ [*see*$(2.37)_3$ *and* $(2.37)_4$)], we find the coefficients $D_n$ and $F_n$ as

$$F_n = -\frac{2}{\mu^2} D_n \frac{\cosh \beta_n \frac{b}{2}}{\cosh \alpha_n \frac{b}{2}}, \quad D_n = \frac{R_n}{k \cosh \beta_n \frac{b}{2}} \tag{2.38}$$

where $R_n$ is the coefficient of the Fourier series. Similarly, for the boundary conditions along the edges at $x = \pm\frac{a}{2}$, we find the remaining unknown coefficients $G_n$ and $L_n$ which reads:

$$G_n = -L_n, \quad D_n = -\frac{Q_n}{k}, \tag{2.39}$$

where $Q_n$ is the coefficient of the Fourier series.

Let us assume that the bending moment applied to the boundary of the bilayer membrane is constant and is expanded in Fourier cosine series. Then, the applied edge moments (denoted as $M_x = M_1$ and $M_y = M_2$) can be expanded in terms of Fourier cosine series as

$$M_1 = \sum_{n=1}^{\infty} Q_n \cos \gamma_n y, \quad M_2 = \sum_{n=1}^{\infty} R_n \cos \alpha_n x, \tag{2.40}$$

where $Q_n$ and $R_n$ are obtained as:

$$Q_n = \frac{4M_1}{n\pi}(-1)^{\frac{n-1}{2}}, \quad R_n = \frac{4M_2}{n\pi}(-1)^{\frac{n-1}{2}}. \tag{2.41}$$

Subsequently, the solution of the linearized shape equation of the membrane subjected to the bending moment for simply supported edges is obtained by substituting Eqs. (2.38), (2.39) and (2.41) into (2.34), viz.

$$\begin{aligned} z(x,y) = \frac{4}{\mu^2 k\pi}\Big\{ \sum_{n=1,3,\ldots}^{\infty} \frac{(-1)^{\frac{n-1}{2}}}{n} \Big\{ M_1 \Big(\frac{\cosh \beta_n y}{\cosh \beta_n \frac{b}{2}} - \frac{\cosh \alpha_n y}{\cosh \alpha_n \frac{b}{2}}\Big) \cos \alpha_n x + \\ M_2 \Big(\frac{\cosh \theta_n x}{\cosh \theta_n \frac{a}{2}} - \frac{\cosh \gamma_n x}{\cosh \gamma_n \frac{a}{2}}\Big) \cos \gamma_n y \Big\} \Big\}. \end{aligned} \tag{2.42}$$

## 2.6 Examples and results

As noted in the previous section, the problem to be considered is a rectangular portion of the plane of a bilayer membrane with lengths *a and b* with its edges simply supported. We study the evolution of the membrane shape in response to an applied bending moment $M_1$ and $M_2$ specified across the boundary of the surface for different values of $\frac{b}{a}$ of the sides of the domain (see Fig. 2.3). The boundary of the membrane surface consists of piece-wise

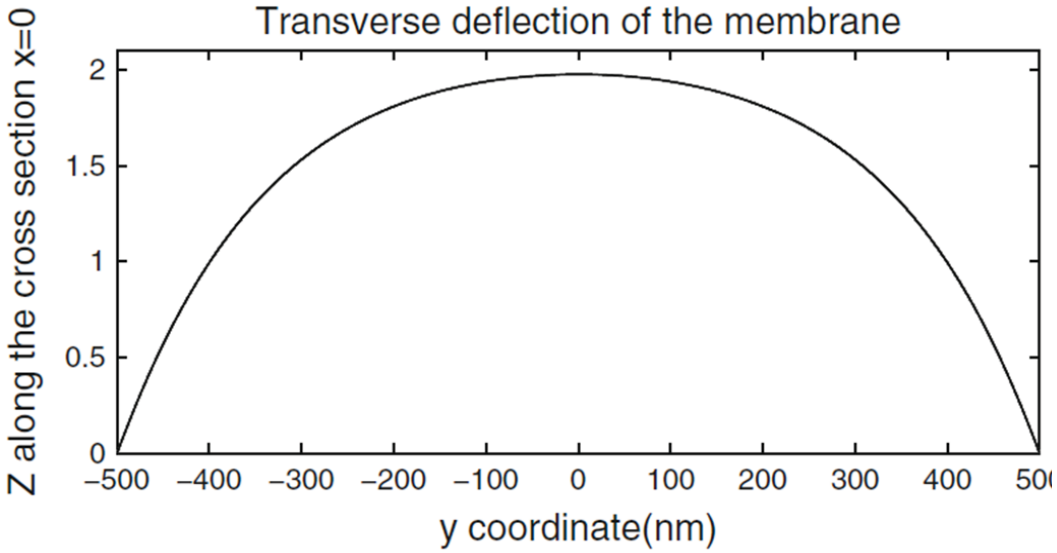


Fig. 2.4 Membrane shape evolution with an applied moment of $M_1 = M_1 = 30 \times 10^{-4}(pNnm)$ and ratio of sides of domain$(\frac{b}{a} = 2)$.

continuous linear segments and there are no jumps in the twist at the corners and therefore, no corner forces. The bilayer membrane is homogeneous, with constant bending modulus, which is assumed to be $k = 82\ pNnm$ [70]. The value of the surface stress $\lambda$ is also constant and is assumed to be $(10^{-4})\ pN/nm$.

We show the height of the membrane $z$ at the center in response to the different values of applied bending moment at different values of the aspect ratio of the membrane patch. From Eq. (2.42), the height $z$ at the center is directly proportional to the applied bending moment and therefore, it increases in response to the increasing applied bending moment as shown Figs. 2.4, 2.5 and 2.6.

For the isotropic membrane, as the shape evolves in response to the bending moment $M$, implicitly the surface pressure develops in the rectangular patch spatially in a homogeneous manner and intensifies as bending moment increases. In this work, the connection of the surface shape and lateral pressure $p$ is interpreted implicitly through the behavior of the applied bending moment. In reality, any lateral pressure gradient across the bilayer membrane can create a bending moment [76]. We demonstrate that by replacing the lateral pressure

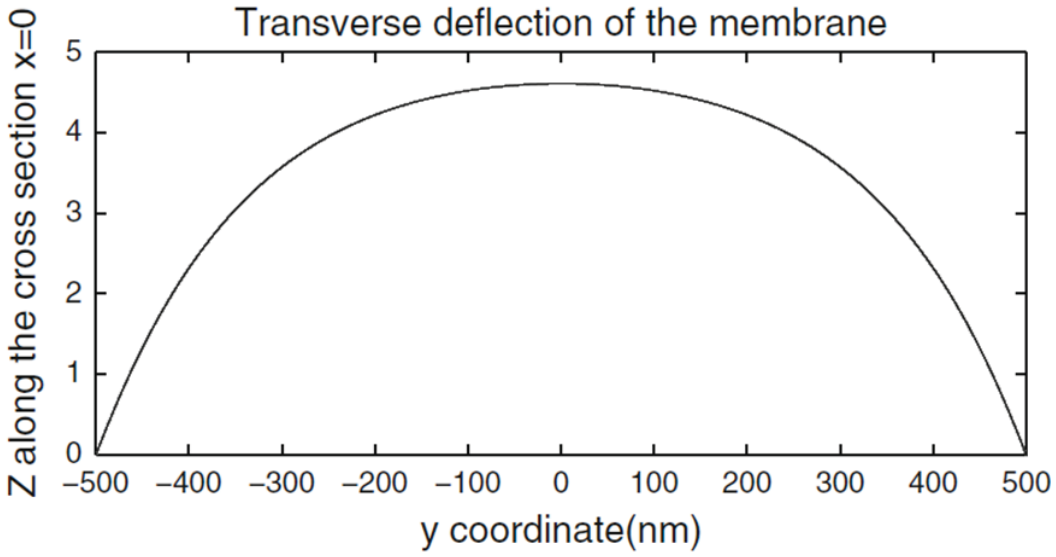


Fig. 2.5 Membrane shape evolution with an applied moment of $M_1 = M_1 = 70 \times 10^{-4}(pNnm)$ and ratio of sides of domain$(\frac{b}{a} = 2)$ .

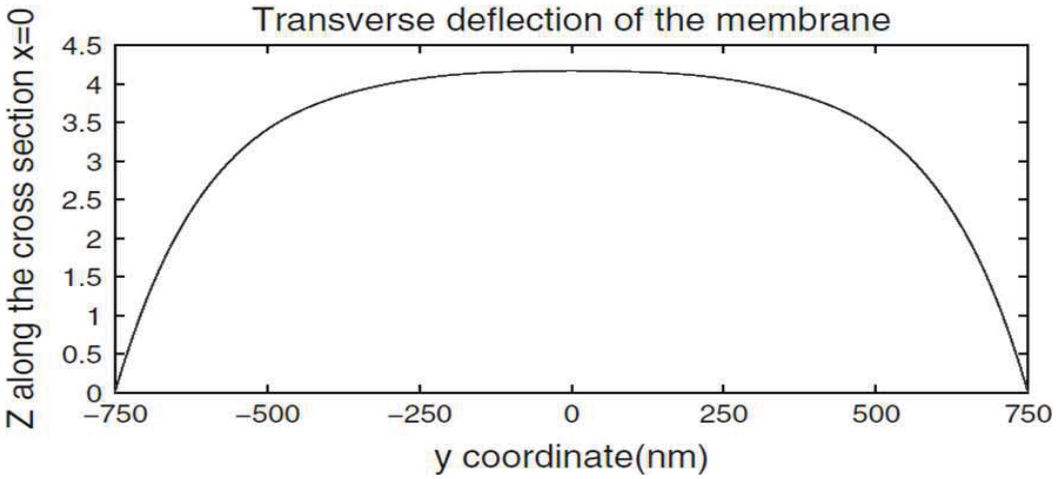


Fig. 2.6 Membrane shape evolution with an applied moment of $M_1 = M_1 = 70 \times 10^{-4}(pNnm)$ and ratio of sides of domain$(\frac{b}{a} = 3)$.

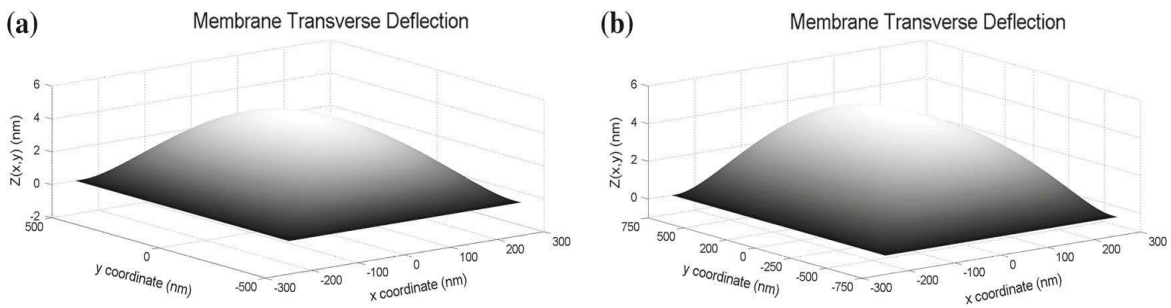


Fig. 2.7 Membrane shape evolution with ratio of sides of domain: (i)$(\frac{b}{a} = 2)$, (ii)$(\frac{b}{a} = 3)$

with the applied bending moment at the boundaries, the shape evolution behavior can be analyzed in a similar manner to that in lateral pressure load. Fig. 2.7 depicts the symmetric shape deformation of the membrane for different values of the ratio of the sides of the rectangular domain. Thus, the choice of bending moment $M$ at the boundaries is important in analyzing how the membrane shape evolves and could be used in various applications such as in the study of tether formation [88] in membrane bending stiffness measurement and checking the convergence, validity and accuracy of numerical methods for the analysis of lipid bilayer membranes.

## 2.7 Conclusion

This research presents an analytical expression for the deformations of a rectangular lipid membrane in the case of vanishing lateral pressure, subjected to various boundary forces acting on their edges. Emphasis is placed on the cases where the membrane is subjected to applied boundary moments, since the corresponding deformation profiles are quantitatively equivalent to those induced by the lateral pressure gradient in the membrane conformation. The principle of superposed incremental deformation is effectively applied to reduce the highly non-linear shape equation of the lipid membrane to a single mathematically tractable PDE with minimum loss of generality. Hence, a complete analytical solution is obtained which predicts smooth membrane morphological transitions over the domain of interest and satisfies the imposed boundary conditions. A number of examples which demonstrate the evolution of the membrane shape in response to an applied bending moment for different values of the aspect ratio of the sides of the rectangular patch have been presented. In all the examples, it has been found that for isotropic membranes, as the shape evolves in response to the bending moment, the surface pressure develops in the rectangular patch spatially in a homogeneous manner and intensifies as bending moment increases.

Finally, the analysis presented here can serve as a guide in solving problems involving rectangular lipid membranes subjected to different types of set boundary conditions/forces. Potential applications includes the study of spontaneous curvature of a membrane, tether formation in bending stiffness measurements and more importantly as a benchmark solution for checking the convergence and accuracy of numerical methods for the analysis of lipid bilayer membranes.

# Chapter 3

# Interaction Induced Morphological Transitions of Lipid Membranes in Contact with an Elliptical Cross Section of a Rigid Substrate

*We present a complete analysis for the deformation profiles of lipid membranes induced by their interactions with solid elliptical cylinder substrates (e.g., proteins). The theoretical framework for the mechanics of lipid membranes is described in terms of the classical Helfrich model and the resulting shape equation is formulated in general curvilinear coordinates to accommodate the elliptical shape of the contour surrounding the contact area. Admissible boundary conditions for the contact region are taken from the existing literature but reformulated and adapted to the current framework. A complete semi-analytic solution (in terms of Mathieu functions) is obtained within the limitation of superposed incremental deformations and the Monge representation in the deformed configuration functions. The results predict smooth morphological transitions over the domain of interest when a lipid membrane interacts with a rigid substrate through an elliptical contact region.*

## 3.1 Introduction

Lipid molecules are biologically important molecules which contain hydrocarbon chains and make up the structural and functional building blocks for all living cells. Lipid molecules are amphiphilic in that they have hydrophilic polar head groups and a hydrophobic nonpolar tail end. The hydrophilic molecules dissolve readily in water and have the tendency to interact or form hydrogen bonds with water molecules. The hydrophobic molecules, however,

don't dissolve in water. When dispersed in water, the difference in solvation preference of these two parts of the lipid molecules forces them to assemble spontaneously into lipid bilayer structures (lipid membranes). In fact, it is known that a lipid bilayer structure is characteristic of all biomembranes [33, 73]. Depending on the specific size and shape of the hydrophobic and hydrophilic parts, lipid molecules can also form other structures such as micelles, ellipsoids, and cylinders (e.g., see Fig. 3.1).

Although they are negligibly thin (typically 5-10nm), lipid membranes represent a critically important interface within biological cells providing a selective permeability barrier around each cell. In addition, lipid membranes mediate all interactions between cells and their surrounding environment through the involvement of a variety of proteins. Proteins coexist and co-evolve with lipid bilayers in the membrane composition (approxinately thirty per cent) and are involved in the process of various essential cellular activities across the membrane, for example, transportation of molecules, ion pumps and signal transduction in and out of the cell. In particular, so-called "trans-membrane proteins" assist morphological aspects of cellular processes such as fusion, fission, and envagination [15, 53, 71] regulated by membrane forces. In addition, interactions between "trans-membrane proteins" and the membranes themselves produce necessary mechanical forces to regulate desired morphological transitions for the aforementioned cellular processes [11, 13, 15, 53, 63]. Consequently, the study of the morphological aspects of such interactions is crucial to the understanding of a wide variety of essential cellular functions.

Recent studies have indicated that the mechanism of lipid membrane interaction with trans-membrane proteins can be examined by quantitative theoretical models through so-called "compatible deformations" and the consideration of necessary equilibrium conditions on the boundaries and/or some parts of the lipid membrane interacting with a substrate (see, for example, Refs. [1, 2, 23, 74] and the references contained therein). Artificially produced lipid bilayer membranes [99] are used as cell membrane systems *in vitro* and can be used to

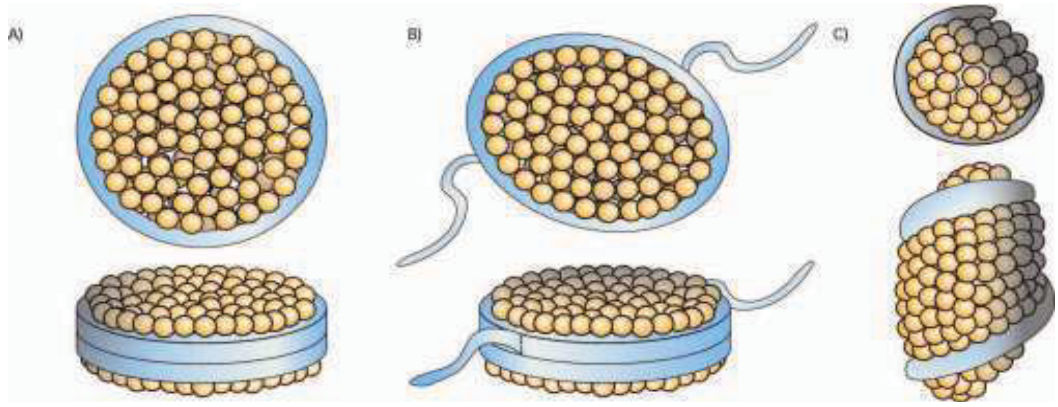


Fig. 3.1 Circular, cylindrical and elliptical structure formed from lipid molecules.(*Picture taken from: Skar-Gislinge, N., et al. 2010*).

study the dynamics of lipid membranes, for example, domain formation, hydrophobic mismatching, and lipid diffusion. In this regard, phospholipid bilayer membranes of elliptical shape can also be stabilized allowing for unprecedented studies of the functions of membrane proteins and their interaction with lipid membranes [87] (see Fig. 3.1). Within this context, solid cylindrical [1] and elliptical substrate structures can be used to study lipid membrane-protein interactions. Since lipid membranes are negligibly thin and fragile, any empirical examination of the above-mentioned conditions can present formidable difficulties. Consequently, it is of interest to develop analytical models to predict and describe the morphological transitions of lipid membranes. Such analytical models are largely absent from the literature, in particular in cases when lipid membranes interact through the elliptical contact domain of a trans-membrane protein substrate. Perhaps this is most likely explained by the massive analytical and numerical complexity arising from the highly nonlinear nature of the corresponding systems of equations defined in the necessary curvilinear setting. In the context of analytical modelling, few successful attempts have been reported under the assumption of superposed incremental deformations of lipid membranes while incorporating the generality and complexity of the associated boundary forces and domains of interest [1, 9].

In the present work, we develop a complete analytical framework describing the deformations of lipid membranes resulting from their interaction with solid elliptical cylinder substrates along their edges. Emphasis is placed on the representation of the film/substrate interaction boundary conditions by means of Mathieu functions, at the same time, maintaining the rigor and generality in the derivation of compatible shape equations within the prescription of superposed incremental deformations. We obtain a complete semi-analytical solution by reducing the corresponding problem to a system involving a single partial differential equation. Our results indicate smooth transition of deformation profiles over the domain of interest and also accommodate solutions in Ref. [1] when the magnitude of the two parameter families coincide.

The chapter is organized as follows. Sections 3.2 and 3.3 introduce a formulation of the problem which includes a brief review of the geometry and kinematics of the membrane surface, description of the generalized equilibrium-shape equation of the lipid membrane and the corresponding boundary conditions. Sections 3.4 and 3.5 present the derivation of the solutions and a discussion of the results with examples. Finally, Section 3.6 presents our conclusions.

## 3.2 Formulation

### 3.2.1 Surface geometry, shape equation and boundary conditions

In much of the literature on lipid membrane mechanics, it has been noted that a bilayer membrane can be modeled as a continuous elastic two-dimensional geometric surface embedded in three-dimensional Euclidean space relying on the classical Helfrich theory [37] to provide the theoretical framework for modeling the shape changes in the membrane. Thus, the mechanical response and associated morphological transitions of lipid membranes can be described entirely by the deformation and geometry of the membrane surface. In this work,

we study a simplified uniform bilayer membrane in which the areal free-energy density for the membrane can be expressed within the framework of the well-known Helfrich model as

$$W(H,K;x_\alpha) = kH^2 + \bar{k}K. \tag{3.1}$$

Here and in what follows, Greek indices take the value 1,2 and we sum over repeated indices. The parameters $k$ and $\bar{k}$ are bending rigidities which pertain to lipid membranes with uniform properties. While $\bar{k}$ is unrestricted, $k$ is found to be positive [1] . In the above, $H$ is called the mean curvature of the membrane surface $\omega$ (with boundary $\partial\omega$), and $K$ is the Gaussian curvature. These curvatures are defined by

$$H = \frac{1}{2}a^{\alpha\beta}b_{\alpha\beta}, \quad K = \frac{1}{2}\varepsilon^{\alpha\beta}\varepsilon^{\lambda\mu}b_{\alpha\lambda}b_{\beta\mu}, \tag{3.2}$$

where $(a^{\alpha\beta})$ is the matrix of dual metric components (i.e, the contravariant components of the surface metric tensor), the inverse of the metric $(a_{\alpha\beta})$; $\varepsilon^{\alpha\beta} = \frac{e^{\alpha\beta}}{\sqrt{a}}$ is the permutation tensor density with $a = det(a_{\alpha\beta})$; $e^{12} = -e^{21} = 1$, $e^{11} = e^{22} = 0$; and $b_{\alpha\beta}$ are the symmetric coefficients of the second fundamental form on $\omega$. The latter are the covariant components of the surface curvature tensor. The contravariant cofactor of the curvature is given by [90]

$$\tilde{b}^{\alpha\beta} = 2Ha^{\alpha\beta} - b^{\alpha\beta}. \tag{3.3}$$

In Eqs. $(3.2)_1$ and $(3.3)$, the metric is defined by $(a_{\alpha\beta} = \mathbf{a}_\alpha \cdot \mathbf{a}_\beta)$, where $(\mathbf{a}_\alpha = \mathbf{r}_{,\alpha})$ are the tangent vectors to $\omega$ induced by the parametrization $\mathbf{r}(x_\alpha)$, the position in $\mathbb{R}^3$ of a point on the membrane surface with coordinates $x_\alpha$. The unit vector field which defines the local surface orientation of the membrane can also be given by $\mathbf{n} = \frac{1}{2}\varepsilon^{\alpha\beta}\mathbf{a}_\alpha \times \mathbf{a}_\beta$.

According to the classical Helfrich theory [37], the shape equation describing the equilibrium configurations of the membrane can be obtained by minimization of the free energy $\int_\omega W(H,K;x_\alpha)da$ leading to [1]

$$k[\Delta H + 2H(H^2 - K)] - 2\lambda H = P, \tag{3.4}$$

where $\lambda$ is a constitutively indeterminate Lagrange-multiplier field associated with the lipid membrane surface area constraint [1, 41, 70] and $P$ is mechanically interpreted as net lateral pressure exerted on the membrane in the direction of its orientation $\mathbf{n}$.

The associated admissible boundary conditions (e.g., boundary forces $\mathbf{f}$ and moments $M$ on $\partial\omega$) of Eq. (3.4) are derived in detail in Refs. [1, 70, 90, 91]. These are given by

$$\mathbf{f} = F_\upsilon \upsilon + F_\tau \tau + F_n \mathbf{n}, \tag{3.5}$$

$$M = \frac{1}{2} W_H + \kappa_\tau W_K, \tag{3.6}$$

where $\upsilon$ and $\tau = \mathbf{n} \times \upsilon$ correspond to the exterior unit normal and unit tangent to $\partial\omega$, respectively, and

$$F_\upsilon = W + \lambda - \kappa_\upsilon M, \quad F_\tau = -\tau M, \quad F_n = (\tau M)' - (\frac{1}{2} W_H)_{,\upsilon} - (W_K)_{,\beta} \tilde{b}^{\alpha\beta} \upsilon_\alpha, \tag{3.7}$$

are, respectively, the $\upsilon$-,$\tau$- and $\mathbf{n}$-components of distributed forces per unit length applied to $\partial\omega$ (we note here the use of the subscripts $H$ and $K$ to also denote partial derivatives with respect to the indicated variables, e.g., $W_H = \frac{\partial W}{\partial H}$ etc...). For example, the force applied to the membrane at the $i$th corner of $\partial\omega$ is

$$\mathbf{f_i} = W_K[\tau]_i n, \tag{3.8}$$

where,

$$\tau = b^{\alpha\beta} \tau_\alpha \upsilon_\beta, \tag{3.9}$$

is the twist of the membrane surface $\omega$ on the $(\upsilon, \tau)$- axes with $(\upsilon_\alpha = \mathbf{a}_\alpha \cdot \upsilon$ and $\tau_\beta = \mathbf{a}_\beta \cdot \tau)$, and

$$\kappa_\upsilon = b^{\alpha\beta}\upsilon_\alpha\upsilon_\beta, \quad \kappa_\tau = b^{\alpha\beta}\tau_\alpha\tau_\beta. \tag{3.10}$$

are the normal curvatures of $\omega$ in the directions of $\upsilon$ and $\tau$, respectively.

### 3.2.2 Lipid molecule-substrate interaction model

In contrast to trans-membrane proteins which are held within the interior of the lipid bilayer in an aqueous environment, many membrane proteins are anchored to the surface of the membrane by special molecules that are associated with lipids and these substrates are free to move on the surface of the membrane. The membrane-solid substrate-liquid interaction is schematically demonstrated in Fig. 3.2. The interaction between lipid molecules and a homogeneous isotropic solid substrate may be modeled using conical anchoring [49, 101]. In this work, we utilize the contact boundary conditions developed (for lipid membranes interacting with curved substrates) by Agrawal and Steigmann [1] in order to analyze the behavior of elliptical lipid membranes resulting from their interaction with solid elliptical cylindrical substrates (e.g., proteins) along their edges.

Let $\Gamma$ represent the wall of the elliptical substrate, $\mathbf{B}$ the (symmetric) curvature tensor of $\Gamma$, and $\mathbf{N}$ the unit normal to the wall at a point of $\partial\omega$. The boundary $\partial\omega$ is a simple closed smooth curve on $\Gamma$. Now we consider a system consisting of a volume of bulk liquid with uniform properties bounded by the lipid bilayer membrane $\omega$ (with configurations of $\mathbf{n}$ ) and the wall of the solid elliptical cylindrical substrate $\Gamma$. The interaction in this system is considered to be energetically costly for configurations of $\mathbf{n}$ to deviate from $\mathbf{N}$ and this situation is idealized by the following constraint in the conical anchoring models as [101]:

$$\mathbf{n} \cdot \mathbf{N} = \cos\gamma, \tag{3.11}$$

in which $\gamma$ is assigned.

Since $\Gamma$ is a curved structure, then $\dot{\mathbf{N}}$ does not vanish at a membrane point of $\partial\omega$ for all variations $\mathbf{u} \in T_\Gamma$, where $\mathbf{u}$ is a virtual displacement and $T_\Gamma$ is the tangent plane at a point on the lipid membrane boundary $\partial\omega$. Instead, the variation of (3.11) may result in the possibility of a non-uniform membrane/wall interaction; i.e., $\gamma$ is not constant on $\Gamma$. In contrast, $\gamma$ is assigned a constant value in the case of a uniform film/wall interaction (details in Ref. [1]). Furthermore, the boundary condition for the membrane/curved substrate interactions is given by [1]

$$F_\upsilon \cos\gamma + F_n \sin\gamma - M\mathbf{n}\cdot(\nabla_\Gamma\gamma - \mathbf{Bn}) = \sigma, \quad F_\tau - M\boldsymbol{\tau}\cdot(\nabla_\Gamma\gamma - \mathbf{Bn}) = \mathbf{0}, \tag{3.12}$$

where $\sigma$ is an empirical constant which accounts for the wetting of the wall by the volume of the liquid. Positive values of $\sigma$ promote wetting, while negative values penalize wetting. Here, $F_\upsilon$, $F_n$ and $M$ are boundary force components and moments, respectively, on $\partial\omega$.

## 3.3 Linearized shape equation and boundary conditions

The evaluation of the shape equation Eq. (3.4) (within the Monge representation) furnishes a highly non-linear problem which most often requires heavy computational resources. In our previous study [9], we considered an "admissible linearization" method to make the system mathematically tractable without compromising generality and obtained the mean and Gaussian curvatures etc to linear order as

$$a \simeq 1, \quad \mathbf{n} \simeq \mathbf{k} - \nabla z, \quad \textit{and} \quad \mathbf{b} \simeq \nabla^2 z, \tag{3.13}$$

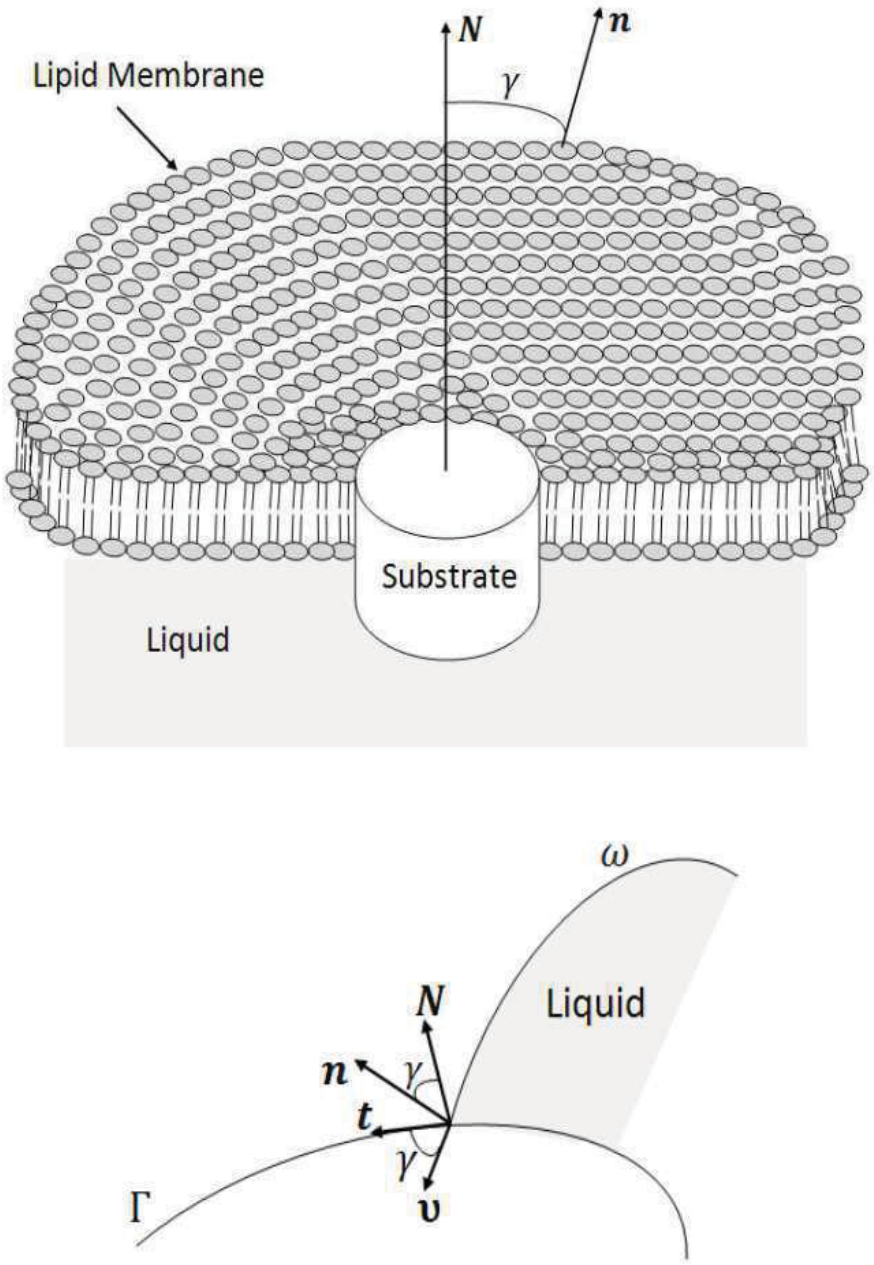


Fig. 3.2 Schematics of interaction of membrane, substrate and bulk liquid: (a) three-dimensional and (b) two-dimensional representations.

$$H \simeq \frac{1}{2}\Delta z \quad and \quad K \simeq 0, \tag{3.14}$$

where $z(x_\alpha)$ is the height function that describes the bilayer membrane mid-plane shape, $\nabla^2 z = z_{,\alpha\beta}\mathbf{e}_\alpha \otimes \mathbf{e}_\beta$ is the second gradient on the plane and $\Delta z = tr(\nabla^2 z)$ is the corresponding Laplacian in the plane. It follows from Eqs. (3.13), (3.14), and (3.4) that the linearized shape equation describing membrane morphology in the case of the Helfrich uniform membrane is obtained as

$$\frac{1}{2}k\Delta(\Delta z) - \lambda\Delta z \simeq P. \tag{3.15}$$

The associated boundary conditions (see Eqs. (3.5)-(3.7) ) in terms of the unit tangents and normals of the projected curve $\partial\omega$ on the plane can be linearized as

$$M \simeq \frac{1}{2}k\Delta z + \bar{k}\bar{\tau}.(\nabla^2 z)\bar{\tau}, \tag{3.16}$$

$$f_\upsilon \simeq \lambda, \quad f_\tau \simeq 0, \quad and \quad f_n \simeq \bar{k}\bar{\tau}\cdot\nabla\tau - k\bar{\upsilon}\cdot\nabla H, \tag{3.17}$$

and $\tau$ (see Eq. (3.9)) is reduced to

$$\tau \simeq \bar{\tau}\cdot(\nabla^2 z)\bar{\upsilon}. \tag{3.18}$$

Here, $\bar{\tau}$ and $\bar{\upsilon}$ are the unit tangent and normal vectors to the projected curve, respectively (see, for example, Ref. [9]).

### 3.3.1 Linearized shape equation and boundary conditions in elliptical coordinates

Here, we consider deformations of an elliptical lipid membrane, in the case of vanishing lateral pressure and superposed incremental deformations, subjected to the interaction of the lipid molecules in the membrane with an isotropic solid elliptical cylindrical substrate (which may represent the action of, e.g., proteins). The deformation problem on an elliptical domain can be rigorously analyzed by introducing the elliptical coordinates $(\xi,\eta)$ defined as

$$x+iy = c\cosh(\xi+i\eta) \tag{3.19}$$

such that

$$\begin{aligned} x &= c\cosh(\xi)\cos(\eta),\\ y &= c\sinh(\xi)\sin(\eta),\\ z &= z. \end{aligned} \tag{3.20}$$

where the semi-focal length $c$ is given by $c=\sqrt{a^2-b^2}$ and $\xi$, $\eta$ are radial and angular coordinates, respectively. The ranges of these parameters are given by $\xi\in[0,\infty)$, $\eta\in[0,2\pi]$, and $-\infty<z<\infty$ . The constant values of $\xi$ and $\eta$ form a family of confocal ellipses and hyperbolas, respectively.

The gradient ($\nabla$) and Laplacian ($\Delta$) operators in elliptical coordinates are (see Ref. [62], p. 18)

$$\nabla = \frac{1}{\sqrt{c^2(\cosh^2\xi-\cos^2\eta)}}\left(\frac{\partial}{\partial\xi}\mathbf{e}_\xi,\frac{\partial}{\partial\eta}\mathbf{e}_\eta\right), \tag{3.21}$$

$$\Delta = \frac{1}{c^2(\cosh^2\xi-\cos^2\eta)}\left(\frac{\partial^2}{\partial\xi^2}+\frac{\partial^2}{\partial\eta^2}\right), \tag{3.22}$$

The interaction problem under consideration is analyzed by solving the linearized shape equation (3.15) on an unbounded elliptical domain $\xi \geq \xi_0$. We represent the wall of the hydrophobic elliptical cylinder by $\Gamma$ with $\xi_0(>0)$, corresponding to the edge of the bounding elliptical $(\mathbf{N} = \mathbf{e}_\xi)$ substrate on $\Gamma$, such that the length of the semi-major axis is given by $a = c\cosh(\xi_0)$, whilst that of the semi-minor axis is $b = c\sinh(\xi_0)$. In addition, the empirical constant $\sigma$ in Eq. (3.12) is assigned a negative value so that wetting of the wall by the volume of the surrounding bulk liquid is suppressed, i.e., energetically disfavored. Further, we also assign $\gamma = \pi/2$ so as to minimize the energy cost for configuration $\mathbf{n}$ to deviate from the elliptical cylinder. This yields the kinematic edge condition $\mathbf{n} \simeq \mathbf{k} - \nabla z = \mathbf{k}$ at the wall, implying that the lipid molecule tail groups of the bilayer form a full contact around the elliptical cylinder which is thus shielded from the surrounding bulk liquid.

To express the boundary conditions in terms of elliptical coordinates, we assign $\gamma = \pi/2$ in Eqs. $(3.12)_{1,2}$. Then, Eq. $(3.12)_1$ reduces to

$$F_n - M\mathbf{n}\cdot(-\mathbf{B}\mathbf{n}) = \sigma, \tag{3.23}$$

where the curvature of the elliptical cylinders is found to be

$$\mathbf{B} = \frac{-c^2\cosh\xi\sinh\xi}{(c^2(\cosh^2\xi - \cos^2\eta))^{3/2}}\mathbf{e}_\eta \otimes \mathbf{e}_\eta. \tag{3.24}$$

Since $\mathbf{n} - \nabla z = \mathbf{k}$, we impose $\nabla z = 0$ on the boundary $\partial\omega$ and also find $\mathbf{B}\mathbf{n} = \mathbf{0}$. Accordingly, Eqs. (3.18) and (3.23) are reduced respectively to

$$\tau \simeq \bar{\tau}\cdot(\nabla^2 z)\bar{\upsilon} = 0. \tag{3.25}$$

$$F_n = \sigma. \tag{3.26}$$

Substituting in Eq. $(3.17)_3$ yields

$$f_n \simeq -k\bar{\upsilon} \cdot \nabla H = \sigma, \tag{3.27}$$

where $\bar{\tau}$ and $\bar{\upsilon}$ are identified in the elliptical coordinate system as $\mathbf{e}_\eta$ and $-\mathbf{e}_\xi$, respectively. Finally, writing $\nabla H$ in elliptical coordinates using the definition of the gradient operator in Eq. $(3.21)$ and substituting into Eq. $(3.27)$ furnishes the boundary condition for the lipid membrane/solid elliptical substrate as

$$\frac{1}{h}\frac{\partial H}{\partial \xi} = \frac{\sigma}{k}, \quad on \quad \partial\omega \tag{3.28}$$

where

$$h(\xi,\eta) = c(\cosh^2\xi - \cos^2\eta)^{1/2} \tag{3.29}$$

The above film/substrate interaction conditions together with the kinematic edge condition $z = 0$ are here demonstrated by solving the linearized shape equation $(3.15)$ with $P = 0$. Therefore, the shape equation for the surface deformation of the membrane reduces to

$$\frac{1}{2}k\Delta(\Delta z) - \lambda\Delta z \simeq 0, \quad in \quad \omega \tag{3.30}$$

subject to the boundary conditions

$$z = 0, \quad \nabla z = 0, \quad and \quad \frac{1}{h}\frac{\partial H}{\partial \xi} = \frac{\sigma}{k}, \quad on \quad \partial\omega \tag{3.31}$$

where $k$ is the bending modulus and $\lambda$ is a Lagrange-multiplier field associated with the lipid membrane surface area constraint. Note that the latter is not a material property and hence can be assigned any value in the equation of equilibrium and any related conditions in a particular problem whenever deemed necessary. For example, if the surface area of the lipid membrane is fixed and prevents local dilation of the area, then $\lambda$ can be physically

interpreted as surface pressure and thus may be a spatially varying field [70]. Accordingly, in the case of constant surface pressure, $\lambda$ can be assigned a negative value, $\lambda < 0$. On the other hand, $\lambda$ can also be mechanically interpreted as the traction acting on the surface of the lipid membrane induced by the bending couple and assuming this stress to be tensile, it can be assigned a positive constant value, $\lambda > 0$. Note that although $\lambda > 0$ and $\lambda < 0$ have quantitatively different behaviours, each of these cases can be treated analytically in a similar manner as special cases of the following equation:

$$\Delta H - \zeta \mu^2 H = 0, \tag{3.32}$$

in which $H = \frac{1}{2}\Delta z$ (Eq. $(3.14)_1$) and

$$\mu^2 = \frac{2\lambda}{k}, \quad \text{and } k > 0. \tag{3.33}$$

In fact, when $\lambda < 0$, Eq. (3.15) can be recast in the form of the two-dimensional Helmholtz equation (Eq. (3.32) with $\zeta = -1$) and the case $\lambda > 0$, corresponds to the modified Helmholtz equation (Eq. (3.32) with $\zeta = +1$).

Using the definition of the Laplacian, Eq.(3.32) may be written as

$$\frac{\partial^2 H}{\partial \xi^2} + \frac{\partial^2 H}{\partial \eta^2} - \frac{\mu^2 c^2}{2}(\cosh 2\xi - \cos 2\eta) H = 0. \tag{3.34}$$

In addition, the boundary conditions of the system under consideration (see Eq. $(3.31)$) are written in elliptical coordinates as

$$\begin{gathered} \frac{1}{h}\frac{\partial}{\partial \xi} H(\xi_0, \eta) = \frac{\sigma}{k}, \\ \frac{\partial}{\partial \xi} z(\xi_0, \eta) = 0, \quad \frac{\partial}{\partial \eta} z(\xi_0, \eta) = 0, \\ z(\xi_0, \eta) = 0, \end{gathered} \tag{3.35}$$

where $z = z(\xi, \eta)$ and $h(\xi_0, \eta)$ is given by Eq. $(3.29)$.

## 3.4 Analytical solution of the linearized shape equation

The general solution of Eq. (3.30) can be established by combining Eqs. $(3.14)_1$ and (3.30), which furnishes $\Delta[z-(\frac{2}{\mu^2})H]=0$. Hence, we obtain the solution $z(\xi,\eta)$ as

$$z(\xi,\eta)=\frac{2}{\mu^2}H(\xi,\eta)+\phi(\xi,\eta), \tag{3.36}$$

where $\phi$ is a plane harmonic function.

The general solution to the modified Helmholtz equation in Eq. (3.34) can be obtained through the method of separation of variables and may be written as (see Ref. [62], p. 20)

$$H(\xi,\eta)=F(\xi)G(\eta), \tag{3.37}$$

with which $F(\xi)$ and $G(\eta)$ respectively satisfy the following differential equations

$$\frac{\partial^2 F}{\partial \xi^2}-(\alpha-2q\cosh(2\xi))F=0 \tag{3.38a}$$

$$\frac{\partial^2 G}{\partial \eta^2}+(\alpha-2q\cos(2\eta))G=0 \tag{3.38b}$$

Here, $\alpha$ is the constant of separation and is also referred to as the Mathieu characteristic number; $q$ is the Mathieu parameter which can be positive or negative depending on the value of $\lambda$ (i.e., $q=-\mu^2c^2/4$, when $\lambda>0$ and $q=\mu^2c^2/4$, when $\lambda<0$). Equations $(3.38a)$ and $(3.38b)$ are modified Mathieu differential equations of the radial and circumferential kind, respectively [59]. In the subsequent subsections, we first obtain solutions to these differential equations with positive and negative values of $\lambda$ and then the corresponding general solution $z(\xi,\eta)$ will be obtained.

### 3.4.1 Deformation of the elliptical lipid membrane when $\lambda > 0$

As noted earlier, the bending of the elliptical lipid membrane resulting from the film/substrate interaction can induce a tensile stress on the surface of the membrane and this can be physically represented in the shape equation by assigning a positive value of $\lambda$, $(i.e, \lambda > 0)$. Thus, the parameter $q < 0$. We now proceed to solve Eqs. $(3.38a)$ and $(3.38b)$. Since we seek a bounded solution to a problem in an unbounded domain, the free-space solutions to Eqs. $(3.38a)$ and the corresponding general solution to $(3.38b)$ may be written, respectively as:

$$F(\xi) = \sum_{m=0}^{\infty} C_m Ke_{2m}(\xi, -q) + \sum_{m=1}^{\infty} \bar{C}_m Ko_{2m}(\xi, -q), \tag{3.39}$$

$$G(\eta) = \sum_{m=0}^{\infty} D_m ce_{2m}(\eta, -q) + \sum_{m=1}^{\infty} \bar{D}_m se_{2m}(\eta, -q), \tag{3.40}$$

where $C_m$, $\bar{C}_m$, $D_m$ and $\bar{D}_m$ are arbitrary constants to be determined from the admissible boundary condition. Here, the functions $Ke_{2m}(\xi, -q)$ and $Ko_{2m}(\xi, -q)$ are the even and odd, $2mth$-order, second kind, modified Mathieu functions, respectively. Similarly, the periodic functions $ce_{2m}(\eta, -q)$ and $se_{2m}(\eta, -q)$ are the even and odd, $2mth$-order, first kind modified Mathieu functions which can also appropriately satisfy the single-valuedness of $z(\xi, \eta)$ in Eq. $(3.36)$. Since we study the deformation field in an unbounded domain of the elliptical lipid membrane, in order to have a unique single-valued solution, $G(\eta)$ must return to the same value as $\eta$ increases by $2\pi$. In addition, it will be simpler to solve the linearized shape equation if we assume a symmetric deformation of the elliptical membrane about the major and minor axes simultaneously. Therefore, we choose $ce_{2m}(\eta, -q)$ which satisfies the quadrant symmetry behavior of the ellipse. Accordingly, we choose the solution $Ke_{2m}(\xi, -q)$ for $(3.38b)$ since this also satisfies the requirement that the solution be bounded in the unbounded domain; i.e., at a large distance from the boundary $\xi_0$, $(\xi \geq \xi_0, \xi \to \infty)$,

and $Ke_{2m}(\xi,-q) \to 0$ as required. Therefore, the solution $H(\xi,\eta)$ may now be written in the form

$$H(\xi,\eta) = \sum_{m=0}^{\infty} L_{2m} Ke_{2m}(\xi,-q) ce_{2m}(\eta,-q), \tag{3.41}$$

where the constant $L_{2m}$ must be determined from a given boundary condition. Here, the most appropriate representations for $ce_{2m}(\eta,-q)$ and $Ke_{2m}(\xi,-q)$ are [59]

$$ce_{2m}(\eta,-q) = (-1)^m \sum_{r=0}^{\infty} (-1)^r A_{2r}^{(2m)} \cos(2r\eta), \tag{3.42}$$

$$Ke_{2m}(\xi,-q) = (-1)^m \frac{p_{2m}}{\pi A_0^2} \sum_{r=0}^{\infty} A_{2r}^{(2m)} I_r(v_1) k_r(v_2), \tag{3.43}$$

where $A_{2r}^{(2m)}$ are coefficients associated with and determined through a recurrence relation once the values of $\alpha_{2m}$ (see Eqs. $(3.38a)$ and $(3.38b)$) have been evaluated as functions of $q$. Here, $p_{2m} = ce_{2m}(0,q)ce_{2m}(\pi/2,q)$, $I_r(v_1)$ and $k_r(v_2)$ are, respectively, modified Bessel functions of the first and second kind of order $r$ and $v_1(\xi) = \sqrt{q}\exp(-\xi)$, $v_2(\xi) = \sqrt{q}\exp(\xi)$. It should also be noted that with the asymptotic value of $Ke_{2m}(\xi,-q)$, Eq. $(3.41)$ yields $H^2 \propto \frac{p_{2m}^2 \exp(2v_2)}{2\pi v_2 A_0^2}$, which is a bounded multiplicative function of $\eta$ as $\xi \to \infty$. Accordingly, the associated contribution to the net bending energy is finite.

The detailed procedure by which the Mathieu characteristic number $\alpha_{2m}$ and the associated coefficients $A_{2r}^{(2m)}$ are obtained has been addressed in Ref. [59]. For the sake of brevity here, we report only a summary of that procedure. When the infinite series given in Eq. $(3.42)$ is substituted into the differential equation in Eq. $(3.38b)$, an infinite set of coupled equations associated with an infinite matrix defining a recurrence relation for the coefficients which involve ($q$, $\alpha$, and $A_{2r}^{(2m)}$) is obtained. After truncating the infinite matrix at an appropriately chosen row and column, this problem is reduced to an eigenvalue-eigenvector problem in which $\alpha_{2m}$ become the eigenvalues, and the coefficients $A_{2r}^{(2m)}$ are those of the

corresponding eigenvectors. MATLAB code was written for computing these eigenvalues and eigenvectors.

In the case of $\phi$ in Eq. (3.36), we choose among the following periodic harmonic functions of $\xi$ and $\eta$, which satisfy the condition which ensures that $\mathbf{n} \to \mathbf{k}$ for large $\xi \to \infty$. This condition is satisfied by imposing the requirement that $|\nabla z| \to 0$ which further entails, $\frac{\partial z}{\partial \xi} \to 0$ and $\frac{\partial z}{\partial \eta} \to 0$

$$\begin{gathered} e^{-2m\xi}\cos(2m\eta), \quad e^{-2m\xi}\sin(2m\eta), \\ \sum_{m=0}^{\infty}\sum_{r=0}^{\infty} A_{2r}^{(2m)} e^{-2r\xi} ce_{2m}(\eta,-q); \quad \textit{and} \quad \log(e^{\xi}/e^{\xi_0}). \end{gathered} \tag{3.44}$$

Thus, the general solution in Eq. (3.36) can be written in the form

$$\begin{gathered} z(\xi,\eta) = \frac{2}{\mu^2}\sum_{m=0}^{\infty} L_{2m} Ke_{2m}(\xi,-q) ce_{2m}(\eta,-q) + \beta + D\Big\{\log(\frac{ce^{\xi}}{2}) - \log(\frac{ce^{\xi_0}}{2})\Big\} + \\ \sum_{m=0}^{\infty}\sum_{r=0}^{\infty} \beta_{2r} A_{2r}^{(2m)} e^{-2r\xi} ce_{2m}(\eta,-q), \end{gathered} \tag{3.45}$$

where $L_{2m}$, $\beta$, $D$, and $\beta_{2r}$ are arbitrary constants to be determined from the given boundary conditions.

Finally, the procedure for the computation of the analytical solution is completed by the determination of the four unknown coefficients. Thus, by substituting the expressions (3.41) and (3.45) into Eq. (3.35), we obtain

$$\begin{aligned}
\frac{1}{h(\xi_0,\eta)}\frac{\partial}{\partial\xi}H(\xi_0,\eta)=\frac{\sigma}{k}, \quad \Rightarrow \qquad & \frac{1}{h(\xi_0,\eta)}\sum_{m=0}^{\infty}L_{2m}Ke'_{2m}(\xi_0,-q)ce_{2m}(\eta,-q)=\frac{\sigma}{k},\\
\frac{\partial}{\partial\eta}z(\xi_0,\eta)=0, \quad \Rightarrow \quad & \sum_{m=0}^{\infty}\left\{\frac{2}{\mu^2}L_{2m}Ke_{2m}(\xi_0,-q)+\sum_{r=0}^{\infty}\beta_{2r}A_{2r}^{(2m)}e^{-2r\xi_0}\right\}ce'_{2m}(\eta,-q)=0,\\
\frac{\partial}{\partial\xi}z(\xi_0,\eta)=0, \quad \Rightarrow \quad & \sum_{m=0}^{\infty}\left\{\frac{2}{\mu^2}L_{2m}Ke'_{2m}(\xi_0,-q)+\sum_{r=0}^{\infty}\beta_{2r}A_{2r}^{(2m)}(-2r)e^{-2r\xi_0}\right\}ce_{2m}(\eta,-q)+\frac{2D}{ce^{\xi_0}}=0,\\
z(\xi_0,\eta)=0, \quad \Rightarrow \quad & \sum_{m=0}^{\infty}\left\{\frac{2}{\mu^2}L_{2m}Ke_{2m}(\xi_0,-q)+\sum_{r=0}^{\infty}\beta_{2r}A_{2r}^{(2m)}e^{-2r\xi_0}\right\}ce_{2m}(\eta,-q)+\beta=0,
\end{aligned} \tag{3.46}$$

where the prime ($'$) attached to $Ke_{2m}$ and $ce_{2m}$ denotes the $\xi-$ and $\eta-$derivatives, respectively.

### 3.4.2 Determination of the coefficients

The solution procedure for the unknown coefficients in Eq. (3.46) continues by making use of the orthogonality of the angular Mathieu functions, and the relations are summarized in the following equations [59]:

$$\begin{gathered}
\int_0^{2\pi} ce_{2m}se_{2n}=0,\\
\textstyle\int_0^{2\pi}(ce_0)^2=2\pi,\\
\displaystyle\int_0^{2\pi} ce_{2m}ce_{2n}=\int_0^{2\pi} se_{2m}se_{2n}=\pi\delta_{mn}, \quad m\geq 1, \quad n\geq 1
\end{gathered} \tag{3.47}$$

where $\delta_{mn}$ is the Kronecker delta.

For example, let us consider the boundary condition in Eq. $(3.46)_1$. Multiplying both sides of the equation by $ce_{2m}(\eta,-q)$ and integrating over the domain $(0\rightarrow 2\pi)$ results in an integral expression for the coefficient $L_{2m}$

$$\sum_{m=0}^{\infty}L_{2m}Ke'_{2m}(\xi_0,-q)\textstyle\int_0^{2\pi}[ce_{2m}(\eta,-q)]^2/h(\xi_0,\eta)\,d\eta=\frac{\sigma}{k}\int_0^{2\pi}ce_{2m}(\eta,-q)\,d\eta. \tag{3.48}$$

Now

$$h(\xi_0,\eta) = c(\cosh^2\xi_0 - \cos^2\eta)^{1/2} = c\cosh\xi_0(1-(\cos\eta/\cosh\xi_0)^2)^{1/2} = a(1-e^2\cos^2\eta)^{1/2} \tag{3.49}$$

where $e$ is the eccentricity of the bounding ellipse. Thus, the integral expression of the coefficient $L_{2m}$ is

$$L_{2m} = \frac{\sigma a}{k}\frac{\int_0^{2\pi} ce_{2m}(\eta,-q)\,d\eta}{Ke'_{2m}(\xi_0,-q)\int_0^{2\pi}[ce_{2m}(\eta,-q)]^2/(1-e^2\cos^2\eta)^{1/2}\,d\eta}. \tag{3.50}$$

On substituting the infinite cosine series for $ce_{2m}(\eta,-q)$ in Eq. (3.50), and using the integral definition for Mathieu function in Ref. [59], p.177, we obtain

$$L_{2m} = \frac{2\pi\sigma a(-1)^m A_0^{(2m)}}{kKe'_{2m}(\xi_0,-q)S_{2m}}. \tag{3.51}$$

Here,

$$S_{2m} = \pi[1+\tfrac{1}{4}e^2(1+\Theta_{2m})+\ldots] \tag{3.52}$$

where $\Theta_{2m}$ is

$$\Theta_{2m} = A_0^{(2m)}A_2^{(2m)} + \sum_{r=0}^{\infty} A_{2r}^{(2m)}A_{2r+2}^{(2m)} \tag{3.53}$$

The substitution of Eq. (3.51) into Eq. $(3.46)_2$ yields an infinite system of simultaneous linear equations

$$\sum_{r=0}^{\infty}\beta_{2r}c_{mr} = -\tfrac{2}{\mu^2}\gamma_m \tag{3.54}$$

where

$$\begin{aligned} c_{mr} &= A_{2r}^{(2m)}e^{-2r\xi_0}, \\ \gamma_m &= L_{2m}Ke_{2m}(\xi_0,-q). \end{aligned} \tag{3.55}$$

Then, the solution of Eq. (3.54) can be obtained as (see also Ref. [78])

$$\beta_{2r} = -\frac{2}{\mu^2} T_{2r}(\xi_0, -q), \quad T_{2r}(\xi_0, -q) = \Delta^{(r)}/\Delta, \quad r = 0, 1, 2, \ldots, \tag{3.56}$$

where

$$\Delta = \begin{vmatrix} c_{00} & c_{01} & c_{02} & \cdots & \cdots \\ c_{10} & c_{11} & c_{12} & \cdots & \cdots \\ c_{20} & c_{21} & c_{22} & \cdots & \cdots \\ . & . & . & \cdots & \cdots \\ . & . & . & \cdots & \cdots \end{vmatrix}$$

$$\Delta^{(r)} = \begin{vmatrix} c_{00} & c_{01} & \cdots & \gamma_0 & \cdots \\ c_{10} & c_{11} & \cdots & \gamma_1 & \cdots \\ c_{20} & c_{21} & \cdots & \gamma_2 & \cdots \\ . & . & \cdots & . & \cdots \\ . & . & \cdots & . & \cdots \end{vmatrix}$$

Similarly, with some effort, we obtain the remaining coefficients as:

$$\begin{aligned} \beta &= -\frac{1}{2} \sum_{m=0}^{\infty} \left\{ \frac{4\pi\sigma a}{\mu^2 k} \frac{Ke_{2m}(\xi_0, -q)}{S_{2m} Ke'_{2m}(\xi_0, -q)} + \frac{1}{(-1)^m A_0^{(2m)}} \sum_{r=0}^{\infty} -\frac{2}{\mu^2} T_{2r}(\xi_0, -q) A_{2r}^{(2m)} e^{-2r\xi_0} \right\}, \\ D &= -\frac{c e^{\xi_0}}{4} \sum_{m=0}^{\infty} \left\{ \frac{4\pi\sigma a}{\mu^2 k S_{2m}} + \frac{1}{(-1)^m A_0^{(2m)}} \sum_{r=0}^{\infty} -\frac{2}{\mu^2} T_{2r}(\xi_0, -q) A_{2r}^{(2m)} (-2r) e^{-2r\xi_0} \right\}. \end{aligned} \tag{3.57}$$

Subsequently, the solution of the linearized shape equation of the membrane subjected to the lipid membrane/solid elliptical cylindrical substrate is obtained by substituting Eqs. (3.51) and (3.57) into Eq. (3.45), namely:

$$z(\xi,\eta)=\sum_{m=0}^{\infty}\left\{\frac{4\pi\sigma a}{\mu^2 k}\frac{(-1)^m A_0^{(2m)}}{S_{2m}}\frac{Ke_{2m}(\xi,-q)}{Ke'_{2m}(\xi_0,-q)}-\frac{2}{\mu^2}\sum_{r=0}^{\infty}T_{2r}(\xi_0,-q)A_{2r}^{(2m)}e^{-2r\xi}\right\}ce_{2m}(\eta,-q)$$
$$-\frac{1}{2}\sum_{m=0}^{\infty}\left\{\frac{4\pi\sigma a}{\mu^2 k}\frac{Ke_{2m}(\xi_0,-q)}{S_{2m}Ke'_{2m}(\xi_0,-q)}+\frac{1}{(-1)^m A_0^{(2m)}}\sum_{r=0}^{\infty}-\frac{2}{\mu^2}T_{2r}(\xi_0,-q)A_{2r}^{(2m)}e^{-2r\xi_0}\right\}$$
$$-\frac{ce^{\xi_0}}{4}\sum_{m=0}^{\infty}\left\{\frac{4\pi\sigma a}{\mu^2 k S_{2m}}+\frac{4}{\mu^2(-1)^m A_0^{(2m)}}\sum_{r=0}^{\infty}T_{2r}(\xi_0,-q)A_{2r}^{(2m)}(-2r)e^{-2r\xi_0}\right\}\left\{\log\left(\frac{ce^{\xi}}{2}\right)-\log\left(\frac{ce^{\xi_0}}{2}\right)\right\}. \tag{3.58}$$

### 3.4.3 Deformation of the elliptical lipid membrane when $\lambda < 0$

In Sec. (3.4.1), the general solution for Eq. (3.36) was derived for the condition $\lambda > 0$. Here, we briefly discuss the procedure for the computation of the analytical solution for the case when $\lambda < 0$, which is mechanically interpreted as induced surface pressure on the lipid membrane. In the case $\lambda < 0$, we have $q > 0$. For Mathieu equations, a change in the sign of the parameter $q$ corresponds to the replacement $\eta$ by $(\frac{\pi}{2}-\eta)$. According to the theory of Mathieu functions [59], the following relation can be found by applying this replacement in the infinite Fourier series corresponding to $ce_{2m}$ and $Ke_{2m}$,

$$\begin{aligned} ce_{2m}(\eta,-q) &= (-1)^m ce_{2m}(\eta-\frac{\pi}{2},q),\\ Ke_{2m}(\eta,-q) &= (-1)^m Ke_{2m}(\xi,q+i\tfrac{\pi}{2}),\\ \alpha_{2m}(q)=\alpha_{2m}(-q),\quad A_{2r}^{(2m)}(-q) &= (-1)^{m+r}A_{2r}^{(2m)}(q). \end{aligned} \tag{3.59}$$

Thus, the solution for Eqs. (3.38$a$) and (3.38$b$) having a positive parameter $q$, can be written as (see Ref. [59] for details)

$$ce_{2m}(\eta,q)=\sum_{r=0}^{\infty}A_{2r}^{(2m)}(q)\cos(2r\eta), \tag{3.60}$$

$$Ke_{2m}(\xi,q)=\frac{1}{A_0^{2m}(q)}\sum_{r=0}^{\infty}(-1)^{r+1}A_{2r}^{(2m)}(q)J_r(v_1)J_r(v_2), \tag{3.61}$$

where $J_r$ represents the Bessel function of order $r$.

The solution of the linearized shape equation with a positive parameter $q > 0$ can now be rewritten using the characteristic number, the Fourier coefficients, the Mathieu functions, and the modified Mathieu functions using the expressions found above.

### 3.4.4 Transition to circular lipid membrane

When the elliptical cylinder tends to a circular cylinder of radius $\rho$, we recover the circular solution of Agrawal and Steigmann [1]. This limiting case (when $e \to 0$) can be obtained with the following simplifications [78]:

$$\begin{gathered} A_{2r}^{(2m)} \to 1/\sqrt{2}(m=r=0), \quad 1(m=r\neq 0) \quad 0(m\neq r) \quad m,r=0,1,2,\ldots \\ \alpha_{2m} \to 4m^2, \quad ce_{2m}(\eta,-q) \to 1/\sqrt{2}(m=0), \quad \cos 2m\theta(m\neq 0) \quad m=0,1,2,\ldots \\ Ke_{2m}(\eta,-q) \to G_{2m}K_{2m}(\mu\rho), \quad Ke'_{2m}(\eta,-q) \to G_{2m}\mu K'_{2m}(\mu\rho), \quad m=0,1,2,\ldots. \end{gathered} \tag{3.62}$$

where $K_{2m}$ is the second-kind modified Bessel function of order $2m$ and $G_{2m}$ is a constant multiplier. The prime ($\prime$) attached to $K$ represents the $\rho$-derivative. Next, by defining the circular radius $\rho = \frac{ce^{\xi}}{2}$ (details in Ref. [35]), then, the circular cylinder solution can be derived from Eq. (3.58) as

$$z(\rho) = \frac{2\sigma\rho_0}{\mu^3 k}\frac{K_0(\mu\rho)}{K'_0(\mu\rho_0)} - \frac{2\sigma\rho_0}{\mu^3 k}\frac{K_0(\mu\rho_0)}{K'_0(\mu\rho_0)} - \frac{2\sigma\rho_0^2}{\mu^2 k}\log(\frac{\rho}{\rho_0}). \tag{3.63}$$

Normalizing the deflection of the lipid membrane $z(\rho)$ by the radius of the circular cylinder $\rho_0$ and substituting $\mu^2 = \frac{2\lambda}{k}$, the above expression can be further reduced to give the solution in Agrawal and Steigmann [1]:

$$z(\rho) = \frac{2\sigma}{\mu^3 k K'_0(\mu\rho_0)}\Big\{K_0(\mu\rho) - K_0(\mu\rho_0)\Big\} - \frac{\sigma\rho_0}{\lambda}\log(\frac{\rho}{\rho_0}). \tag{3.64}$$

It should be noted that the above solution is independent of $\theta$, that is, only the first term in the series Eq. $(3.58)$ is retained.

## 3.5 Examples and results

As noted above, we consider the deformation problem on an unbounded domain of an elliptical lipid membrane subjected to the interaction of the lipid molecules in the membrane with an isotropic solid elliptical cylindrical substrate. In the numerical calculations presented below, $\xi_0$, $a$, $b$, $c$, and $e$ denote the boundary of the substrate, the length of the semi-major axis, the length of the semi-minor axis, the half-focal length and the eccentricity of the substrate ellipse, respectively. We study the evolution of the shape of the membrane in response to the membrane's interaction with the solid elliptical substrate for different values of the eccentricity of the bounding elliptical substrate. It should be noted that in the limiting cases, the elliptical cylinder degenerates to the corresponding circular ($e = 0$) and strip ($e = 1$) cross-sections.

In Figs. (3.3)-(3.5), we show the membrane deformation $z$ in response to the different values of the hydrophobicity $|\sigma/\lambda|$. Furthermore, from the contour plot of the deflection of the membrane shown in Fig. 3.6, we observe that the membrane deformation profile exhibits a "wavy pattern" along the circumferential direction near the contour of the contact region. This "pattern" may be associated with the non-uniform force generated by the elliptic cylinder on the membrane in the corresponding direction. The shape is controlled by the eccentricity of the ellipse. In all of these results, we clearly observe that large values of $|\sigma/\lambda|$ induce a significant depression in the lipid membrane which can be easily verified by noting the direct proportionality of $z$ and its derivatives to $\sigma$ as shown in Eq. (3.58). Further, for a given $e$, comparing the induced depressions in the membrane along the major and minor axes of the ellipse, the latter increase with the values of the hydrophobicity (see Figs. $3.3(b)$, $3.4(b)$ and $3.5(b)$). This also reflects the obvious difference between the ellip-

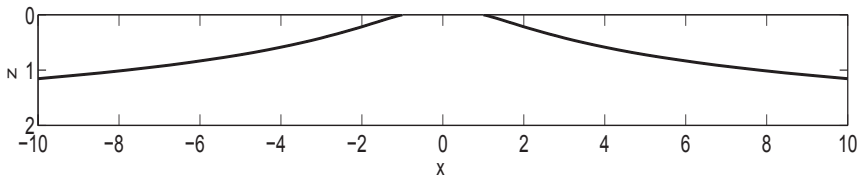


(a)

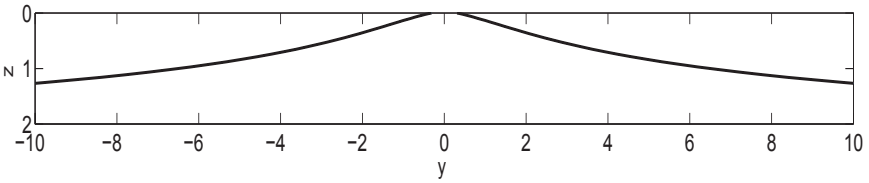


(b)

Fig. 3.3 Deflection of lipid membrane along the (a) major (b) minor axes with ($\gamma = \pi/2$, $e = 0.95$, $\sigma/\lambda = -3$).

tical and circular cylindrical substrates in which the deflection behavior of the membrane resulting from elliptical substrate interaction can be expressed in terms of elliptical coordinate arguments $(\xi, \eta)$ and $q^{(\pm)}$, in Eqs. (3.20), (3.38$a$) and (3.38$b$) while in the circular case in only one parameter, $\rho$, in Eq. (3.64).

Finally, when the elliptical cylinder degenerates to the corresponding circular cross-section, the deformation profile of the lipid membrane induced by its interaction with the now circular cylinder substrate coincides with the solution of Agrawal and Steigmann ( [1]). This is shown in Figs. (3.7)-(3.9). While Fig. 3.7 shows the contour plot of the deflection

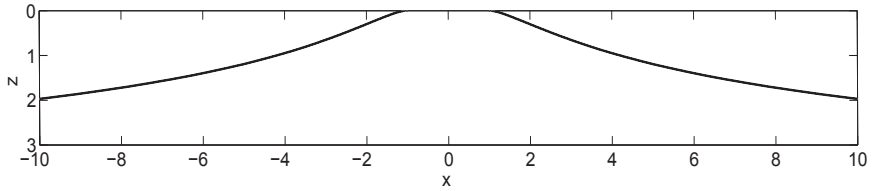


(a)

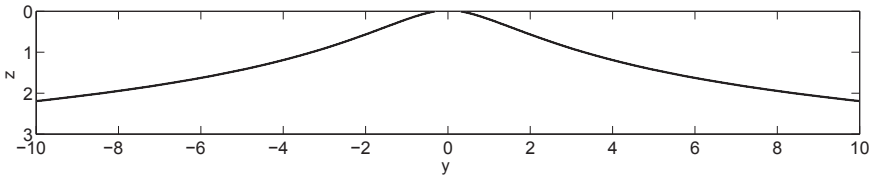


(b)

Fig. 3.4 Deflection of lipid membrane along the (a) major (b) minor axes with ($\gamma = \pi/2$, $e = 0.95$, $\sigma/\lambda = -9$).

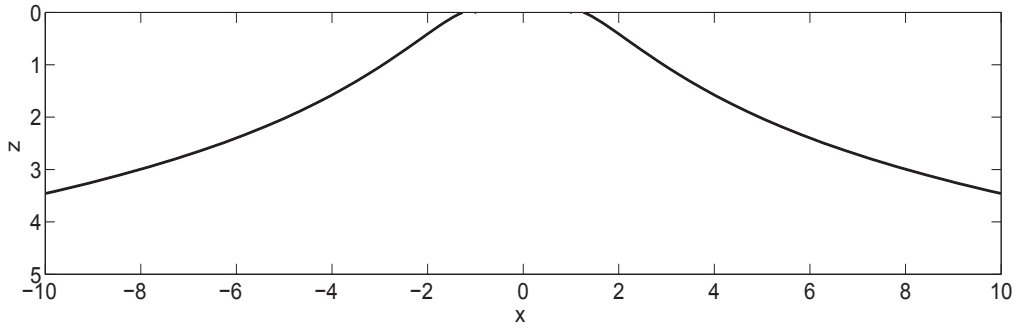


(a)

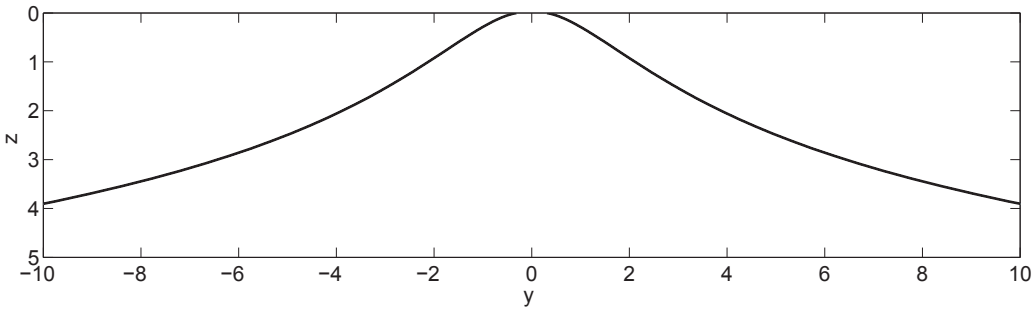


(b)

Fig. 3.5 Deflection of lipid membrane along the (a) major (b) minor axes with ($\gamma = \pi/2$, $e = 0.95$, $\sigma/\lambda = -15$).

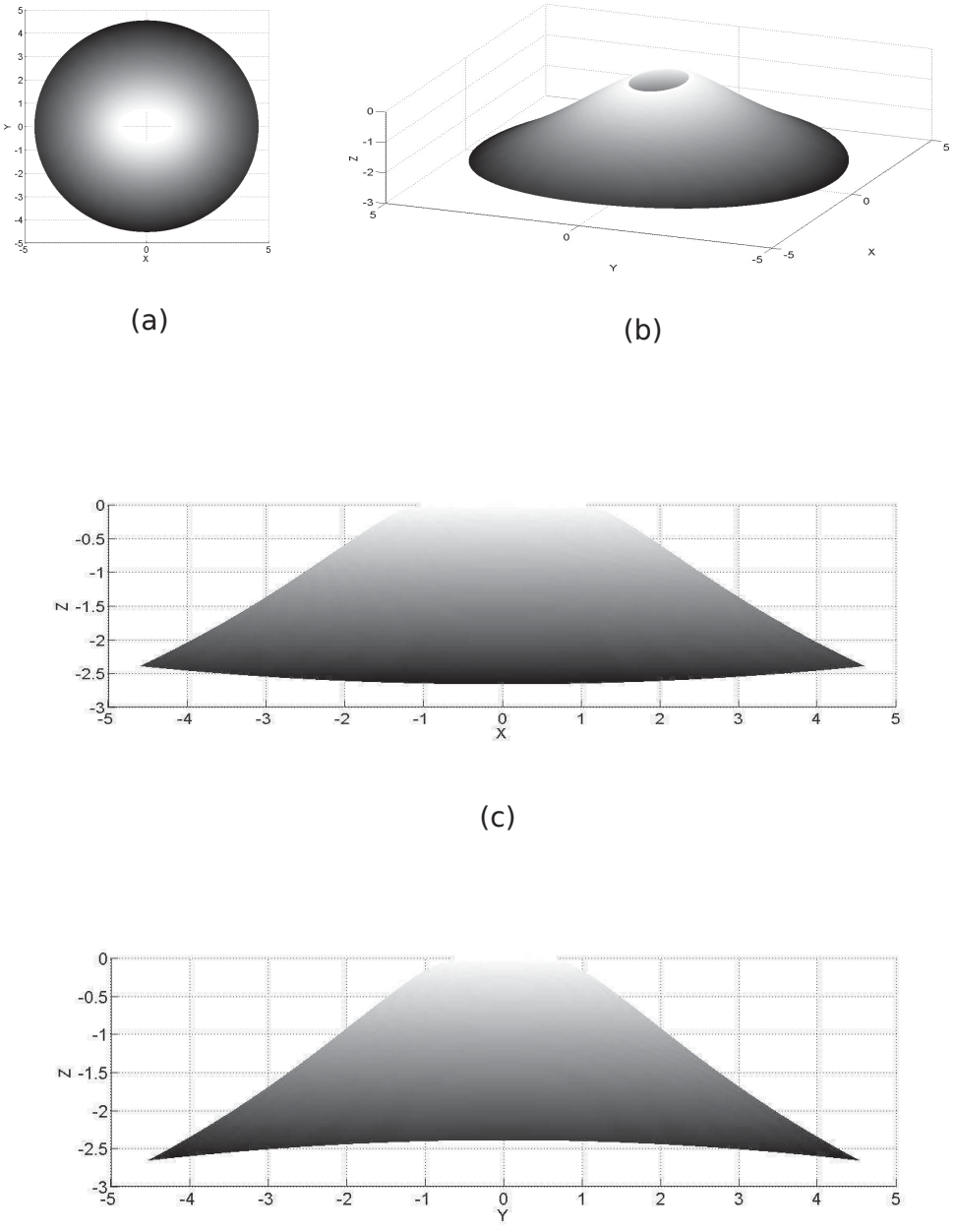


Fig. 3.6 Contour plot of lipid membrane deflection with elliptical substrate ($\gamma = \pi/2$, $e = 0.75$, $\sigma/\lambda = -15$).

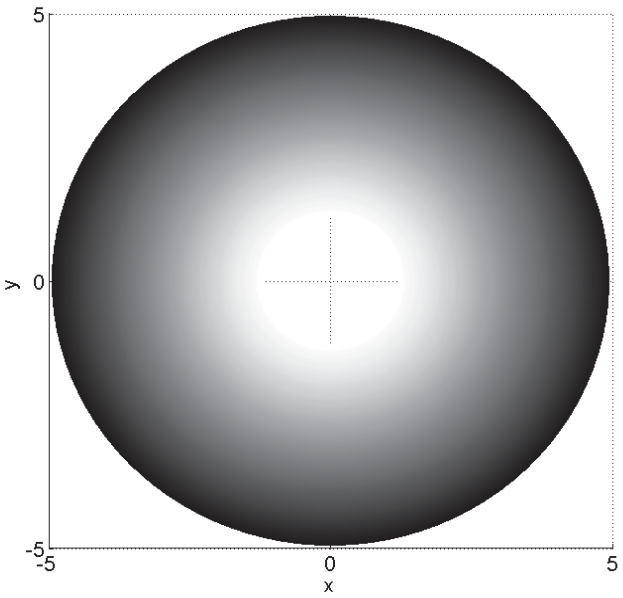


(a)

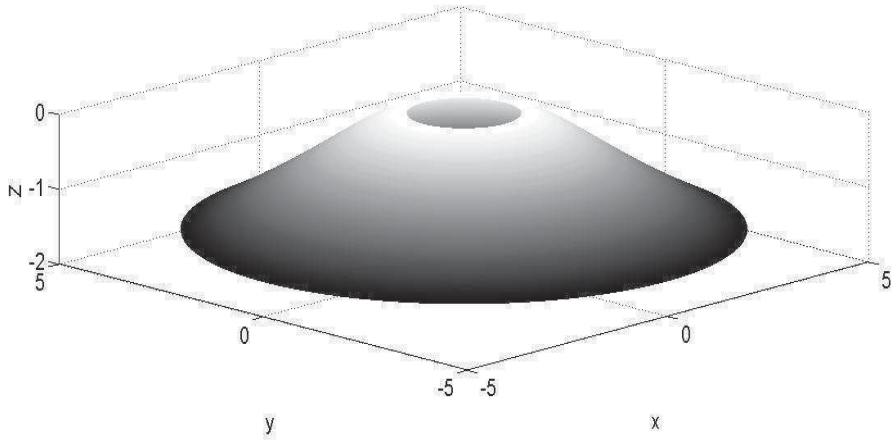


(b)

Fig. 3.7 Contour plot of lipid membrane deflection with circular substrate interaction ($\gamma = \pi/2$, $\sigma/\lambda = -3$).

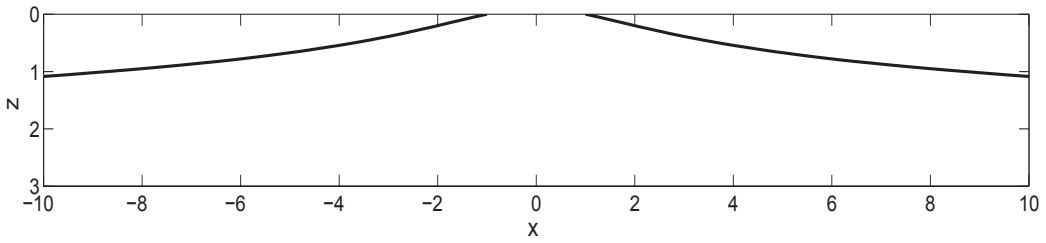


(a)

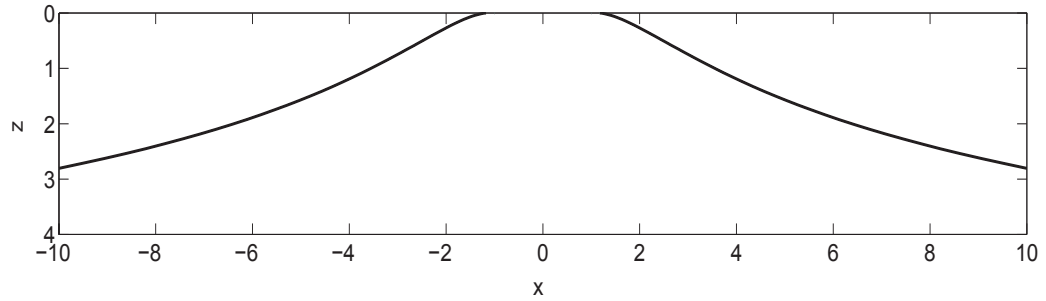


(b)

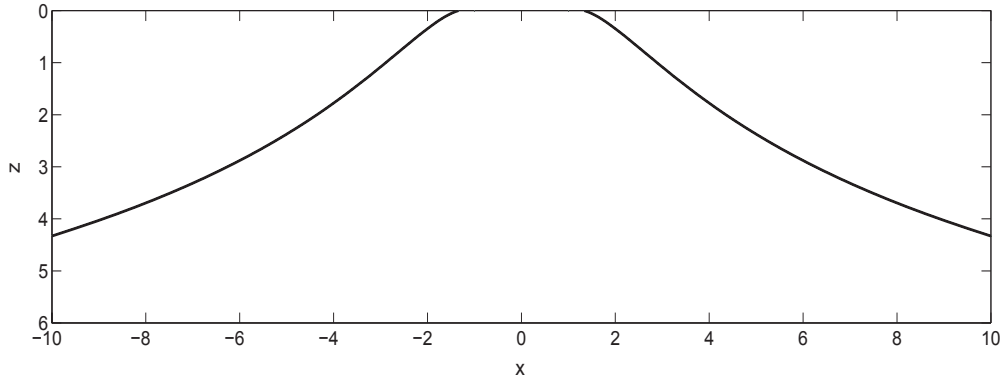


(c)

Fig. 3.8 Linear solution of lipid-membrane circular cylinder substrate interaction ($\gamma = \pi/2$, (a) $\sigma/\lambda = -3$, (b) $\sigma/\lambda = -9$, (c) $\sigma/\lambda = -15$).

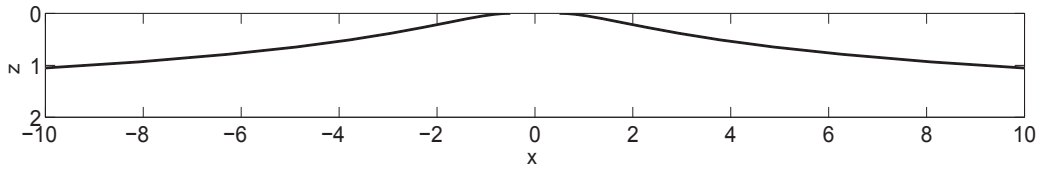


(a)

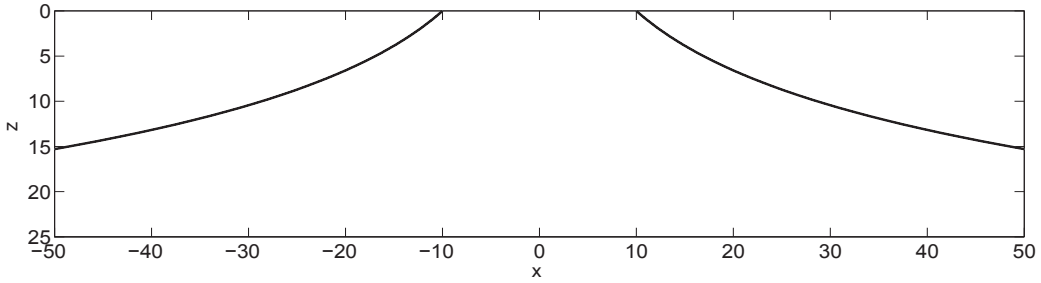


(b)

Fig. 3.9 Effect of substrate cylinder radius with (a) $\mu\rho_0 = 0.05$, (b) $\mu\rho_0 = 10$.

of the membrane, in Fig. 3.8, we show the membrane deformation $z$ in response to the different values of the hydrophobicity $|\sigma/\lambda|$. The circular cylinder generates a vertical load on the membrane and as a result the magnitude of the depressed region on the membrane as well as the non-linear response of the membrane varies with the change of the radius of the cylinder. Figure 3.9, depicts the effect of increasing the radius of the cylinder on the membrane depression at fixed hydrophobicity. These observations make it clear that the solutions obtained here for the film/elliptical substrate interactions generalize, in some sense, the solutions of the corresponding case of a circular lipid membrane interacting with a circular cylinder substrate in which the circular membrane solutions are merely limiting cases of the elliptical membrane solutions. Furthermore, based on the solution for the circular cylinder [1], the linear solution of Eq. $(3.64)$ was found to be valid in the range in which $|\sigma/\lambda|$ is sufficiently small. Consistent with this, we expect that the linear solution for the elliptical substrate is valid for sufficiently small values of $|\sigma/\lambda|$. The verification of this result will form part of a future work on this subject.

## 3.6 Conclusions

We have obtained a semi-analytical solution describing the morphological transitions of lipid membranes when interacting with solid elliptical cylindrical substrates through an elliptical contact region. The deformation mode is characterized by the modified Mathieu functions and performed in the framework of a general curvilinear coordinate system. A linearized version of the shape equation for the corresponding system is obtained via the principle of superposed incremental deformations and is reduced to a single partial differential equation with minimum loss of generality. Hence, a complete semi-analytical solution is obtained which predicts the deformations of lipid membranes as a result of lipid membrane/elliptical substrate interactions. The actual deformation profiles are computed from the infinite series of the eigenfunctions for the desired elliptical domain. A number

of examples which demonstrate the evolution of the membrane shape in response to the film/substrate interaction for various values of hydrophobicity have been presented. In all the examples, it has been found that, larger values of hydrophobicity create a depressed region in the membrane and this intensifies as the value of hydrophobicity increases. Consequently, the significant depression induced in the membrane indicates a dominant non-linear response and thus the linear solution developed for the linearzed shape equation is valid for only sufficiently small values of hydrophobicity. Finally, the results obtained predict "smooth" morphological transitions over the domain of interest and accommodate solutions in Ref. [1] when the magnitudes of the two parameter families coincide.

# Chapter 4

# Bud Formation of Lipid Membranes in Response to the Surface Diffusion of Transmembrane Proteins and Line Tension

*We study the formation of membrane budding in model lipid bilayers with the budding assumed to be driven by means of diffusion of trans-membrane proteins over a composite membrane surface. The theoretical model for the lipid membrane incorporates a modified Helfrich-type formulation as a special case. In addition, a spontaneous curvature is introduced into the model in order to accommodate the effect of the non-uniformly distributed proteins in the bending response of the membrane. Furthermore, we discuss the effects of line tension on the budding of the membrane, and the necessary adjustments to the boundary conditions. The resulting shape equation is solved numerically for the parametric representation of the surface which has one to one correspondence to the membrane surface in consideration. Our numerical results successfully predict the vesicle formation phenomenon on a flat lipid membrane surface, since the present analysis is not restricted to the conventional Monge representation often adopted to the problems of these kind for the obvious computational simplicity, despite it's limited capability on describing the deformed configuration of membranes. In addition, we show that line tension at the interface of the protein concentrated domain makes a significant contribution to the bud formation of membranes.*

## 4.1 Introduction

Lipid bilayer membranes are negligibly thin (typically 5-10nm) but represent a critically important interface within biological cells mediating all interactions between cells and their surrounding environment through the involvement of a variety of proteins [33]. These pro-

teins can aggregate into clusters or domains on the membrane surface. In particular, so-called "trans-membrane proteins" domain, which, for example, covers more than 30% of the plasma membrane, the inner mitochondrial membrane and other membranes such as synaptic vesicles [67, 82], can induce local curvature [104] and hence assist morphological aspects of cellular processes such as fission, fusion and budding [10, 15, 53, 71] regulated by membrane forces. Specifically, membrane budding, which manifests as spherical protrusions emerging out of a flat or curved bilayer membrane, is one particular phenomenon and is an important step in cellular vesicular transport such as exocytosis and endocytosis processes [50, 75]. This intracellular vesicle transport is promoted by vesicle transport proteins, which are required to move molecules between cellular organelles. Another typical example concerns the many viruses which can cause diseases such as AIDS, H1N1 influenza and Lassa fever. These are membrane enveloped and escape from still living host cells by membrane budding events [44, 79]. In the above cellular activities, the topology change (budding) involves novel mechanisms, but the development of proper medicine for some of the diseases caused by these viruses has proved challenging, in part because of the poor understanding of the mechanics of the bud formation process. Therefore, it is critically important to understand the physical mechanisms for the above shape transformation, and consequently several studies have been made on the mechanics and influence of membrane proteins on membrane bud formation ( e.g., see Refs. [42, 72, 79, 3, 26, 60] and the references therein). These studies are mostly confined to the context of curvature changes ascribed to changes in protein distribution on the membrane, although the full understanding of the mechanics still remains challenging. For example, some of the proposed mechanisms which explain the way proteins induce high curvature in biological membranes and bud formation are: high concentration of proteins locally can drive membrane curvature by a crowding mechanism [89]; intrinsically curved proteins which have a high affinity for membranes such as BAR domain [66] and dynamin [97] may wrap around the membrane to

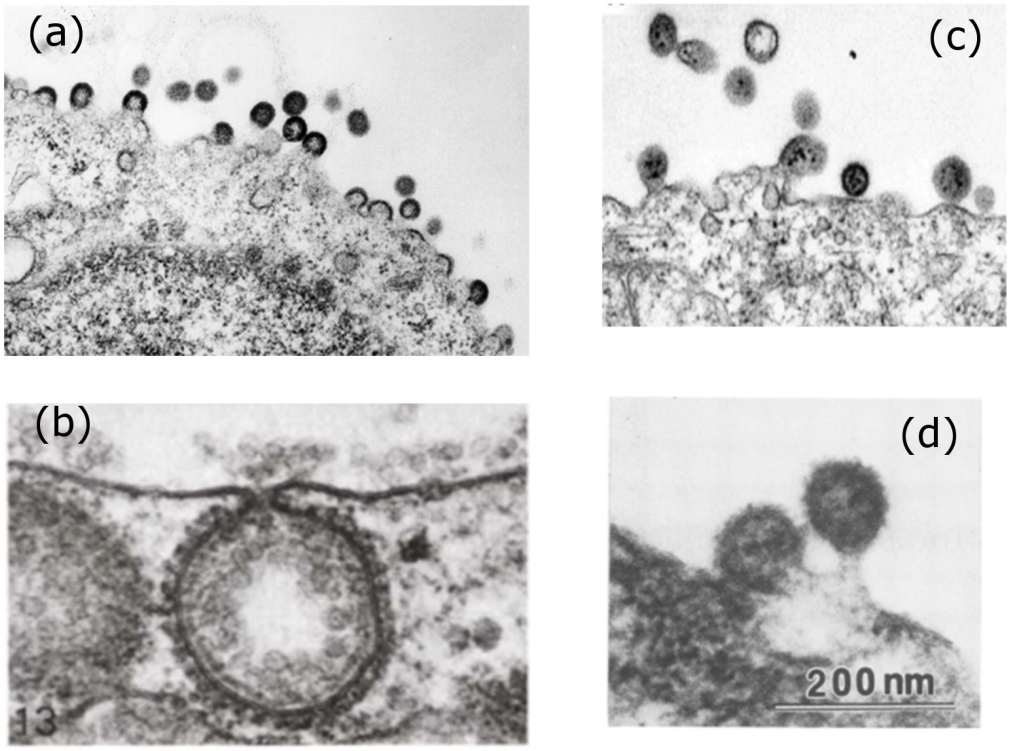


Fig. 4.1 (**a**) HIV-1 Gag assembling into capsids and budding from the plasma membrane. Transmission electron micrograph, (The Lingappa Lab & The Fred Hutchinson Cancer Research EM facility, 2006), (**b**) Clathrin-coated vesicle prior to fission, observed by [65] (1979, reproduced by permission of the Company of Biologists), (**c**) Electron micrographs of arenavirus particles emerging from an infected cell (*Picture taken from: Schley, D., et. al., 2013*) and (**d**) Electron micrographs of virions budding from the surface a human embryonic lung cell. (*Picture taken from: Grimwood, B.G., 1985*).

form buds and triggering of membrane bending by conformational change, causing part of a protein such as Sarlp [51] and Epsin [12] to be inserted like a wedge in the membrane and consequently causing the membrane to form vesicle budding in response. Some examples for membrane bud formation are shown in Figure 4.1.

The work described here is motivated by the approach in [3] to consider the use of surface diffusion of trans-membrane proteins on the membrane as one possible driving mechanism for membrane budding. Diffusion of membrane proteins is considered an important step in the assembly of macromolecular structures on a membrane surface, which lead to the shape transformation of the membrane, including viral buds, endocytic pits and cell-to-cell

junction [48]. Hence, determining/identifying the forces and energies involved in the bud formation induced by the diffusion of trans-membrane proteins is a key step towards the understanding of the mechanics of bud formation by this mechanism. In this context, several studies have indicated that the interactions of intermembrane proteins provide necessary mechanical forces to regulate the membrane′s morphological transitions and the induced morphological profiles are also dependent on the mechanical responses of lipid bilayers. In fact, most protein-induced deformations of lipid membranes can be examined through the "compatible deformations" assimilated by resultant tensions, bending moments and intra-bilayer pressures on the boundaries and/or some parts of lipid membranes. Relevant developments and reviews can be found in Refs. [1, 3, 10, 41, 90, 91, 94] and the references therein. In addition, another example of membrane energy such as line tension (interfacial energy), which arises locally at the interface between the protein concentration domain and the bulk lipid boundary due to the difference in bending modulus and thickness of the heterogeneous membrane, can physically determine or influence the distribution of proteins [28] as well as the formation of bud [55] on the membrane. Thus, line tension, which is suppressed in [3], can have a non-negligible effect on the formation of membrane budding, and is considered to persist in the geometrically nonlinear limit considered in [3]. Therefore, this work also will examine the potential role of line tension in orchestrating membrane shape transformation (bud formation). In other words, we hypothesize that bud formation is related to the line tension at the boundary of protein domain and surrounding bulk lipid of the membrane. Furthermore, we assume that the bud formation occurs on a relatively much slower time scale than the fission of the bud, and therefore we don't model the dynamics of the pinching off of the bud. In other words, we model the stage from nucleation to bud formation prior to pinching off.

In the present study, the mechanical response and associated morphological transitions of membranes is described based on a continuum model which incorporates a modified local

form of the Helfrich energy-type formulation [37]. This modification is taken into account to reflect the effect of protein diffusion on the membrane local curvature change. In addition, a spontaneous curvature is introduced into the model in order to accommodate the effect of the non-uniformly distributed proteins in the bending response of the membrane. However, the resulting shape equation is highly nonlinear, and the corresponding analysis most often involves heavy numerical treatments. In addition, in most cases, the derived equilibrium shape equations are solved based on linear geometric approximations in the Monge representation of the membrane surfaces, and this is limited in scope to small deviations of the membrane shape from a plane [52, 72]. In the present work, the description of the shape equation is based on a parametric representation of the surface (not limited within the Monge representation) and hence applicable for general membrane geometries.

Boundary conditions are central to the modelling of functions of lipid membranes interacting with biological structures such as transmembrane proteins [42]. Here, the need is even more pressing, since line tension is induced by local interactions at the boundaries between the proteins domain and the surrounding bulk lipids at phase interface. For this reason, we extend the work described in [3] to obtain the appropriate set of boundary conditions in the presence of line tension and study its influence on the formation of bud on the membrane.

In this chapter, Sections 4.2 and 4.3 introduce a summary of the formulation of the problem which includes a brief review of the geometry and kinematics of the membrane surface, description of the generalized equilibrium-shape equation of the lipid membrane and the corresponding boundary conditions. These matters are addressed in detail elsewhere [1, 3, 41]. Vesicle formation of the membrane is possible when the membrane is subjected to the tension field together with the internal pressure. However, we mention here that this is not the only case. Boundary interactions and local membrane bending in certain directions together with other intercellular activities may also result in vesicle formation [69]. Section

4.4 presents the membrane surface representation, numerical solutions and a discussion of the results with examples. Finally, Section 4.5 summarizes our conclusions.

## 4.2 Problem formulation

### 4.2.1 Energy functional

The present model is an extension of that discussed in [3] for lipid membranes with diffusion of trans-membrane proteins domain on the membrane surface and the line tension $\gamma$ of the domain edge. The constitutive response and associated shape transformation of the lipid membrane induced by a diffusion of proteins which has an areal concentration of proteins, $\sigma(\theta^{\alpha},t)$, on the membrane surface can be described by the deformation and geometry of the membrane. In this work, we study a non-uniform bilayer membrane in which the areal energy density for the lipid membrane is a natural extension of the Helfrich energy [37] and is necessarily assumed of the form

$$W(H,K,\sigma;\theta^{\alpha}) = \eta(\sigma)+k(\sigma)[H-C(\sigma)]^2+\bar{k}(\sigma)K. \tag{4.1}$$

Here, and in what follows, Greek indices take the value 1,2 and we sum over repeated indices. The parameters $k(\sigma)$ and $\bar{k}(\sigma)$ are bending rigidities which pertain to lipid membranes with non-uniform properties. In the above, $\eta(\sigma)$ is the energy contribution associated with bending deformation induced from protein density $\sigma$, $H$ is the mean curvature of the membrane surface $\omega$ and $K$ is the Gaussian curvature. These curvatures are defined by

$$H=\frac{1}{2}(\kappa_{\upsilon}+\kappa_t), \quad K=\kappa_{\upsilon}\kappa_t-\tau^2, \tag{4.2}$$

where $\upsilon$ and $t=\mathbf{n}\times\upsilon$ correspond to the exterior unit normal and unit tangent to a smooth surface boundary $\partial\omega$, respectively; $\kappa_{\upsilon}$ and $\kappa_t$ are the normal curvatures on these axes and

$\tau$ is the twist. The unit vector field $\mathbf{n} = (\mathbf{a}_1 \times \mathbf{a}_2)/|\mathbf{a}_1 \times \mathbf{a}_2|$ is the local surface orientation. Here, $(\mathbf{a}_\alpha = \mathbf{r}_{,\alpha})$, are the tangent vectors to $\omega$ induced by the parametrization $\mathbf{r}(\theta^\alpha)$, the position in $\mathbb{R}^3$ of a point on the membrane surface with coordinates $\theta^\alpha$. The surface metric tensor is also defined by $(a_{\alpha\beta} = \mathbf{a}_\alpha \cdot \mathbf{a}_\beta)$. The local curvature of the membrane by the surface-tensor field is $(\mathbf{b} = b_{\alpha\beta}\mathbf{a}^\alpha \otimes \mathbf{a}^\beta)$, where $(b_{\alpha\beta} = \mathbf{n} \cdot \mathbf{r}_{,\alpha\beta} = -\mathbf{a}_\alpha \cdot \mathbf{n}_{,\beta})$ are the symmetric coefficients of the second fundamental form on $\omega$. The contravariant cofactor of the curvature is given by [90]

$$\tilde{b}^{\alpha\beta} = 2Ha^{\alpha\beta} - b^{\alpha\beta}, \tag{4.3}$$

where $(a^{\alpha\beta})$ is the matrix of dual metric components (i.e, the contravariant components of the surface metric tensor), the inverse of the metric $(a_{\alpha\beta})$; and $(b^{\alpha\beta})$ is also the inverse of $(b_{\alpha\beta})$. Furthermore, the local curvature of the membrane can be described in terms of the orthonormal vectors $(\upsilon, t)$ in the tangent plane as [3]

$$\mathbf{b} = \kappa_\upsilon \upsilon \otimes \upsilon + \kappa_t t \otimes t + \tau(\upsilon \otimes t + t \otimes \upsilon). \tag{4.4}$$

In equation (4.1), the spontaneous curvature $C(\sigma)$ is introduced in order to accommodate the effect of non-uniformly distributed proteins which interact with the lipid bilayer to generate a distribution of spontaneous curvature fields. Local hydrophobic lipid-protein interactions can promote a specific local curvature in lipid bilayers, and this curvature depends on protein geometry and density [10, 42]. The shape of transmembrane proteins can be analogized to a cone, a cylinder or an inverted cone, with its axis of revolution directed along the surface normal $\mathbf{n}$. To quantify the distribution of the spontaneous curvature induced by the diffusion of proteins, we consider a hypothesized spontaneous curvature proportional to protein density, consistent with the viewpoint presented in [3]. A simple

proposal for the distribution of the spontaneous curvature which ensures bilayer symmetry in the absence of proteins is

$$C(\sigma) = (\mu\varphi)\sigma, \tag{4.5}$$

where $(\mu\varphi)$ is a constant of proportionality. Here, $\mu$ is a positive constant and $\varphi$ is the angle made by the meridian of the cone with $\mathbf{n}$.

As mentioned earlier, we consider the possibility that the diffusion of transmembrane proteins on the membrane surface promote membrane bending and subsequently formation of a bud as the area covered by the protein increases with time. We also hypothesize that bud formation is related to the line tension at the boundary of the protein concentration domain and the surrounding bulk lipid of the membrane. This means that bud formation can be analyzed as an interplay between bilayer bending energies and the domain line tension. Thus, if $\gamma$ is the line tension energy per unit length, the total energy of the lipid membrane may be expressed as

$$E = \int_{\omega} W(H,K,\sigma;\theta^{\alpha})da + \int_{\partial\omega} \gamma ds, \tag{4.6}$$

where *ds* is the length element along the boundary curve.

To accommodate the constraint of bulk area incompressibility, an augmented energy functional is considered

$$E^{*} = \int_{\Omega} [JW(H,K,\sigma;\theta^{\alpha}) - \lambda(J-1)]dA + \int_{\partial\Omega} \gamma ds, \tag{4.7}$$

where $\lambda(\theta^{\alpha})$ is a Lagrange multiplier field [1, 3, 41] associated with the incompressiblity constraint, and $J$ is the local areal stretch induced by the map from a fixed reference surface $\Omega$ to the current surface configuration $\omega$.

### 4.2.2 Convected coordinates

In order to ease the formulation of balance laws, we apply the convected coordinate ($\xi^\alpha$) technique to parametrize the material manifold. A material point on the membrane may be labeled by a convected coordinate system $\mathbf{x}(\xi^\alpha)$. Initially, at time $t_0$, these may be distinctly identified with the coordinate $\theta^\alpha$. The associated surface $\Omega$, with parametric representation $\mathbf{x}(\xi^\alpha) = \mathbf{r}(\xi^\alpha, t_0)$, may serve as a reference configuration of the material body in a Lagrangian description of the motion. This configuration represents the membrane surface at a fixed instant $t_0$. This same material points may peruse a spatial trajectory in time in which their current position at time $t$ is defined by the convected coordinate system using the parametrization, via a map $\mathbf{r}(\xi^\alpha) = \mathbf{r}(\xi^\alpha, t)$. This functional relation gives the current position at time $t$ of a particular material point that originally occupied the position $\mathbf{x}(\xi^\alpha) \in \Omega$ at time $t_0$. The connection with the $\theta^\alpha$ parametrization of $\omega$ is provided by [4, 83]

$$\hat{\mathbf{r}}(\xi^\alpha, t) = \mathbf{r}(\theta^\alpha(\xi^\beta, t), t) \tag{4.8}$$

Thus, we specify the fixed surface coordinates $\theta^\alpha$ as functions of $\xi^\alpha$ and $t$ subject to the initial condition, and such a coordinate can be written generally as $\theta^\alpha(\xi^\beta, t_0) = \xi^\alpha$. We note that once it is specified, any function, $f(\theta^\alpha, t)$, say, may be expressed in terms of convected coordinates as $f(\xi^\alpha, t)$, where

$$\hat{f}(\xi^\alpha, t) = f(\theta^\alpha(\xi^\beta, t), t). \tag{4.9}$$

The partial time derivative of a function defined on a surface given in the convected parametrization is $\dot{f} = \partial \hat{f}(\xi^\alpha, t)/\partial t$, whereas that in the fixed-coordinate parametrization is $f_t = \partial f(\theta^\alpha, t)/\partial t$. The two are related by $\dot{f} = f_t + (\theta^\alpha)^{\cdot} f_{,\alpha}$.

The velocity vector of the convected material point in the current configuration $\omega$ may thus be defined as $\mathbf{u} = \dot{\mathbf{r}} = \partial \hat{\mathbf{r}}/\partial t$. Furthermore, this velocity may be written terms of

components on the natural basis as

$$\mathbf{u} = u^{\alpha}\mathbf{a}_{\alpha} + u\mathbf{n}, \tag{4.10}$$

where $u^{\alpha}$ and $u$ are respectively the tangential and normal variations of the position field induced by the fixed-coordinate $(\theta^{\alpha})$ parametrization. This is not the same as the time derivative $\mathbf{r}_t$. By chain rule, the two are related by

$$\mathbf{u} = (\theta^{\alpha})^{\cdot}\mathbf{a}_{\alpha} + u\mathbf{n}. \tag{4.11}$$

Following [3, 4], we adopt the notion of the time derivative of the fixed-coordinate parametrization defined by

$$\frac{d}{dt}\theta^{\alpha}{}_{|\xi^{\alpha}} = u^{\alpha}(\theta^{\beta}, t), \quad \theta^{\alpha}_{|t_0} = \xi^{\alpha}, \tag{4.12}$$

where the subscript refers to the derivative evaluated at a fixed value of the doublet $\{\xi^{\alpha}\}$; i.e., with $t$ fixed in the function $\theta^{\alpha}(\xi^{\beta}, t)$ and is therefore equal to $(\theta^{\alpha})^{\cdot}$. In this connection we note that the normal velocity of the point on the surface in Eq. (4.10) is given by

$$u\mathbf{n} = \mathbf{r}_t, \tag{4.13}$$

and the convected and fixed-coordinate time derivatives satisfy

$$\dot{f} = f_t + u^{\alpha} f_{,\alpha}. \tag{4.14}$$

### 4.2.3 Mass balance

The foregoing relationships facilitate the reduction of global balance laws. For example, if $\sigma$ is the areal density of the transmembrane protein concentration on $\omega$, then the rate of change of the total quantity of $\sigma$ in a part $\pi$ of $\omega$ is

$$\frac{d}{dt}\int_{\pi}\sigma da = \frac{d}{dt}\int_{\Pi}\sigma J dA = \int_{\pi}(\dot{\sigma}+\sigma\dot{J}/J)da \tag{4.15}$$

where $\Pi$ is the part of the fixed surface $\Omega$ that is convected to $\pi$ and $J$ is the local areal dilation of the surface; i.e.,

$$\int_{\pi} da = \int_{\Pi} J dA \quad for\ all \quad \Pi \in \Omega \tag{4.16}$$

To express the right-hand side of Eq. (4.15) in terms of the fixed-coordinate parametrization, we use [94]

$$\dot{J}/J = u^{\alpha}_{;\alpha} - 2Hu \tag{4.17}$$

### 4.2.4 Shape equation and boundary conditions

We note that the equations characterizing membrane equilibrium (or shape equations) and boundary conditions can be obtained by applying variational methods to the total energy functional in Eq. (4.7), which includes contributions from the total line tension energy. Thus, the induced variation of the total energy of the membrane-protein system is

$$\frac{d}{dt}E^{*} = \int_{\omega}[\dot{W}+(W+\lambda)\dot{J}/J+\dot{\lambda}(1-J^{-1})]da + \int_{\partial\omega}\gamma(ds)^{\cdot}, \tag{4.18}$$

where

$$\dot{W} = W_H\dot{H} + W_K\dot{K} + W_\sigma\dot{\sigma}. \tag{4.19}$$

Here, and henceforth, the subscripts $H$, $K$, and $\sigma$ denote partial derivatives with respect to the indicated variables (e.g., $W_H = \frac{\partial W}{\partial H}$ etc...).

To compute the variation of the energy, we use Eq. (4.17) and the explicit formulas for the variational derivative of $H$ and $K$ from Ref. [94]. Thus, following the procedures outlined in [3, 41, 90, 91], the Euler equation which describes the geometry of the membrane

in mechanical equilibrium under a net lateral pressure $p$ in the direction of its orientation $\mathbf{n}$ is obtained as

$$\frac{1}{2}\Delta(W_H) + (W_K)_{;\alpha\beta}\tilde{b}^{\alpha\beta} + W_H(2H^2 - K) + 2H(KW_K - W) - 2\lambda H = p, \tag{4.20}$$

where $\Delta(\cdot) = (\cdot)_{;\alpha\beta}a^{\alpha\beta}$ is the surface Laplacian. The Lagrange multipier $\lambda$ satisfies [3],

$$\nabla\lambda = -W_\sigma \nabla\sigma, \tag{4.21}$$

in which the right hand side of Eq. (4.21) accommodates any non-uniformity in the bending properties of the membranes that may be generated by the constitutive response of the membrane to transmembrane proteins, and $W_\sigma$ is the chemical potential for the diffusing proteins.

In addition, the variation of the energy membrane also yields terms that define boundary forces and moments on a smooth boundary $\partial\omega$ of the membrane, and hence we obtain the following admissible boundary conditions

$$\mathbf{f} = f_\upsilon \upsilon + f_t \tau + f_n \mathbf{n}, \tag{4.22}$$

$$M = \frac{1}{2}W_H + \kappa_t W_K, \tag{4.23}$$

$$f_\upsilon = W + \lambda - \kappa_\upsilon M + c_g\gamma, \tag{4.24}$$

$$f_t = -\tau M, \tag{4.25}$$

$$f_n = (\tau M)' - (\frac{1}{2}W_H)_{,\upsilon} - (W_K)_{,\beta}\tilde{b}^{\alpha\beta}\upsilon_\alpha + c_n\gamma. \tag{4.26}$$

Here, $f_\upsilon$, $f_t$ and $f_n$ are, respectively, the $\upsilon$-,$\mathbf{t}$- and $\mathbf{n}$-components of distributed forces per unit length applied to $\partial\omega$. We also note here that $c_n$ is the normal curvature and $c_g$ is the geodesic curvature. The force applied to the membrane at the $i$th corner of $\partial\omega$ is also

obtained as

$$\mathbf{f_i} = W_K[\tau]_i n, \tag{4.27}$$

where,

$$\tau = b^{\alpha\beta}\tau_\alpha \upsilon_\beta, \tag{4.28}$$

is the twist of the membrane surface $\omega$ on the $(\upsilon, \mathbf{t})$- axes with ($\upsilon_\alpha = \mathbf{a}_\alpha \cdot \upsilon$ and $\tau_\beta = \mathbf{a}_\beta \cdot \mathbf{t}$), and

$$\kappa_\upsilon = b^{\alpha\beta}\upsilon_\alpha \upsilon_\beta, \quad \kappa_t = b^{\alpha\beta}\tau_\alpha \tau_\beta. \tag{4.29}$$

are the normal curvatures of $\omega$ in the directions of $\upsilon$ and $\mathbf{t}$, respectively.

For a bilayer membrane that has no natural orientation, a simple energy function $W$ that satisfies the influence of protein density on the membrane shape, and which also conforms to the conventional theory of bending elasticity in the absence of protein diffusion, is given by [3]

$$W = (\alpha\sigma - \beta)^2 + k[H - C]^2. \tag{4.30}$$

We note that $W$ in Eq. (4.30) corresponds to the restriction of Eq. (4.1) to the case of constant bending moduli ($k > 0$) and $\bar{k}$. The assumption of uniform bending moduli is justifiable for dilute concentration of proteins on the membrane. However, here, we make the assumption primarily to ensure that their effect on the bending stiffness remains negligible. This also allows us to avoid any influence of non-uniformity of the bending moduli on the spontaneous curvature in equation (4.5). In addition, for the sake of simplicity, the term involving $K$ is suppressed in this study.

The shape equation in Eq. (4.20) reduces to

$$k\Delta(H - C) + 2k(H - C)(2H^2 - K) - 2H[(\alpha\sigma - \beta)^2 + k(H - C)^2] - 2\lambda H = p, \tag{4.31}$$

and the Lagrange multiplier is simplified to

$$\nabla\lambda = 2[k\mu\varphi(H-C) - \alpha(\alpha\sigma-\beta)]\nabla\sigma, \tag{4.32}$$

The full set of boundary conditions for the foregoing assumed energy function is

$$M = k(H-C), \tag{4.33}$$

$$f_\upsilon = (\alpha\sigma-\beta)^2 + k[H-C]^2 + \lambda - \kappa_\upsilon M + c_g\gamma, \tag{4.34}$$

$$f_t = -\tau M, \tag{4.35}$$

$$f_n = (\tau M)' - M_{,\upsilon} + c_n\gamma. \tag{4.36}$$

## 4.3 Protein diffusion

Here it is assumed that the transmembrane proteins are continuously distributed over the membrane surface, and the associated areal concentration, $\sigma(\theta^\alpha,t)$, is assumed to evolve in a diffusive manner. Thus, for any simply connected part $\pi$ of the current configuration surface $\omega$, we have

$$\frac{d}{dt}\int_\pi \sigma da = -\int_{\partial\pi} \mathbf{m}\cdot\upsilon ds, \qquad \text{all} \quad \pi\subset\omega, \tag{4.37}$$

where the surface vector $\mathbf{m} = m^\alpha\mathbf{a}_\alpha$ is the protein flux. Here, and in what follows, $\upsilon = \upsilon^\alpha\mathbf{a}_\alpha$ is the exterior unit normal to the edge $\partial\pi$, defined by $\upsilon = t\times\mathbf{n}$, where $t = \mathbf{a}_\alpha(d\theta^\alpha/ds)$ and $\theta^\alpha(s)$ is the arclength parametrization of $\partial\pi$ at time $t$. We assume that there is no transfer of proteins between the membrane and the bulk fluid in which it is immersed.

For an incompressible membrane, we note that the local constraint equations are $J=1$ and $\dot{J}=0$. A diffusive balance law which satisfies this bulk areal incompressiblity constraint

is derived from Eq. (4.37) using a combination of the the transport Eq. (4.15), Stoke's theorem, together with Eq. (4.17) and the local areal constraint. Thus, the normal surface velocity field in Eq. (2.13) and the protein concentration satisfy [3]

$$u^{\alpha}_{;\alpha} = 2Hu \quad \text{and} \quad \sigma_t + u^{\alpha}\sigma_{,\alpha} + m^{\alpha}_{;\alpha} = 0 \quad \text{on} \quad \omega \tag{4.38}$$

where

$$m^{\alpha}_{;\alpha} = (\sqrt{a}m^{\alpha})_{,\alpha}/\sqrt{a} \tag{4.39}$$

in which $a = det(a_{\alpha\beta})$, is the surface divergence of $\mathbf{m}$. In this study, a simple constitutive equation for $\mathbf{m}$ which accommodates classical Fickean diffusion is adopted from the works of [3]

$$\mathbf{m} = -c\nabla(W_{\sigma}), \tag{4.40}$$

where $c$ is a positive constant and $W_{\sigma}$ is the chemical potential for the diffusing proteins. With the assumed energy function in Eq. (4.30), we have

$$W_{\sigma} = 2[\ \alpha(\alpha\sigma - \beta) + k\mu\varphi(C - H)], \tag{4.41}$$

and the protein flux is

$$\mathbf{m} = -2c\{[\ \alpha^2 + k(\mu\varphi)^2]\nabla\sigma - k\mu\varphi\nabla H\}, \tag{4.42}$$

in which $\nabla C = \mu\varphi\nabla\sigma$.

## 4.4 Surface representation and numerical solutions

### 4.4.1 Surfaces of revolution

In our model, budding is assumed to be driven by the change of curvature of the membrane caused by the diffusion of the transmembrane proteins over the composite membrane surface. Thus, the shape of the bud evolves dynamically as the diffusion proceeds. In this model, the intra-membrane viscous flow is not taken into account in the consideration of the evolution of the bud, since the area $a_p(s)$ covered by the diffusion of the transmembrane protein increases with time. Here, as mentioned in the introduction, since we exclude the budding scission process in our study, we impose the criteria in equation $(4.43)$ to halt the membrane surface penetration around the necking region during the bud formation process, with the assumption that the resulting vesicle develops into a spherical-like shape which corresponds to the most stable membrane curvature. The surface area of this sphere is $4\pi R^2$, where $R$ is the radius of the sphere. Imposing the criteria in equation $(4.43)$ also avoids difficulties associated with heavy numerical computational.

Outside the budding region, for the sake of simplicity, the spontaneous curvature of the membrane is assumed to be constant, $C = \mu\varphi\sigma_0$ where $\sigma_0 = \beta/\alpha$ (i.e. in the absence of protein diffusion, the infimum of the energy can be achieved if $\lambda = 0$ and $H = C(\sigma_0)$). Furthermore, this assumption is equally applied to the membrane immediately around the budding region, and so the model is also applicable to a deformed and/or non-uniform membrane.

In order to treat the possible membrane budding transitions, we assume that the diffusion of the protein forms in an axisymmetric region of area $a_p(s)$ and that the bud that forms will also possess axisymmetry (i.e., the budding region maintains a circular boundary on the membrane). Consequently, we seek a simple class of axisymmetric solution in the surface of revolution parametrized by meridional arclength $s$ and azimuthal angle $\theta$. If $a(s)$ is the

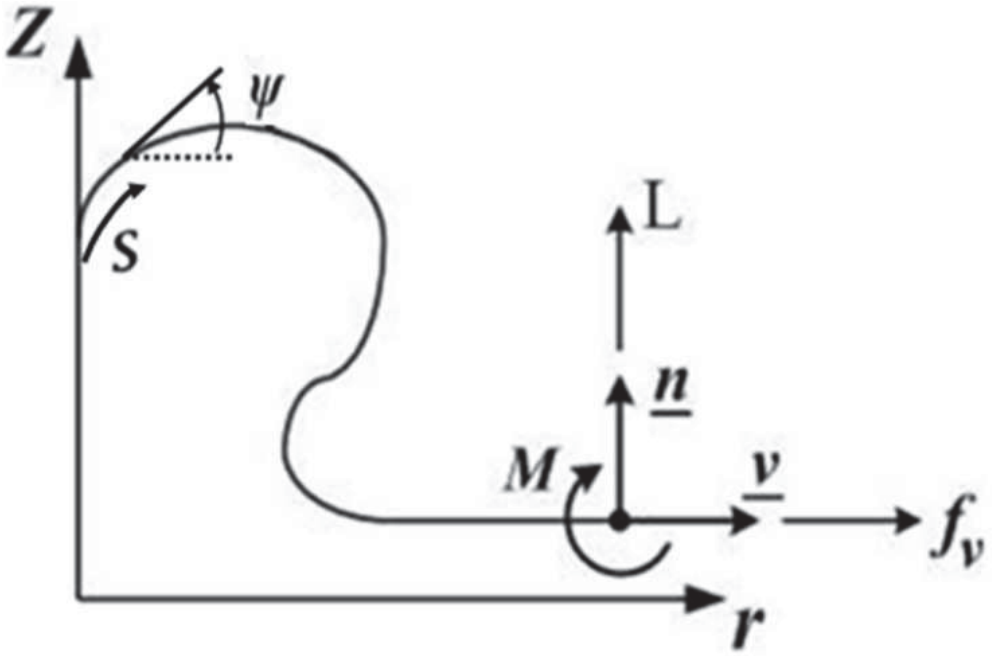


Fig. 4.2 Representation of surface revolution.

area of the membrane within a distance of $s$ of the axis of symmetry, from the assumptions above, we then have that the spontaneous curvature is given by

$$C(s) = \begin{cases} \mu\varphi\sigma & : \quad a(s) \leq a_p(s) \\ \mu\varphi\sigma_0 & : \quad a(s) > a_p(s) \end{cases} \tag{4.43}$$

whereas the Lagrange multiplier is given by

$$\nabla\lambda = \begin{cases} 2[k\mu\varphi(H-C) - \alpha(\alpha\sigma - \beta)]\nabla\sigma & : \quad a(s) \leq a_p(s) \\ 0 & : \quad a(s) > a_p(s) \end{cases} \tag{4.44}$$

Here, we use a cylindrical polar coordinate system $(r, \theta, z)$ to represent a material point in the deformed membrane. Thus, a continuum point on the membrane surface of revolution may be represented as

$$\mathbf{r}(s, \theta, t) = r(s,t)\mathbf{e}_r(\theta) + z(s,t)\mathbf{k}, \tag{4.45}$$

where, $r(s,t)$ is the radial distance of a material point from the axis of symmetry, $z(s,t)$ is the elevation above the base plane, and $\{\mathbf{e}_r, \mathbf{e}_\theta, \mathbf{k}\}$ is the orthonormal basis in the cylindrical polar coordinate system. Since $s$ measures arclength along meridians, we have

$$r'^2 + z'^2 = 1, \tag{4.46}$$

where $(\cdot)' = d(\cdot)/ds$. We choose surface coordinates $\theta^1 = s$ and $\theta^2 = \theta$. The induced tangent vectors are

$$\mathbf{a_1} = r'\mathbf{e}_r + z'\mathbf{k}, \quad \textit{and} \quad \mathbf{a_2} = r\mathbf{e}_\theta, \tag{4.47}$$

and it follows from Eq. (4.46) that there is a local tangent angle $\psi(s)$ relative to a horizontal, flat conformation, such that

$$r' = \cos\psi(s) \quad \textit{and} \quad z' = \sin\psi(s). \tag{4.48}$$

Since $\mathbf{a_1}$ is orthogonal to a parallel of latitude, we identify it with $\upsilon$ Fig. 4.2. Consequently,

$$\upsilon = \cos\psi(s)\mathbf{e}_r + \sin\psi(s)\mathbf{k}, \quad \mathbf{t} = \mathbf{e}_\theta \quad \textit{and} \quad \mathbf{n} = \cos\psi(s)\mathbf{k} - \sin\psi(s)\mathbf{e}_r. \tag{4.49}$$

The metric and dual metric are $a_{\alpha\beta} = diag(1, r^2)$ and $a^{\alpha\beta} = diag(1, r^{-2})$, respectively, and the later can be used to compute

$$\mathbf{a}^1 = \upsilon \quad \textit{and} \quad \mathbf{a}^2 = r^{-1}\mathbf{e}_\theta \tag{4.50}$$

At any given position, the components of curvature of the membrane can be obtained by combining the value of $(b_{\alpha\beta} = diag(\psi', r\sin\psi))$ with Eqs. (4.4) and (4.49) as

$$\kappa_\upsilon = \psi', \quad \kappa_t = r^{-1}\sin\psi(s), \quad \tau = 0, \quad c_g = \cos\psi(s)/r \quad \text{and} \quad c_n = \sin\psi(s)/r. \tag{4.51}$$

In the previous sections, relevant boundary forces and moment (per unit length) acting on the membrane are derived. In this model, we consider that there exists a non-zero traction force $f_\upsilon$ that is the projection onto $\upsilon$ of the force per unit length transmitted across a curve (in this case, particularly, the boundary of the protein concentration domain interface where line tension exists) with unit normal $\upsilon$ and is compressive when diffusion proceeds. Due to the presence of this compressive force, a large bending moment will be generated at the edge arising from the possible high curvature, that must be in a clockwise direction in order to maintain equilibrium. Now, the deformation of the membrane by this compressive force, which in turn is generated by the interaction of the diffusing proteins, may encourage/assist the formation of a growing bud on the membrane surface. It should also be noted that the traction force $f_\upsilon$ is used to relate the line tension energy and the surface tension with the membrane shape. In this regard, for the sake of convenience, we describe the model equations of the membrane in terms of the specified boundary conditions such as bending moment $M$, which is generated by the change in the difference in the mean curvature and the spontaneous curvature, and the traction force $f_\upsilon$. It should also be mentioned that we use the fully coupled systems for diffusion of proteins and membrane shape to obtain the distribution of $\lambda$ in the interior of the membrane, but we specify a uniform value of $\lambda$ at the boundary far from the budding regime of the membrane. If the membrane remains flat under specified boundary conditions, then $\lambda$ affects the diffusion of protein through $(\nabla\lambda = 0)$. Thus, the sum of the normal curvatures is twice the mean curvature $H(s,t)$ and together with the bending moment equation in (4.33), the following differential equation is obtained

$$\psi' = \frac{2M}{k} - \frac{\sin\psi(s)}{r} + 2C. \tag{4.52}$$

The product of the normal curvatures is the Gaussian curvature $K(s,t)$; thus,

$$K = (M/k + C)^2 - (M/k + C - \sin\psi(s)/r). \tag{4.53}$$

The traction force in Eq. (4.34) is expressed by

$$f_\upsilon = (\alpha\sigma - \beta)^2 + M^2/k + \lambda - (\frac{2M}{k} - \frac{\sin\psi(s)}{r} + 2C)M + \gamma\frac{\cos\psi}{r}, \tag{4.54}$$

and the shape equation (4.31), with $P = 0$, simplifies to

$$L' = r\{(F_\upsilon - \gamma\frac{\cos\psi}{r})(\frac{2M}{k} - \frac{\sin\psi}{r} + 2C) + (F_\upsilon - \gamma\frac{\cos\psi}{r})\frac{\sin\psi}{r} + 2M(\frac{M}{k} - \frac{\sin\psi}{r} + C)\frac{\sin\psi}{r}\}, \tag{4.55}$$

where

$$L = \frac{1}{2}r(W_H)' = rM', \tag{4.56}$$

and the Lagrange multiplier $\lambda$ also satisfies [1]

$$\lambda' = 2[\mu\varphi M - \alpha(\alpha\sigma - \beta)]\sigma'. \tag{4.57}$$

The normal and tangential velocities of the surface, which are related by Eq. $(4.38)_1$, is reduced to

$$(rv)' = 2(\frac{M}{k} + C)u, \tag{4.58}$$

where $v(s,t)$ is the velocity component in the direction of the tangent to the meridian; we assume that the velocity in the azimuthal direction vanishes. This furnishes the tangential velocity gradient and thus may be used to estimate the error incurred by neglecting intramembrane viscosity.

The protein flux in Eq. (4.42) becomes

$$m = -c(W_\sigma)' = 2c[\mu\varphi M' - \alpha^2\sigma'], \tag{4.59}$$

where $m = \mathbf{m}\cdot\upsilon$ is the component of the flux $m$ in the direction tangent to the meridian; the azimuthal component of this vector also vanishes. Finally the diffusive balance law $(4.32)_2$

reduces to

$$\sigma_t + v\sigma' = \frac{2c}{r}\{r[\alpha^2\sigma' - \mu\varphi M']\}', \tag{4.60}$$

In order to maintain control over the domain over which the transmembrane proteins interact with the membrane and on which the preceding differential equation is to be solved, the surface area enclosed by the sector $(0,s)$ is specified by the following relation as

$$a' = 2\pi r, \tag{4.61}$$

in which a global constraint on the area of the current surface is enforced by applying the local constraint, $\dot{J} = 0$.

In addition, we non-dimensionlized lengths using the assumed radius of curvature of $R$ of the budding regime, whereas force and moment variables are scaled by the membrane bending rigidity $k$. Thus we define,

$$\begin{gathered}
\bar{s} = s/R, \quad \bar{r} = r/R, \quad \bar{z} = z/R, \quad \bar{H} = RH, \quad \bar{C} = RC, \quad \bar{a} = a/R^2, \quad \bar{\mu} = \mu/R, \\
\bar{u} = u\hat{\tau}/R, \quad \bar{v} = v\hat{\tau}/R, \quad \bar{\sigma} = R^2\sigma, \quad \bar{t} = t/\hat{\tau}, \quad \bar{\alpha} = \alpha/(R\sqrt{k}), \quad \bar{\beta} = \beta R/\sqrt{k}, \\
\bar{L} = RL/k, \quad \bar{\lambda} = R^2\lambda/k, \quad \bar{M} = RM/k, \quad \bar{F}_\upsilon = R^2F_\upsilon/k, \quad \bar{F}_n = R^2F_n/k, \\
\bar{\gamma} = R\gamma/k,
\end{gathered} \tag{4.62}$$

where $\hat{\tau} = (ck)^{-1}$ is used as a measure of time scale from a dimensional analysis of the balance law [3]. For the sake of brevity, we don't list the associated systems of dimensionless equations.

### 4.4.2 Boundary conditions

In the following, we denote the cross-sectional curve at the boundary between the protein concentration domain and the surrounding bulk lipids by $\Gamma$ (assumed circular). The non-

dimensionalized form of the nonlinear equations $(4.48)_1$, $(4.48)_2$, (4.52), (4.55)-(4.57) and (4.61) are solved between $\bar{s} = 0$ at the center of the axis of symmetry of the bud and $\bar{s} = \bar{s}_{max}$ which is an unknown arclength yet to be determined as part of the solution. However, in the numerical simulation we specify $\bar{s}_{max}$ a sufficiently large length from the center of the bud in order to model an isolated bud on an unbounded domain. Symmetry dictates that the shear force vanishes at the pole where $\bar{s} = 0$, and at far end of the cross-section of the membrane where $\bar{s} = \bar{s}_{max}$ i.e.,

$$L(\bar{s} = 0) = 0 \quad \text{and} \quad \bar{L}(\bar{s} = \bar{s}_{max}) = 0. \tag{4.63}$$

The slope is zero at both ends of the cross-section of the membrane, i.e.,

$$\psi(\bar{s} = 0) = 0 \quad \text{and} \quad \psi(\bar{s} = \bar{s}_{max}) = 0. \tag{4.64}$$

Also, at these ends, we have

$$\bar{r}(\bar{s} = 0) = 0 \quad \text{and} \quad \bar{z}(\bar{s} = \bar{s}_{max}) = 0. \tag{4.65}$$

The equations are solved on a flat circular membrane with radius $\rho$. Thus, since there is no area enclosed at $\bar{s} = 0$, and the total area of the membrane is fixed to be $\pi\rho^2$, we have the following additional conditions at the two ends of the cross-section of the membrane

$$\bar{a}(\bar{s} = 0) = 0 \quad \text{and} \quad \bar{a}(\bar{s} = \bar{s}_{max}) = \pi\rho^2. \tag{4.66}$$

Equation (4.55) involves the traction force $f_\upsilon$, which relates the line tension and membrane surface tension $\lambda$ to the membrane shape at the boundary. Thus, we choose and specify a suitable value for $f_\upsilon$ based on the condition given by Eq. (4.54) at $\Gamma$. Further-

more, at the interface $\Gamma$, two additional boundary conditions which must be satisfied are the continuity of $\bar{r}(\bar{s})$ and $\psi(\bar{s})$ at the boundary.

Note that $\lambda$ is nonlinear function of the protein density (see Eq. 4.57). If there is no diffusion of proteins on the membrane, then the inhomogeneity in the value of the local tension $\lambda$ is insignificant. In the region where there is no protein diffusion $\partial\bar{\sigma}/\partial\bar{s}$ goes to zero, and $\lambda$ may be given by a constant value at the boundary, say $\lambda_0$. At the boundary of the protein concentration domain where line tension exists, the actual mean curvature is less than the spontaneous curvature and hence ($M \neq 0$). Also, ($\partial\bar{\sigma}/\partial\bar{s} \neq 0$). This implies that the gradient in the tension $\lambda$ is not zero (using Eq. (4.32)). However, the value of $\lambda$ is equal to the tension outside the budding region plus the jump in tension at the boundary immediately near the budding regime, thereby making the change in tension an effect confined to the budding region.

It is also a possibility that a jump in bending rigidities exist at the boundary between the membrane covered with protein by the diffusion and the surround bulk lipid. In this case the ratio of the bending rigidities in the budding region (covered with dilute concentration of proteins) and near or far away from the budding regime may fix the ratio of the radii away from the interface and of the surface tensions in the two regions. We assume this bending rigidities ratio to be unity. In other words, we assume the bending rigidities of the membrane to be uniform. Note that, for convenience, we also suppress the jump in Gaussian rigidity of the membrane.

Finally, the equations are solved by specifying zero initial value for the protein density at every mesh point in the membrane except at the boundary which we impose a value $\bar{\sigma} = \bar{\sigma}_\Gamma$ in order to expose the membrane to a protein bath and no protein flux ($m$) is assumed at $\Gamma$.

### 4.4.3 Numerical solutions in the budding region and examples

This highly nonlinear coupled two-point boundary value problem, with boundary conditions Eqs. (4.63) - (4.66) is solved using the Matlab boundary value problem solver routine *bvp4c* [85]. The equations were solved on a weakly curved or nearly flat circular domain of radius $\rho = 10$ with $\bar{\alpha} = 1.5$, $\bar{\beta} = 0.75$, $\bar{\mu}\varphi = -\pi$, $\bar{\tau} = 1$ and $\Delta\bar{t} = 0.001$ [3]. It should be noted that there is a singularity at $\bar{s} = 0$. To mitigate this problem, we sought an asymptotic solution near $\bar{s} = 0$ and solved the boundary value problem at $\bar{s} = \delta \ll 1$ and $\bar{s} = \bar{s}_{\max} \gg 1$. Near the origin, $\delta = 0.0001$ gives sufficiently accurate results. The boundary at the far end of the membrane from the axis of symmetry is applied at a large value of $\bar{s} = \bar{s}_{\max}$; $\bar{s}_{\max} \geq 10$ effectively models an unbounded domain or, in other words, an isolated bud sufficiently removed from its neighbors such that the effect of interaction may be ignored. This also provides more than sufficient for far-field behavior to become clear.

The equations are solved by specifying a protein distribution function defined by $\bar{\sigma} = \exp\tilde{\sigma}$ at an initial time $\bar{t} = 0$. This distribution ensures that the numerical solutions yield positive values of the protein density. In addition, the initial surface velocity (both normal and tangential) is assigned zero values at $\bar{t} = 0$. Then, we integrate numerically equations (4.48), (4.52),(4.55)-(4.57) and (4.61) using Matlab routine (*bvp4c*) in order to obtain the initial membrane shape at $\bar{t} = 0$. Next, taking a suitable time step $\Delta\bar{t}$, we use the forward Euler approximation scheme to compute the distribution of the protein density in equation (4.60) and the corresponding membrane shape at this time step is calculated by integrating equations (4.48), (4.52),(4.55)-(4.57) and (4.61) as before. Now, with the time derivative $\mathbf{r}_t$ in (4.13) known at time zero and $\Delta\bar{t}$, we form a backward Euler approximation at each mesh point to compute the normal velocity $u = \mathbf{n}\cdot\mathbf{r}_t$, in which surface normal is evaluated at the initial instant. This normal surface velocity is used to integrate (4.58) for the tangential velocity field at time $\Delta\bar{t}$, assuming the tangential velocity at $\bar{s} = 0$ to vanish, and with the mean curvature equal to the initial distribution. As a result, this tangential velocity is then

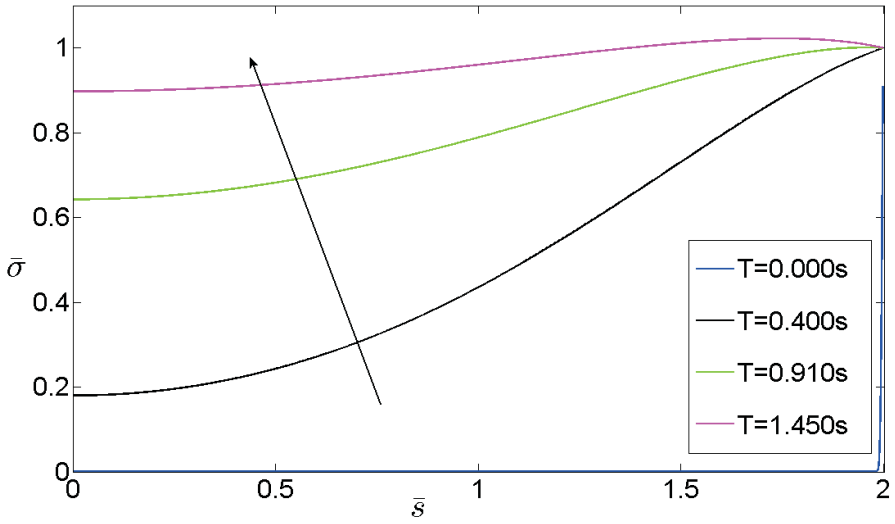


Fig. 4.3 Spatial distribution of protein concentration on the membrane surface. Arrow pointing upwards indicates an increase of diffusion time for the proteins.

used with (4.60) to evaluate the time derivative of the protein density at $\Delta\bar{t}$, in a similar manner as before by forward Euler integration scheme. The procedure is repeated for a specified time interval or until an equilibrium state is reached.

During budding, the first stage is initiation of the bud by the diffusion of the transmembrane over the surface of the membrane, inducing a change in the membrane curvature and local elastic energy. This local elastic energy of the deformed surface tends to pull the unreformed membrane (see Figures 4.4 and 4.5). In other words, the local curvature change further promotes the protein to diffuse on the surface in order to accommodate the changes in membrane curvature. During this process, the membrane may sustain a residual local tension to balance local moment generated due to the difference between the actual mean curvature and the spontaneous curvature. Thus, this residual local tension may alter the shape of the membrane by influencing the pulling forces in the presence of the transmembrane proteins.

Here, we mention that it is not a straightforward matter to locate and prescribe line tension, particularly in the initial stage of the protein diffusion process, since the transmem-

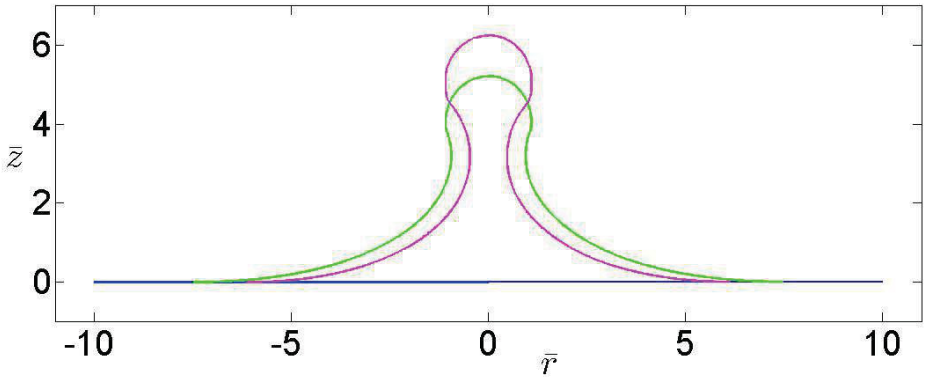


Fig. 4.4 Sequence of membrane shape-changes as the protein diffuses proceeds with $(\gamma = 0)$, and weak membrane tension of $(f_\upsilon = 0.001)$. The associated diffusion time for the protein is (t=0 s,0.91s,1.45s)

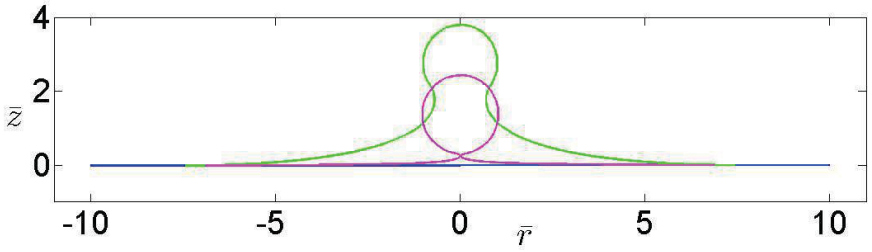


Fig. 4.5 Sequence of membrane shape-changes as the protein diffuses proceeds with $(\gamma = 0.1)$, and weak membrane tension of $(f_\upsilon = 0.001)$.The associated diffusion time for the protein is (t=0 s,0.91s,1.45s)

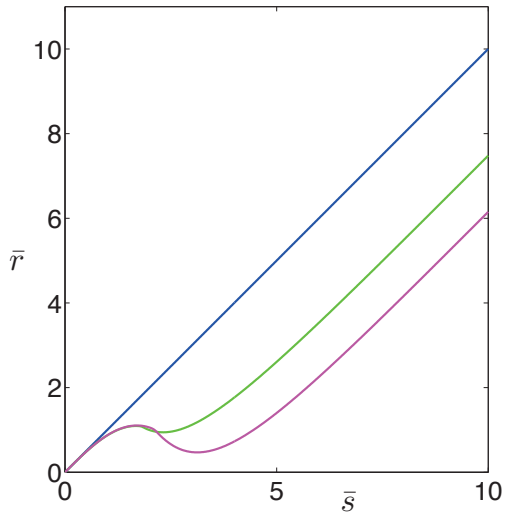


Fig. 4.6 Sequence of radial distance of a membrane point from the axis of symmetry as the protein diffuses proceeds with $(\gamma = 0)$, and weak membrane tension of $(f_\upsilon = 0.001)$. The associated diffusion time for the protein is (t=0 s,0.91s,1.45s)

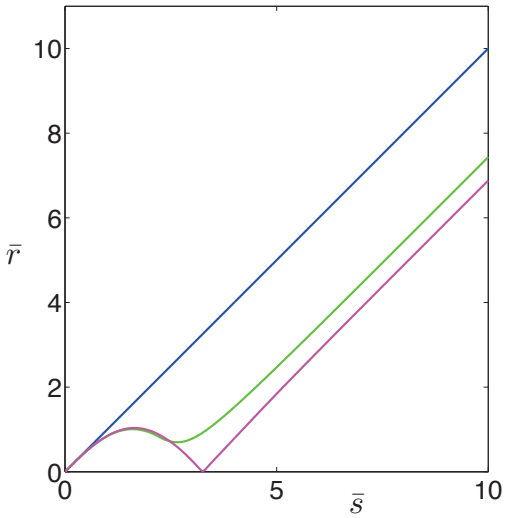


Fig. 4.7 Sequence of radial distance of a membrane point from the axis of symmetry as the protein diffuses proceeds with $(\gamma = 0.1)$, and weak membrane tension of $(f_\upsilon = 0.001)$.The associated diffusion time for the protein is (t=0 s,0.91s,1.45s)

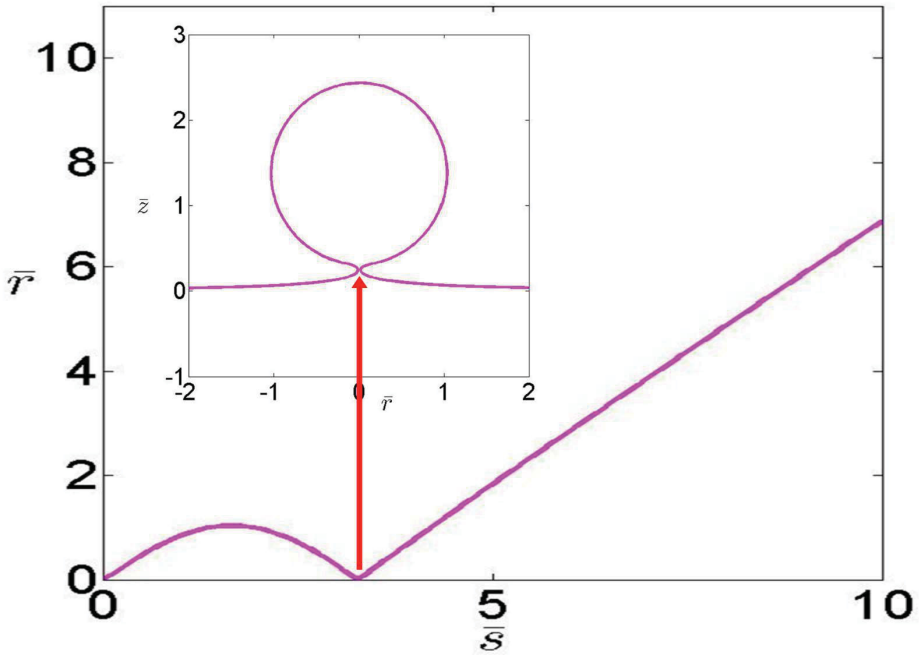


Fig. 4.8 Location of line tension on the evolved membrane bud at (t=1.45s) is shown with an arrow.

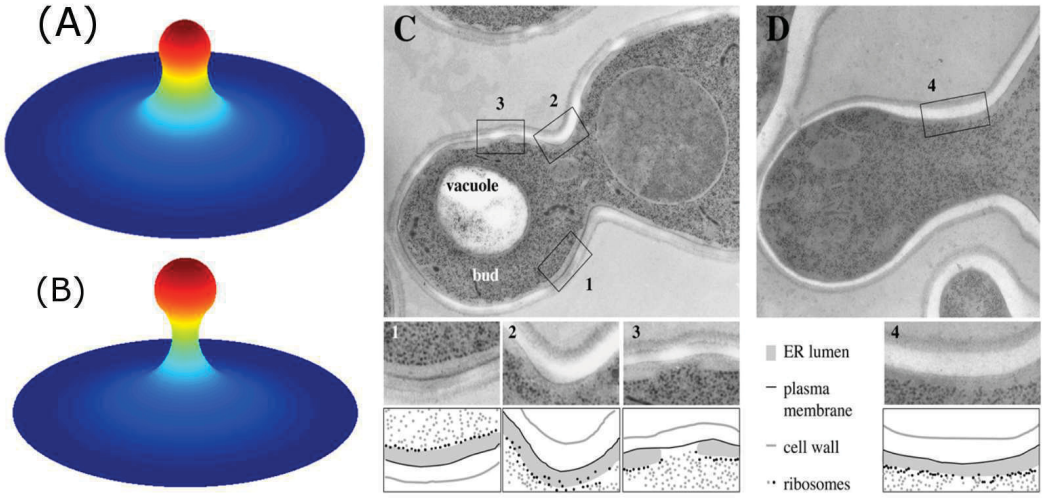


Fig. 4.9 (**A & B**) Sequence of membrane budding evolution as the protein diffuses over the membrane with ($\gamma = 0.0$), and weak membrane tension of ($f_\upsilon = 0.001$) and the corresponding diffusion time for the protein is (t=0.91s,1.45s) and (**C**) Transmission electron microscopy images of the bud neck of a WT yeast cell. (**D**) Transmission electron microscopy images of the bud neck of a shs1Δ mutant cell. (*Pictures* (***C***) *and* (***D***) *are taken from: Cosima, L., et al., 2005*).

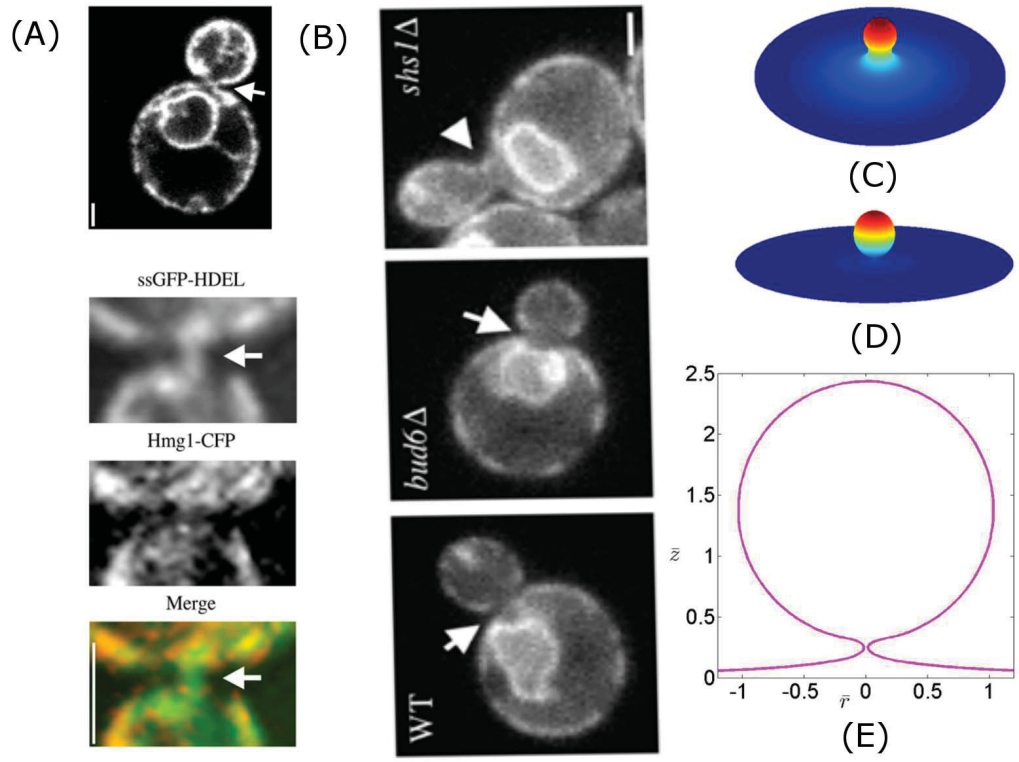


Fig. 4.10 (**A**) Spinning disk confocal images through the bud neck of a yeast cell expressing ssDFP-HDEL. Arrows point at GFP-HDEL localization to the bud neck, (**B**) Images of WT, bud6Δ, and shs1Δ mutant cell expressing Sec61-GFP localization at the bud neck and (**C**&**D**) Sequence of membrane budding evolution as the protein diffuses over the membrane with $(\gamma = 0.1)$, and weak membrane tension of $(f_\upsilon = 0.001)$. The associated diffusion time for the protein is (t=0.91s,1.45s). (**E**) is the 2D plot of the membrane shape corresponding to the counter plot in **D**. (*Pictures* (***A***) *and* (***B***) *are taken from: Cosima, L., et al., 2005*).

brane proteins have a continuous spatial distribution with no distinct boundary separating the protein-free planar membrane from the protein-coated domain. The explicit interface separating the protein-free domain from the protein-coated domain evolves as the diffusion of proteins proceeds with time. As the proteins diffuse, during the process of vesicle formation, a highly concentrated local protein domain develops at the base of the resulting bud and this induces the formation of interface between the protein-free planar membrane and the protein-covered bud. This interface is evolves into a well-defined circular boundary perpendicular to the axis of revolution of the bud and consequently a line tension is induced at this interface. This interface is also responsible to minimize any possible energetically unfavorable contacts between the protein-free planar membrane and the protein-covered bud. Figure 4.8 shows the location of line tension on the resulting membrane bud.

Figures (4.4) - (4.10) illustrate the different effects that line tension has on the bud formation. As shown in Fig. 4.4, each of the spherically-shape domains with positive and negative Gaussian curvatures are generated by a sequence of changes in protein distribution covering the area of the membrane as the protein diffuses from the outer boundary into the membrane. The protein covers the bud regions in both vesicle shapes but the area covered in each case is different depending on the sequence of protein diffusion. The vesicle shape with positive Gaussian curvature has less area covered by the protein compared with the vesicle shape corresponding to the negative Gaussian curvature, since the former shape evolves first followed by the shape with negative Gaussian curvature as the protein diffusion process proceeds. At the early stages of protein diffusion, the growth of the protein domain in the membrane induces bending and helps promote budding with positive Gaussian curvature. As the membrane surface area covered by the protein increases (as a result of the subsequent protein diffusion), the formation of a vesicle with defined neck region increases. When the surface of the bud is saturated with proteins, further diffusion leads to development of a highly concentrated local protein domain at the base of the resulting bud. This local concentration

of protein is responsible for shifting the Gaussian curvature of the neck membrane towards negative values, possibly via protein shape effects, changes in the membrane shape and the gradual evolution of interface formation between the protein-free planar membrane and the protein-covered bud. Thus, the generation of the negative Gaussian curvature during protein diffusion on the membrane surface is a clear indication of the formation of bud and necking. In fact, as reported in [80], the negative Gaussian curvature is necessary, geometrically, for membrane remodeling in biological processes including budding and scission. It should also be noted that, when the diffusion of protein proceeds in the absence of line tension (see Fig. 4.4), the area covered by the protein increases and, consequently, the formation of the spherical-like shape bud increases. The associated displacement in the center of the budding regime increases for the corresponding area covered by the proteins. However, in this case, the neck formation process in the evolution of the membrane bud is slow. On the other hand, the diffusion of the protein in the presence of the line tension has a stronger effect in the bud formation as well as the necking process, to the extent that the displacement in the center of the budding regime decreases as the areas covered by the protein increases (see Fig. 4.5).

Without line tension, the radius decreases smoothly towards the neck of the budding regime, but with a remarkable structural feature; a small plateau (i.e., a membrane region with a nearly horizontal tangent) occurs around this region (see Fig. 4.6).

When line tension dominates (Fig. 4.7), numerical evidence suggests that the radius at the interface decreases with increasing line tension. It nearly vanishes all the way down to zero for a large line tension. Note that this description breaks down at scales comparable to the bilayer width. Despite the fact that the radius goes closer to zero, the difference between the mean curvature and the spontaneous curvature distribution remains finite; in the highly pinched limit, a saddle point develops at the neck which keeps the total curvature energy finite. The result may also suggest that the presence of the neck seems to favor the breaking

process. In this case, fission may occur exactly at the neck. Details of the fission mechanism is outside of the scope of this study and will be the subject of a future work.

## 4.5 Conclusions

We have proposed a continuum based model describing bud formation of lipid membranes induced by the surface diffusion of transmembrane proteins and acting line tension on the membrane. As such, the protein distribution over the membrane in consideration is assumed to be non-uniform. The proposed model is based on the free energy functional accounting for the bending energy of the membrane, including the spontaneous curvature and the acting line tension energy on the boundary of the protein concentrated domain and the surrounding bulk lipid. In the analysis, the protein concentration level is coupled to the deformation of the membrane through the spontaneous curvature term appearing in the resulting shape equation. Our results successfully predict the vesicle formation phenomenon on a flat lipid membrane surface, which were possible under the parametric representation of the membrane surface (not limited to the Monge representation) together with the presence of the acting line tension. In fact, the acting line tension takes a significant role in the bud formation process which was analyzed as an interplay between the bilayer bending energy and the line tension on the domain of interest. This, in turn, suggests that the bud formation is potentially driven by the acting line tension on the membrane surface. It is also found that the final deformed configuration of the membrane (in the form of a spherical bud) is energetically favourable state and, therefore, the bud formation of the membrane is natural and stable.

We conclude that a sufficient amount of line tension energy at the boundary between protein concentrated domain and the surrounding bulk lipid is a major role player in controlling the bud formation process of the lipid bilayer membranes. Therefore, the result can be further extended to the study of important cellular functions associated with budding, mor-

phological aspects of cellular processes in particular, by providing necessary quantitative information for the bud formation of cellular membranes.

# Chapter 5

# Mechanics of a Lipid Bilayer Subjected to Thickness Distension and Membrane Budding

*We study the distension-induced gradient capillarity in membrane budding formation. The budding process is assumed to be primarily driven by a diffusion of trans-membrane proteins and acting line tensions on the protein-concentrated interface. The proposed model, based on the Helfrich type potential, is designed to accommodate inhomogeneous elastic responses of the membrane, non-uniform protein distributions over the membrane surface and more importantly, the thickness distensions induced by the membrane's budding formations. The latter are employed via the augmented energy potential of bulk incompressibility in a weakened manner. By computing the variations of the proposed membrane energy potential, we obtained the corresponding equilibrium equation (membrane's shape equation) describing the morphological transitions of the lipid membrane undergoing the bud formation and the associated thickness distensions. The effects of lipid distension on the shape equation and the necessary adjustments to the accompanying boundary conditions are also derived in detail. The resulting shape equation is solved numerically for the parametric representation of the surface which has one-to-one correspondence with the membrane surface under consideration. The proposed model successfully predicts the bud formation phenomenon on a flat lipid membrane and the associated thickness distension of the membrane demonstrating a smooth transition from one phase to the other (including necking domains). It is also found that the final deformed configuration is energetically favourable and therefore stable. Finally, we show that the inhomogeneous thickness deformation on the membrane in response to transmembrane protein diffusion makes a significant contribution to the membrane's budding and necking processes.*

## 5.1 Introduction

Lipid bilayer membranes are complex assemblies composed of a large variety of transversely oriented two layers of lipid molecules, each of which is characterized by hydrophilic head groups and hydrophobic tails. These membranes play an important role for a wide range of essential cellular functions [33, 67, 82]. Morphological transitions of biological membranes can be regulated by membrane forces induced by the interactions between lipid molecules and proteins. For instance, interactions of trans-membrane proteins with the biological membrane may give rise to local membrane curvature changes (see [26, 31, 60, 104] for a detailed review) and assist morphological aspects of important cellular processes such as fission, fusion and budding [10, 15, 53, 71]. In particular, a bud formation of membranes is an essential initial step in cellular vesicular transport (e.g. exocytosis and endocytosis processes [50, 75]) and in releasing various viral infectious agents in biological cells [79]. Extensive studies have been devoted to this particular subject and evidence has been collected that indicate proteins may drive and/or influence budding on biological membranes (see for example, Refs. [3, 7, 12, 28, 42, 48, 51, 55, 66, 72, 79, 89, 97] and the references therein). Furthermore, the authors in [80] have reported that the positive and negative Gaussian curvature changes are related to the formation of membrane budding. In this respect,the work in [7] showed that, in the presence of acting line tension, spherically-shaped domains with positive and negative Gaussian curvatures can be simulated by a sequence of changes in protein distribution over the membrane as the protein diffusion progresses on the membrane surface. Although, the results in [7] enhanced our understanding of the morphological transitions of biological membranes in bud formation, many of the contributing factors regarding bud formation are still unknown. One of the important factors is the influence of thickness variations of the membranes' deformations (which is not accounted for in [7]). In fact, it is reported in [41] that membranes can undergo rapid thickness changes during the desired deformations (see also [24, 54, 81] and the references therein) and the final

deformed configuration of the membrane is stable with more than one thickness present in a single membrane. Further, experimental evidence [21, 57, 93] suggests that lipid membranes may experience thickness distension with or without tilting motion of lipid molecules. This further suggests that a more accurate prediction of the budding process can be done by incorporating thickness distension of membranes.

In the present work, we consider a lipid bilayer subjected to inhomogeneous thickness distensions and bud formations. The proposed model is based on the modification of the Helfrich type energy potential in [37] to accommodate thickness distensions together with the surface diffusion of trans-membrane proteins and acting line tension on the membrane. The bilayer membrane is assumed to be inhomogeneous and incompressible and the mechanical responses of the membrane are characterized by the changes of mean and Gaussian curvature during deformations. Thickness distension effects are employed by relaxing the constraint of bulk incompressibility in the augmented energy functional via a Lagrange multiplier. This allows the computation of the surface shape (local curvature changes) and distension as essentially independent fields. In addition, we consider lipid bilayers with non-zero spontaneous curvature in order to take into account the effects of non-uniformly distributed proteins in the bending response of the membrane. The corresponding thickness distension profiles inside the boundary layer are calculated on the basis of the modified Helfrich type free energy potential satisfying the influence of protein density distribution on the membrane shape. In this regard, we also adopt the desired energy features given by the Ginzburg-Landau potential to simulate coexistent phase equilibria [41].

The shape equation of the membrane is obtained via variational methods and is solved numerically for a parametric representation of the surface (not limited to the Monge representation) and therefore applicable to general membrane deformations. In addition, a complete analysis of natural boundary conditions has been conducted by extending the results in [7] and is imposed as necessary. The obtained solution successfully predicts the bud

formation phenomenon on a flat lipid membrane and the associated thickness distension of the membrane demonstrating a smooth transition from one phase to the other (including necking domains). It is found that the occurrences of inhomogeneous thickness deformations (distension) in the membrane are able to facilitate the membrane budding and necking during the bud formation process in lipid bilayer membranes.

This chapter is organized as follows. In Section 5.2 we present a concise summary of the membrane model which includes a brief review of the geometry and kinematics of the membrane surface as well as a description of the generalized equilibrium-shape equation of the lipid membrane and the associated admissible boundary conditions ( [1, 3, 41, 90, 91, 94]). In Sections 5.3 and 5.4 we present the membrane surface representation and discuss the numerical solutions and results with examples. Finally, Section 5.5 presents our results and conclusions.

## 5.2 Description of the bilayer membrane model with thickness distension

### 5.2.1 Energy functional

As mentioned in the introduction, in our previous study [7], the thickness distension effect in membrane budding was not taken into consideration. Hence, the current work, which accounts for this effect, is an extension of that discussed in [7] and the total free energy of the lipid bilayer that undergoes inhomogeneous thickness deformation is assumed to be of the form

$$W(H,K,\sigma,\varphi,G;\theta^{\alpha}) = \Upsilon(\sigma)+\zeta(\varphi)+k(\sigma)[H-C(\sigma)]^2+\bar{k}(\sigma)K+\rho(\varphi)G^2. \qquad (5.1)$$

Here and in what follows, Greek indices take the value 1,2 and we sum over repeated indices; $\sigma(\theta^{\alpha},t)$ is the areal concentration of proteins on the membrane surface; $\varphi$ is the lipid

distension and $G = |\nabla\varphi|$, where $\nabla\varphi$ is the gradient of $\varphi$ with respect to material points of the current surface. The parameters $k(\sigma)$ and $\bar{k}(\sigma)$ are bending rigidities which pertain to lipid membranes with nonuniform properties and $\rho(\varphi)$ is a penalty modulus. Further, considerations pertaining to the existence of an energy minimizer [93] require that $k \geq 0$ and $\rho \geq 0$ at values of $\varphi$ associated with stable equilibria. In the above, $\Upsilon(\sigma)$ is the energy contribution associated with bending deformation induced from the non-uniformly distributed protein density $\sigma$, $\zeta(\varphi)$ is the stretching energy density of the membrane which regulates the thickness distension. The Landau expansion of the free energy for $\zeta(\varphi)$, which has the desired energy feature to simulate coexistent phase equilibria [41], would be defined later in the text. $H$ is the mean curvature of the membrane surface $\omega$ and $K$ is the Gaussian curvature. These curvatures are defined by

$$H = \frac{1}{2}(\kappa_\upsilon + \kappa_t), \quad K = \kappa_\upsilon \kappa_t - \tau^2, \tag{5.2}$$

where $\upsilon$ and $t = \mathbf{n} \times \upsilon$ correspond to the exterior unit normal and unit tangent to a smooth surface boundary $\partial\omega$, respectively; $\kappa_\upsilon$ and $\kappa_t$ are the normal curvatures on these axes and $\tau$ is the twist. The unit vector field $\mathbf{n} = (\mathbf{a}_1 \times \mathbf{a}_2)/|\mathbf{a}_1 \times \mathbf{a}_2|$ is the local surface orientation. Here, $(\mathbf{a}_\alpha = \mathbf{r}_{,\alpha})$, are the tangent vectors to $\omega$ induced by the parametrization $\mathbf{r}(\theta^\alpha)$, the position in $\mathbb{R}^3$ of a point on the membrane surface with coordinates $\theta^\alpha$. The surface metric tensor is also defined by $(a_{\alpha\beta} = \mathbf{a}_\alpha \cdot \mathbf{a}_\beta)$. The local curvature of the membrane by the surface-tensor field is

$$\mathbf{b} = b_{\alpha\beta}\mathbf{a}^\alpha \otimes \mathbf{a}^\beta, \tag{5.3}$$

where

$$b_{\alpha\beta} = \mathbf{n} \cdot \mathbf{r}_{,\alpha\beta} = -\mathbf{a}_\alpha \cdot \mathbf{n}_{,\beta}, \tag{5.4}$$

are the symmetric coefficients of the second fundamental form on $\omega$. The contravariant cofactor of the curvature is given by [90]

$$\tilde{b}^{\alpha\beta} = 2Ha^{\alpha\beta} - b^{\alpha\beta}, \tag{5.5}$$

where $(a^{\alpha\beta})$ is the matrix of dual metric components (i.e, the contravariant components of the surface metric tensor), the inverse of the metric $(a_{\alpha\beta})$; and $(b^{\alpha\beta})$ is also the inverse of $(b_{\alpha\beta})$ which can be written as

$$b^{\alpha\beta} = a^{\alpha\lambda}a^{\beta\mu}b_{\lambda\mu}. \tag{5.6}$$

In Eq. (5.1), a non-zero spontaneous curvature, $C(\sigma)$, which takes into account the effects of non-uniformly distributed proteins in the bending response of the membrane, can be written in the following form (see also [3, 7])

$$C(\sigma) = (\mu\Phi)\sigma, \tag{5.7}$$

where $(\mu\Phi)$ is a coupling constant of proportionality. Here, $\mu$ is a positive constant and $\Phi$ is the angle made by the meridian of an assumed conical shape of the transmembrane protein in which its axis of revolution is directed along the surface normal $\mathbf{n}$.

In the presence of acting line tensions [55, 6, 38, 103, 5, 39] on the protein-concentrated interface of the membrane, equilibrium configurations are those which render stationary the potential energy defined by

$$E = \int_{\omega} W(H,K,\sigma,\varphi,G;\theta^{\alpha})da + \int_{\partial\omega} \gamma ds, \tag{5.8}$$

where $ds$ is the length element along the boundary curve and $\gamma$ is the line tension energy per unit length.

In the proposed model, for a quasi-incompressible membrane, the constraint of bulk incompressibility is evaluated on the membrane surface and takes the form $\varphi J = 1$, where $J = \sqrt{a/A}$ in which $A$ is the value of $a$ on the fixed reference surface. Thus, in Eq. (5.1), the thickness distensions induced by the membrane's bud formations are employed by relaxing the constraint of bulk incompressibility in the augmented energy functional potential via a Lagrange multiplier in a weakened manner. This allows the computation of the surface shape (local curvature changes) and distension as essentially independent fields. To accommodate the constraint of bulk area incompressibility, an augmented energy functional is considered

$$E^* = \int_\Omega [JW(H,K,\sigma,\varphi,G;\theta^\alpha) - q(\varphi J - 1)]dA + \int_{\partial\Omega} \gamma ds, \tag{5.9}$$

where $q(\theta^\alpha)$ is a Lagrange multiplier field [3, 41, 1] associated with the incompressiblity constraint, and $J$ is the local areal stretch induced by the map from a fixed reference surface $\Omega$ to the current surface configuration $\omega$.

Before proceeding, we note that the Euler equation emerging from the variation with respect to $q$ is simply the constraint equation, $\varphi J = 1$. Thus, the remaining content of the stationarity condition is extracted as fixed values of the function $q$. For this reason, we henceforth regard this function as being fixed, and therefore suppress the contribution of the associated constant $\int_\Omega q dA$ to the energy; we thus replace Eq. (5.9) by the functional

$$E^* = \int_\Omega J[W(H,K,\sigma,\varphi,G;\theta^\alpha) - q\varphi]dA + \int_{\partial\Omega} \gamma ds \tag{5.10a}$$

$$= \int_\omega [W(H,K,\sigma,\varphi,G;\theta^\alpha) - q\varphi]da + \int_{\partial\omega} \gamma ds \tag{5.10b}$$

### 5.2.2 Membrane protein diffusion balance law

In [3, 7], a suitable format is established to frame the formulation of the protein diffusion balance by applying the convected coordinate $(\xi^\alpha)$ technique to parametrize the material manifold. A brief review of the theory of convected coordinate systems will facilitate our discussion. In this coordinate system, a material point on the membrane is labeled by $\mathbf{x}(\xi^\alpha)$. It is assumed that, at each fixed time $t_0$, $(\xi^\alpha)$ may be distinctly identified with the $\theta^\alpha$. We can identify a body with its reference surface $\Omega$, with parametric representation $\mathbf{x}(\xi^\alpha) = \mathbf{r}(\xi^\alpha, t_0)$ and this surface may serve as a reference configuration of the material body in a Lagrangian description of the motion. That is, we may regard these coordinates as being convected in the sense that they identify, via a map $\mathbf{r}(\xi^\alpha) = \mathbf{r}(\xi^\alpha, t)$, the current position at time $t$ of a point that was located at $\mathbf{x}(\xi^\alpha) \in \Omega$ at time $t_0$. The connection with the $\theta^\alpha$ parametrization of $\omega$ is given as $\hat{\mathbf{r}}(\xi^\alpha, t) = \mathbf{r}(\theta^\alpha(\xi^\beta, t), t)$ [4, 83]. Similarly, the fixed surface coordinates $\theta^\alpha$ can be specified as functions of $\xi^\alpha$ and $t$ subject to the initial condition, and such a coordinate can be written generally as $\theta^\alpha(\xi^\beta, t_0) = \xi^\alpha$. In addition, following [3, 4], the time derivative of the fixed-coordinate parametrization can be defined by $\frac{d}{dt}\theta^\alpha{}_{|\xi^\alpha} = u^\alpha(\theta^\beta, t), \quad \theta^\alpha_{|t_0} = \xi^\alpha$. Thus, the balance law for the surface diffusion of trans-membrane proteins as well as the tangential and normal membrane velocities in in diffusive balance law can be derived based on this coordinate transformation framework. Here, we adopt the expression for the balance law and both components (normal and tangential) of the membrane velocities from [3, 7] relevant to our current work. Thus, we have

$$u\mathbf{n} = \mathbf{r}_t, \tag{5.11}$$

where $u$ is the normal velocity of a material point on the membrane surface,

$$u^\alpha_{;\alpha} = 2Hu \quad \text{and} \quad \sigma_t + u^\alpha \sigma_{,\alpha} + m^\alpha_{;\alpha} = 0 \quad \text{or} \quad \dot{\sigma} = -m^\alpha_{;\alpha} \quad \text{on} \quad \omega \tag{5.12}$$

where $u^\alpha$ is the tangential velocity of a material point on the membrane surface and,

$$m^\alpha_{;\alpha} = (\sqrt{a}m^\alpha)_{,\alpha}/\sqrt{a} \tag{5.13}$$

in which $a = det(a_{\alpha\beta})$, is the surface divergence of $\mathbf{m}$. A simple constitutive equation for $\mathbf{m}$ which accommodates classical Fickean diffusion is adopted from the works of [3]

$$\mathbf{m} = -c\nabla(W_\sigma), \tag{5.14}$$

where $c$ is a positive constant and $W_\sigma$ is the chemical potential for the diffusing proteins.

### 5.2.3 Membrane equilibrium equation and boundary conditions

The shape equation of the membrane and admissible boundary conditions can be obtained via the variational methods. Thus, the variational derivative of the total free energy of the membrane-protein system in Eq. (5.9) is

$$\frac{d}{dt}E^* = \int_\omega [\dot{W} - q\dot{\varphi} + (W - q\varphi)\dot{J}/J]da + \int_{\partial\omega} \gamma(ds)^{\cdot}, \tag{5.15}$$

where

$$\dot{W} = W_H\dot{H} + W_K\dot{K} + W_\sigma\dot{\sigma} + W_\varphi\dot{\varphi} + W_G\dot{G}. \tag{5.16}$$

Here and henceforth, the subscripts $H$, $K$, $\sigma$, $\varphi$ and $G$ denote partial derivatives with respect to the indicated variables (e.g. $W_H = \frac{\partial W}{\partial H}$ etc...).

To compute the variation of the energy, we use Eq. $(5.12)_3$ and the expressions for the variations $\dot{J}$, $\dot{H}$, $\dot{K}$ and $\dot{G}$ from [3, 41, 94]. Consequently, following the procedures outlined

in [3, 41, 90, 91], we found the expression of the shape equation of the membrane as

$$p = \frac{1}{2}\Delta(W_H) + (W_K)_{;\alpha\beta}\tilde{b}^{\alpha\beta} + W_H(2H^2 - K) + 2H(KW_K - W) + 2q\varphi H + G^{-1}W_G b^{\alpha\beta}\varphi_{,\alpha}\varphi_{,\beta}, \tag{5.17}$$

where $\Delta(\cdot) = (\cdot)_{;\alpha\beta}a^{\alpha\beta}$ is the surface Laplacian. The Lagrange multipier $q$ satisfies [41],

$$W_\varphi - q = (G^{-1}W_G a^{\alpha\beta}\varphi_{,\beta})_{;\alpha} \quad \text{on} \quad \omega, \tag{5.18}$$

and

$$\varphi q_{,\alpha} = \partial W/\partial\theta^\alpha \quad \text{on} \quad \omega, \tag{5.19}$$

in which the right hand side of Eq. (5.19) accounts for any explicit coordinate dependence of the material properties arising in non-uniform membranes. In this regard, we adopt the following expression from [3]

$$\varphi q_{,\alpha} = -W_\sigma\sigma_{,\alpha} \quad \text{on} \quad \omega, \tag{5.20}$$

to accommodate any non-uniformity in the bending properties of the membranes which may be generated by the constitutive response of the membrane to transmembrane proteins where $W_\sigma$ is the chemical potential for the diffusing proteins. In the absence of protein concentration effect on the membrane surface [3, 41], the Euler equation arising from Eq. (5.15) under tangential variation are then given by $q_{,\alpha} = 0$; i.e.,

$$q = \text{const.} \quad \text{on} \quad \omega, \tag{5.21}$$

as in the classical Canham-Helfrich theory for lipid bilayers with properties that are uniform in the sense that the energy density $W$ does not depend explicitly on the coordinates $\theta^\alpha$.

In addition, we obtain, after applying the variation of the energy membrane, the admissible boundary conditions on a smooth edge $\partial\omega$ of the membrane:

$$M = \frac{1}{2}W_H + \kappa_t W_K, \tag{5.22}$$

is the bending couple per unit length on $\partial\omega$,

$$\mathbf{f} = f_\upsilon \upsilon + f_t \tau + f_n \mathbf{n}, \tag{5.23}$$

is the edge traction (force per unit length) on $\partial\omega$, with

$$f_\upsilon = W - q\varphi - \kappa_\upsilon M + G^{-1} W_G (\varphi_{,\upsilon})^2 + c_g \gamma, \tag{5.24}$$

$$f_t = -\tau M + G^{-1} W_G \varphi_{,\upsilon} \varphi', \tag{5.25}$$

$$f_n = (\tau M)' - (\frac{1}{2}W_H)_{,\upsilon} - (W_K)_{,\beta} \tilde{b}^{\alpha\beta} \upsilon_\alpha + c_n \gamma. \tag{5.26}$$

Here $(\cdot)_{,\upsilon} = \upsilon^\alpha (\cdot)_{,\alpha}$ and $(\cdot)' = d(\cdot)/ds$ are the normal and tangential derivatives on the boundary; $f_\upsilon$, $f_t$ and $f_n$ respectively, are the components of distributed forces per unit length applied on the boundary in the directions of $\upsilon$, $\mathbf{t}$ and $\mathbf{n}$. We also note here that $c_n$ is the normal curvature and $c_g$ is the geodesic curvature.

Further,

$$\tau = b^{\alpha\beta} \tau_\alpha \upsilon_\beta, \tag{5.27}$$

is the twist of the membrane surface $\omega$ on the $(\upsilon, \mathbf{t})$- axes with $(\upsilon_\alpha = \mathbf{a}_\alpha \cdot \upsilon$ and $\tau_\beta = \mathbf{a}_\beta \cdot \mathbf{t})$, whereas

$$\kappa_\upsilon = b^{\alpha\beta} \upsilon_\alpha \upsilon_\beta \quad \text{and} \quad \kappa_t = b^{\alpha\beta} \tau_\alpha \tau_\beta. \tag{5.28}$$

are the normal curvatures of $\omega$ in the directions of $\upsilon$ and $\mathbf{t}$, respectively.

For a non-uniform bilayer membrane with lipid distension, we adopt a simple modified Helfrich-type free energy function $W$ that satisfies the influence of protein density distribution on the membrane shape and which also conforms to the conventional theory of bending elasticity in the absence of protein diffusion and distension:

$$W = (\alpha\sigma - \beta)^2 + k[H - C]^2 + \zeta(\varphi) + \rho G^2. \tag{5.29}$$

Here, the energy $\zeta(\varphi)$ that regulates the thickness distension can be constructed in a phenomenological Landau expansion of the stretching free energy in powers of the areal stretch $J$ (see, for example, [32, 46, 64, 22]). Thus, in the present work, under the assumption of fixed temperature of the membrane for any configuration setting and bulk quasi-compressibility constraint which takes the form of $\varphi J = 1$, the energy term $\zeta(\varphi)$ is chosen as a simple non-convex function possessing the desired features to simulate coexistent phase equilibria [41] and is given by the Ginzburg-Landau potential as

$$\zeta(\varphi) = W(\varphi^{-1}) = a_1\varphi^{-4} + a_2\varphi^{-3} + a_3\varphi^{-2} + a_4\varphi^{-1} + a_5\varphi + a_6, \tag{5.30}$$

where the phenomenological parameters $a_1 - a_6$ are constants.

We note that $W$ in Eq. (5.29) corresponds to the restriction of Eq. (5.1) to the case of constant bending moduli $(k > 0)$ and $\bar{k}$. The assumption of uniform bending moduli is justifiable for dilute concentration of proteins on the membrane. However, here, we make the assumption primarily to ensure that their effect on the bending stiffness remains negligible. This also allows us to avoid any influence of non-uniformity of the bending moduli on the spontaneous curvature in equation Eq. (5.7). In addition, for the sake of simplicity, the term involving $K$ is suppressed in this study.

For the particular energy given by Eq. (5.29), with

$$W_H = 2k[H-C], \quad W_\sigma = 2[\alpha(\alpha\sigma-\beta)-k\mu\varphi(H-C)], \quad W_G = 2\rho G \tag{5.31a}$$

$$W_\varphi = \zeta(\varphi)_\varphi = -4a_1\varphi^{-5} - 3a_2\varphi^{-4} - 2a_3\varphi^{-3} - a_4\varphi^{-2} - a_5\varphi^{-1} \tag{5.31b}$$

the shape equation reduces to

$$k\Delta(H-C) + 2k(H-C)(2H^2-K) - 2H[(\alpha\sigma-\beta)^2 + k(H-C)^2 - q\varphi + \zeta(\varphi) + \rho G^2] + 2\rho b^{\alpha\beta}\varphi_{,\alpha}\varphi_{,\beta} = p, \tag{5.32}$$

and equations (5.18) and (5.20) are simplified to

$$W_\varphi - q = 2\rho a^{\alpha\beta}(\varphi_{,\beta\alpha} - \varphi_{,\lambda}\Gamma^\lambda_{\beta\alpha}), \tag{5.33}$$

$$\varphi\nabla q = 2[k\mu\Phi(H-C) - \alpha(\alpha\sigma-\beta)]\nabla\sigma. \tag{5.34}$$

where $\Gamma^\lambda_{\beta\alpha}$ are the Christoffel symbols induced by the coordinates of $\omega$.

In addition, the bending moment and edge forces which are assigned on part of the membrane boundary $\partial\omega$ are

$$M = k(H-C), \tag{5.35}$$

and

$$f_\upsilon = (\alpha\sigma-\beta)^2 + k[H-C]^2 - q\varphi + \zeta(\varphi) + \rho G^2 - \kappa_\upsilon M + 2\rho(\varphi_{,\upsilon})^2 + c_g\gamma, \tag{5.36}$$

$$f_t = -\tau M + 2\rho\varphi_{,\upsilon}\varphi', \tag{5.37}$$

$$f_n = (\tau M)' - M_{,\upsilon} + c_n\gamma. \tag{5.38}$$

Finally, using Eq. (5.29) and the chemical potential for the diffusing proteins in Eq. $(5.31b)_2$, the protein flux in Eq. (5.14) is reduced to

$$\mathbf{m} = -2c\{[\,\alpha^2 + k(\mu\Phi)^2]\nabla\sigma - k\mu\Phi\nabla H\}, \tag{5.39}$$

in which $\nabla C = \mu\varphi\nabla\sigma$.

## 5.3 Membrane surface representation

We assume that the diffusion of the protein on the membrane surface forms a bud which possesses axisymmetry (i.e. the budding region maintains a circular boundary on the membrane). Figure 5.1 shows a schematic of an axisymmetric membrane bud generated by a planar curve in which $\varphi$ represents the thickness distension in the current configuration of the membrane surface, $\omega$. Consequently, we seek a simple class of axisymmetric solution in the surface of revolution parametrized by arclength coordinate $s$, which is measured from the center of the vesicle and an angle $\psi(s)$, that the membrane surface makes from the horizontal plane.

$$\mathbf{r}(s,\theta,t) = r(s,t)\mathbf{e}_r(\theta) + z(s,t)\mathbf{k}, \tag{5.40}$$

where, $(r,\theta,z)$ are cylindrical polar coordinate system which represent a material point in the deformed membrane, $r(s,t)$ is the radial distance of a material point from the axis of symmetry, $z(s,t)$ is the elevation above the base plane, and $\{\mathbf{e}_r,\mathbf{e}_\theta,\mathbf{k}\}$ is the orthonormal basis in the cylindrical polar coordinate system. Since $s$ measures arclength along meridians, we have

$$r'^2 + z'^2 = 1, \tag{5.41}$$

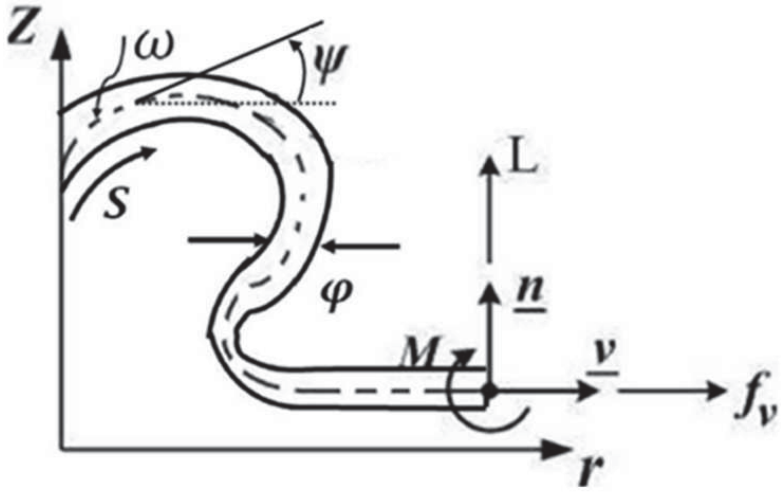


Fig. 5.1 Schematic representation of membrane budding with thickness distension.

where $(\cdot)' = d(\cdot)/ds$. It follows from Eq. (5.41) and the simple geometry in figure 5.1 that $r(s)$ and $z(s)$ can be related to $s$ and $\psi$ by

$$r' = \cos\psi(s) \quad \textit{and} \quad z' = \sin\psi(s). \tag{5.42}$$

We choose surface coordinates $\theta^1 = s$ and $\theta^2 = \theta$. The induced tangent vectors are

$$\mathbf{a_1} = r'\mathbf{e}_r + z'\mathbf{k}, \quad \textit{and} \quad \mathbf{a_2} = r\mathbf{e}_\theta. \tag{5.43}$$

Since $\mathbf{a_1}$ is orthogonal to a parallel of latitude, we identify it with $\upsilon$ (Fig. 5.1). Consequently,

$$\upsilon = \cos\psi(s)\mathbf{e}_r + \sin\psi(s)\mathbf{k}, \quad \mathbf{t} = \mathbf{e}_\theta \quad \textit{and} \quad \mathbf{n} = \cos\psi(s)\mathbf{k} - \sin\psi(s)\mathbf{e}_r. \tag{5.44}$$

The metric and dual metric are $a_{\alpha\beta} = diag(1, r^2)$ and $a^{\alpha\beta} = diag(1, r^{-2})$, respectively, and the later can be used to compute

$$\mathbf{a}^1 = \upsilon \quad \textit{and} \quad \mathbf{a}^2 = r^{-1}\mathbf{e}_\theta \tag{5.45}$$

We can also get all the components of the Christoffel symbols in (5.33):

$$\Gamma^{\theta}_{s\theta} = \Gamma^{\theta}_{\theta s} = \frac{1}{r} \quad \text{and} \quad \Gamma^{s}_{\theta\theta} = -r. \tag{5.46}$$

At any given position, the components of curvature of the membrane can be obtained by combining the value of ($b_{\alpha\beta} = diag(\psi', r\sin\psi)$) with equations (5.6) and (5.44) as

$$\kappa_{\upsilon} = \psi', \quad \kappa_t = r^{-1}\sin\psi(s), \quad \tau = 0, \quad c_g = \cos\psi(s)/r \quad \text{and} \quad c_n = \sin\psi(s)/r. \tag{5.47}$$

In the previous sections, relevant admissible boundary edge forces and moments acting on the membrane are derived. Following the procedures outlined in [7], we obtain the following differential equation as

$$\psi' = \frac{2M}{k} - \frac{\sin\psi(s)}{r} + 2C. \tag{5.48}$$

The product of the normal curvatures is the Gaussian curvature $K(s,t)$; thus,

$$K = (\frac{M}{k} + C)^2 - (\frac{M}{k} - \frac{\sin\psi(s)}{r} + C). \tag{5.49}$$

The traction force in equation (5.36) is expressed by

$$\begin{aligned} f_{\upsilon} = (\alpha\sigma - \beta)^2 + M^2/k - q\varphi + \zeta(\varphi) + \rho G^2 - (\frac{2M}{k} - \frac{\sin\psi(s)}{r} + 2C)M + \\ 2\rho d^2 + \gamma\frac{\cos\psi}{r}, \end{aligned} \tag{5.50}$$

and the shape equation (5.32), with $P = 0$ and ($b^{\alpha\beta} = diag(\psi', r^{-3}\sin\psi)$), simplifies to

$$\begin{aligned} L' = r\{(f_{\upsilon} - \gamma\frac{\cos\psi}{r} - 2\rho d^2)(\frac{2M}{k} - \frac{\sin\psi}{r} + 2C) + (f_{\upsilon} - \gamma\frac{\cos\psi}{r} - 2\rho d^2)\frac{\sin\psi}{r} + \\ 2M(\frac{M}{k} - \frac{\sin\psi}{r} + C)\frac{\sin\psi}{r} - 2\rho d^2(\frac{2M}{k} - \frac{\sin\psi}{r} + 2C)\}, \end{aligned} \tag{5.51}$$

where

$$L = \frac{1}{2} r (W_H)' = rM' \quad \text{and} \quad d = \varphi', \tag{5.52}$$

and the Lagrange multiplier $q$ in equations (5.33) and (5.34) also satisfies

$$W_\varphi - q = 2\rho(\varphi')' = 2\rho(d)', \tag{5.53}$$

and

$$q' = 2[\mu\Phi M - \alpha(\alpha\sigma - \beta)]\sigma'. \tag{5.54}$$

Further, rearranging of Eq. (5.53) gives

$$d' = \frac{1}{2\rho}[-4a_1\varphi^{-5} - 3a_2\varphi^{-4} - 2a_3\varphi^{-3} - a_4\varphi^{-2} - a_5\varphi^{-1}] - \frac{q}{2\rho} - \frac{d}{r}\cos\psi. \tag{5.55}$$

The normal and tangential velocities of the surface, which are related by Eq. $(5.12)_1$, lead to

$$(rv)' = 2(\frac{M}{k} + C)u, \tag{5.56}$$

where $v(s,t)$ is the velocity component in the direction of the tangent to the meridian; we assume that the velocity in the azimuthal direction vanishes. This furnishes the tangential velocity gradient and thus may be used to estimate the error incurred by neglecting intra-membrane viscosity.

The protein flux in Eq. (5.39) becomes

$$m = -c(W_\sigma)' = 2c[\mu\Phi M' - \alpha^2\sigma'], \tag{5.57}$$

where $m = \mathbf{m}\cdot\upsilon$ is the component of the flux $m$ in the direction tangent to the meridian; the azimuthal component of this vector also vanishes. Finally the diffusive balance law $(5.12)_2$

reduces to

$$\sigma_t + v\sigma' = \frac{2c}{r}\{r[\alpha^2\sigma' - \mu\Phi M']\}', \tag{5.58}$$

In order to maintain control over the domain over which the transmembrane proteins interact with the membrane and on which the preceding differential equation is to be solved, the surface area enclosed by the sector $(0,s)$ is specified by the following relation as

$$a' = 2\pi r, \tag{5.59}$$

in which a global constraint on the area of the current surface is enforced by applying the local constraint, $\dot{J} = 0$.

The nine equations (5.42), (5.48), (5.51) – (5.56) and (5.59) form a ninth-order system for the nine unknowns $r, z, a, \phi, L, M, d, q$ and $\psi$ as a function of $s$. We can re-cast these equations as a set of explicit first-order equations:

$$r' = \cos\psi(s). \tag{5.60}$$

$$z' = \sin\psi(s). \tag{5.61}$$

$$a' = 2\pi r, \tag{5.62}$$

$$\psi' = \frac{2M}{k} - \frac{\sin\psi(s)}{r} + 2C. \tag{5.63}$$

$$\begin{aligned} L' = r\{(F_\upsilon - \gamma\frac{\cos\psi}{r} - 2\rho d^2)(\frac{2M}{k} - \frac{\sin\psi}{r} + 2C) + (F_\upsilon - \gamma\frac{\cos\psi}{r} - 2\rho d^2)\frac{\sin\psi}{r} + \\ 2M(\frac{M}{k} - \frac{\sin\psi}{r} + C)\frac{\sin\psi}{r} - 2\rho d^2(\frac{2M}{k} - \frac{\sin\psi}{r} + 2C)\}, \end{aligned} \tag{5.64}$$

$$M' = \frac{L}{r} \tag{5.65}$$

$$d' = \frac{1}{2\rho}[-4a_1\varphi^{-5} - 3a_2\varphi^{-4} - 2a_3\varphi^{-3} - a_4\varphi^{-2} - a_5\varphi^{-1}] - \frac{q}{2\rho} - \frac{d}{r}\cos\psi. \tag{5.66}$$

$$q' = 2[\mu\Phi M - \alpha(\alpha\sigma - \beta)]\sigma'. \tag{5.67}$$

$$\varphi' = d \tag{5.68}$$

In addition, we non-dimensionlized lengths using the assumed radius of curvature of $R$ of the budding regime, whereas force and moment variables are scaled by the membrane bending rigidity $k$. Thus we define,

$$\begin{gathered}
\bar{s} = s/R, \quad \bar{r} = r/R, \quad \bar{z} = z/R, \quad \bar{H} = RH, \quad \bar{C} = RC, \quad \bar{a} = a/R^2, \quad \bar{\mu} = \mu/R, \\
\bar{u} = u\hat{\tau}/R, \quad \bar{v} = v\hat{\tau}/R, \quad \bar{\sigma} = R^2\sigma, \quad \bar{t} = t/\hat{\tau}, \quad \bar{\alpha} = \alpha/(R\sqrt{k}), \quad \bar{\beta} = \beta R/\sqrt{k}, \\
\bar{L} = RL/k, \quad \bar{q} = R^2 q/k, \quad \bar{M} = RM/k, \quad \bar{F}_\upsilon = R^2 F_\upsilon/k, \quad \bar{F}_n = R^2 F_n/k, \\
\bar{\gamma} = R\gamma/k,
\end{gathered} \tag{5.69}$$

where $\hat{\tau} = (ck)^{-1}$ is used as a measure of time scale from a dimensional analysis of the balance law [3]. For the sake of brevity, we don't list the associated systems of dimensionless equations.

## 5.4 Numerical results and discussion

### 5.4.1 Boundary conditions

Here, we have cast our boundary conditions following our previous study [7], with further additional thickness distension related conditions. In the following, we denote the cross-sectional curve at the boundary between the protein concentration domain and the surrounding bulk lipids by $\Gamma$ (assumed circular). The non-dimensionalized form of the nonlinear equations (5.60)-(5.68) are solved between $\bar{s} = 0$ at the center of the axis of symmetry of the bud and $\bar{s} = \bar{s}_{max}$ which is an unknown arclength yet to be determined as part of the solution. However, in order to avoid effects arising from finite boundaries in our numerical simulation analysis, we specify $\bar{s}_{max}$ a sufficiently large length from the center of the bud.

Furthermore, this large value of $\bar{s}_{max}$ assumption is also applied to model an isolated bud on an unbounded domain. Symmetry dictates that the shear force vanishes at the pole where $\bar{s} = 0$, and at far end of the cross-section of the membrane where $\bar{s} = \bar{s}_{max}$ i.e.,

$$L(\bar{s} = 0) = 0 \quad \text{and} \quad \bar{L}(\bar{s} = \bar{s}_{max}) = 0. \tag{5.70}$$

The slope is zero at both ends of the cross-section of the membrane, i.e.,

$$\psi(\bar{s} = 0) = 0 \quad \text{and} \quad \psi(\bar{s} = \bar{s}_{max}) = 0. \tag{5.71}$$

Also, at these ends, we have

$$\bar{r}(\bar{s} = 0) = 0 \quad \text{and} \quad \bar{z}(\bar{s} = \bar{s}_{max}) = 0. \tag{5.72}$$

The equations are solved on a flat circular membrane with radius $\rho$. Thus, since there is no area enclosed at $\bar{s} = 0$, and the total area of the membrane is fixed to be $\pi\rho^2$, we have the following additional conditions at the two ends of the cross-section of the membrane

$$\bar{a}(\bar{s} = 0) = 0 \quad \text{and} \quad \bar{a}(\bar{s} = \bar{s}_{max}) = \pi\rho^2. \tag{5.73}$$

In addition, we impose a constant thickness distension at the outer boundary of the membrane cross-section through the simulation and thus, the variation of the membrane thickness at the outer end of the cross-section is restricted. Thus, we have

$$\bar{\varphi}(\bar{s} = \bar{s}_{max}) = 0.8 \quad \text{and} \quad \bar{d}(\bar{s} = \bar{s}_{max}) = 0. \tag{5.74}$$

Due to a lack of specific experimental data and in order to show the numerical feasibility of the model, we fix the values of phenomenological parameters $a_i$ $(i = 1, ..., 6)$ as shown in

Table 5.1 Parameters used in the proposed Ginzburg-Landau potential

| Phenomenological parameters | Value [N/nm] |
|---|---|
| $a_1$ | -8.7579 |
| $a_2$ | 20.8034 |
| $a_3$ | 2.8 |
| $a_4$ | 2.56 |
| $a_5$ | 80.80 |
| $a_6$ | -8.0458 |

Table. 5.1, dimensionally all multiplied by $[10^{-9}]$. It is also worth mentioning that this specific choice is merely for the sake of illustration of the simulation of the model. In principle, these values must be adjusted to optimize agreement between the numerical prediction and the corresponding experimental data.

Equation (5.51) involves the traction force $f_\upsilon$ which relates the thickness distension, line tension and membrane surface tension $(\varphi q)$ to the membrane shape at the boundary. Thus, we choose and specify a suitable value for $f_\upsilon$ based on the condition given by (5.50) at $\Gamma$.

Note that $(\varphi q)$ is a nonlinear function of the protein density (see Eq. 5.54). If there is no diffusion of proteins on the membrane, then the inhomogeneity in the value of the local tension $(\varphi q)$ as well as the change of thickness is insignificant. In the region where there is no protein diffusion $\partial\bar{\sigma}/\partial\bar{s}$ goes to zero, and $(\varphi q)$ may be given by a constant value at the boundary, say $(\varphi_0 q_0)$. At the boundary of the protein concentration domain where line tension exists, the actual mean curvature is less than the spontaneous curvature and hence $(M \neq 0)$. Also, $(\partial\bar{\sigma}/\partial\bar{s} \neq 0)$. This implies that the gradient in the tension $(\varphi q)$ is not zero. However, the value of $(\varphi q)$ is equal to the tension outside the budding region plus the jump in tension at the boundary immediately near the budding regime, thereby making the change in tension an effect confined to the budding region.

We also assume the bending rigidities of the membrane to be uniform and also suppress the jump in Gaussian rigidity of the membrane for numerical convenience. Finally, the

equations are solved by specifying zero initial values for the protein density at every mesh point in the membrane except at the boundary which we impose a value $\bar{\sigma} = \bar{\sigma}_\Gamma$ in order to expose the membrane to a protein bath and no protein flux ($m$) is assumed at $\Gamma$.

### 5.4.2 Numerical solutions and examples

Here, we start to solve the non-dimensionalized form of the following two-point boundary value problem

$$r' = \cos\psi(s), \tag{5.75}$$

$$z' = \sin\psi(s), \tag{5.76}$$

$$a' = 2\pi r, \tag{5.77}$$

$$\psi' = \frac{2M}{k} - \frac{\sin\psi(s)}{r} + 2C, \tag{5.78}$$

$$\begin{aligned} L' = r\{(F_\upsilon - \gamma\frac{\cos\psi}{r} - 2\rho d^2)(\frac{2M}{k} - \frac{\sin\psi}{r} + 2C) + (F_\upsilon - \gamma\frac{\cos\psi}{r} - 2\rho d^2)\frac{\sin\psi}{r} + \\ 2M(\frac{M}{k} - \frac{\sin\psi}{r} + C)\frac{\sin\psi}{r} - 2\rho d^2(\frac{2M}{k} - \frac{\sin\psi}{r} + 2C)\}, \end{aligned} \tag{5.79}$$

$$M' = \frac{L}{r}, \tag{5.80}$$

$$d' = \frac{1}{2\rho}[-4a_1\varphi^{-5} - 3a_2\varphi^{-4} - 2a_3\varphi^{-3} - a_4\varphi^{-2} - a_5\varphi^{-1}] - \frac{q}{2\rho} - \frac{d}{r}\cos\psi, \tag{5.81}$$

$$q' = 2[\mu\Phi M - \alpha(\alpha\sigma - \beta)]\sigma', \tag{5.82}$$

$$\varphi' = d, \tag{5.83}$$

with boundary conditions Eqs. (5.70) - (5.74), is solved using the Matlab boundary value problem solver routine *bvp4c* [85]. The equations were solved on a weakly curved or nearly flat circular domain of radius $\rho = 10$ with $\bar{\alpha} = 1.5$, $\bar{\beta} = 0.75$, $\bar{\mu}\varphi = -\pi$, $\bar{\tau} = 1$ and $\Delta\bar{t} = 0.001$ [3, 7]. It should be noted that there is a singularity at $\bar{s} = 0$. To mitigate this problem, we sought an asymptotic solution near $\bar{s} = 0$ and solved the boundary value problem at

$\bar{s} = \delta \ll 1$ and $\bar{s} = \bar{s}_{\max} \gg 1$. Near the origin, $\delta = 0.0001$ gives sufficiently accurate results. The boundary at the far end of the membrane from the axis of symmetry is applied at a large value of $\bar{s} = \bar{s}_{\max}$; $\bar{s}_{\max} \geq 10$ effectively models an unbounded domain or in other words, an isolated bud sufficiently removed from its neighbors such that the effect of interaction may be ignored. This also provides more than sufficient for far-field behavior to become clear.

The equations are solved by specifying a protein distribution function defined by $\bar{\sigma} = \exp\tilde{\sigma}$ at an initial time $\bar{t} = 0$. This distribution ensures that the numerical solutions yield positive values of the protein density. In addition, the initial surface velocity (both normal and tangential) is assigned zero values at $\bar{t} = 0$. Then, we integrate numerically equations $(5.60)$-$(5.68)$ using Matlab routine (*bvp4c*) in order to obtain the initial membrane shape at $\bar{t} = 0$. Next, taking a suitable time step $\Delta\bar{t}$, we use the forward Euler approximation scheme to compute the distribution of the protein density in equation (5.58) and the corresponding membrane shape at this time step is calculated by integrating equations $(5.60)$-$(5.68)$ as before. Now, with the time derivative $\mathbf{r}_t$ in (5.11) known at time zero and $\Delta\bar{t}$, we form a backward Euler approximation at each mesh point to compute the normal velocity $u = \mathbf{n} \cdot \mathbf{r}_t$, in which surface normal is evaluated at the initial instant. This normal surface velocity is used to integrate (5.56) for the tangential velocity field at time $\Delta\bar{t}$, assuming the tangential velocity at $\bar{s} = 0$ to vanish and with the mean curvature equal to the initial distribution. As a result, this tangential velocity is then used with (5.58) to evaluate the time derivative of the protein density at $\Delta\bar{t}$, in a similar manner as before by forward Euler integration scheme. The procedure is repeated for a specified time interval or until an equilibrium state is reached.

As reported in [7], the membrane budding is initiated by the diffusion of the transmembrane over the surface of the membrane which induces a local curvature change in the membrane. This local curvature change is also accompanied by an enhanced diffusion of proteins on the surface in order to accommodate the changes in membrane curvature. Besides that, this local disturbance of the membrane may also promote the protein concentration fluctu-

ation on the membrane which may also result in the generation of tensional forces on the membrane. As a result of these forces and the protein diffusion, a local elastic energy will be developed. This local elastic energy of the deformed surface tends to pull the undeformed membrane. During this process, the membrane may sustain a residual local tension to balance local moment generated due to the difference between the actual mean curvature and the spontaneous curvature. Thus, this residual local tension may have an impact to alter the shape of the membrane as well as to induce the thickness distension on the membrane by influencing the pulling forces in the presence of the transmembrane proteins.

Figures (5.3)–(5.12) illustrate the solution of the numerical analysis which include the sequence of membrane shape changes and the corresponding thickness distension induced by membrane budding as the protein diffusion progresses on the membrane surface. In our analysis, since the lipid molecules are not allowed to deviate from the mid-surface normal (without tilt), the thickness changes in membrane are assumed to occur in the direction parallel to the surface normal of the membrane. Besides that, since the thickness distension and local curvature changes are computed essentially as independent fields; for clarity, we make reference to the schematic representation of the membrane deformation depicted in Fig. 5.2 in order to present discussions of our results.

Figures (5.3) and (5.4), respectively, show a sequence of changes in the membrane's local curvature ( surface shape changes) and the corresponding thickness distension changes induced by the membrane deformation as the protein diffusion progresses on the membrane surface. These results are computed in the presence of acting line tension in the membrane interface. The curves in the Fig. 5.3 correspond to the flat state, bulged and fully budded conditions of the membrane. Similarly, the curves in Fig. 5.4 shows the corresponding nonlinear thickness variations for each of the membrane shapes in Fig. 5.3. The solution in Fig. 5.4 shows that there is a strong localization of deformation around the base of the bulged membrane which can locally reduce the membrane thickness. This is probably due

to emergence of membrane-protein mediated forces in the protein concentrated domain and these forces may influence the local tensional forces which may indirectly cause the phase transition from thicker region (ordered phase) to thinner region (disordered phase). Using the curves in Fig. 5.5 **(a)**,**(b)**, Fig. 5.5**(c)** shows a schematic of the thickness distension variation on the bilayer membrane. As noted, this schematic representation is based on the two curves in Fig. 5.5 **(a)** and 5.5 **(b)** which respectively, represent the shape of the mid-surface, $\omega$, and thickness distension, $\varphi$, in the current configuration. The result in Fig. 5.6 can also be interpreted in a similar manner to that of the result in Fig. 5.5.

Furthermore, we also note that in both Figs. 5.5 and 5.6 the thickness distension takes its minimum at two different $\bar{r}$ values near the base of the bulged or fully budded region of the membrane. In addition, the presence of line tension energy in the model further facilitates the reduction of the thickness of the membrane at the base of the generated bud and accelerates the membrane budding process which may also lead to the possible membrane scission. For clarity, Figures 5.5 and 5.6 are included to indicate the nonlinear spatial variation of the thickness distension in each of the spherically-shape curvatures as the protein diffuses from the outer boundary into the membrane surface. From these figures, we conclude that local thickness distension and line tension have a strong impact in altering membrane shape in the bud formation on the bilayer membrane (see for example, the contour plot corresponding to this membrane deformation state in Fig. 5.7).

Figures 5.8 - 5.12 illustrate the effects of thickness distension in the membrane bud formation process in the absence of acting line tension energy on the membrane. As shown in Fig. 5.8, an inhomogeneous thickness variation is observed corresponding to flat state, bulged and fully budded region of the membrane (see Fig. 5.9). In this figure, we show also that the thickness distension takes its minimum at two different curvatures values for different $\bar{r}$ values near the base of the bulged or fully budded region of the membrane. For clarity, figures 5.10 and 5.11 indicate the inhomogeneous variation of the thickness distension in

each of the spherically-shaped curvatures as the protein diffuses from the outer boundary into the membrane. From these figures, we observe that, depending on the sequence of protein diffusion, the influence of thickness distension on the membrane bud formation process is strong compared to the results discussed in our previous study [7]. In view of this, we highlight that local thickness distension generated during membrane budding may have a strong impact in changing the bud formation process on the bilayer membrane by changing the curvature of the membrane in the presence of the transmembrane proteins (see for example, the contour plot corresponding to this membrane deformation state in Fig. 5.12 ).

Furthermore, in Fig. 5.14, we observe that the energy that accommodates the thickness distension on the membrane given by Landau potential in Eq. (5.30) takes its minimum at two different curvature values for different $\bar{s}$ values. The curves in Figure 5.14 correspond to the bulged and fully budded conditions of the membrane, respectively. As indicated in the figure, this result also indicates that the minimum points in the Landau potential free energy function corresponds to the minimum thickness section of the membrane which is at the base of the generated bud.

Our numerical results (see Fig. 5.13) suggest that the radius at the interface decreases smoothly towards the neck of the budding regime with the presence of thickness distension (shown in red curve in the figure) or a combination with line tension (shown in purple curve in the figure). It nearly vanishes all the way down to zero. Note that this description breaks down at scales comparable to the bilayer width. Despite the fact that the radius tends closer to zero, the difference between the mean curvature and the spontaneous curvature distribution remains finite; in the highly pinched limit, a saddle point develops at the neck which keeps the total curvature energy finite. The result may also suggest that the presence of the neck seems to favor the breaking process. In this case, fission may occur exactly at the neck. Details of the fission mechanism is outside of the scope of this study but certainly merits further investigation.

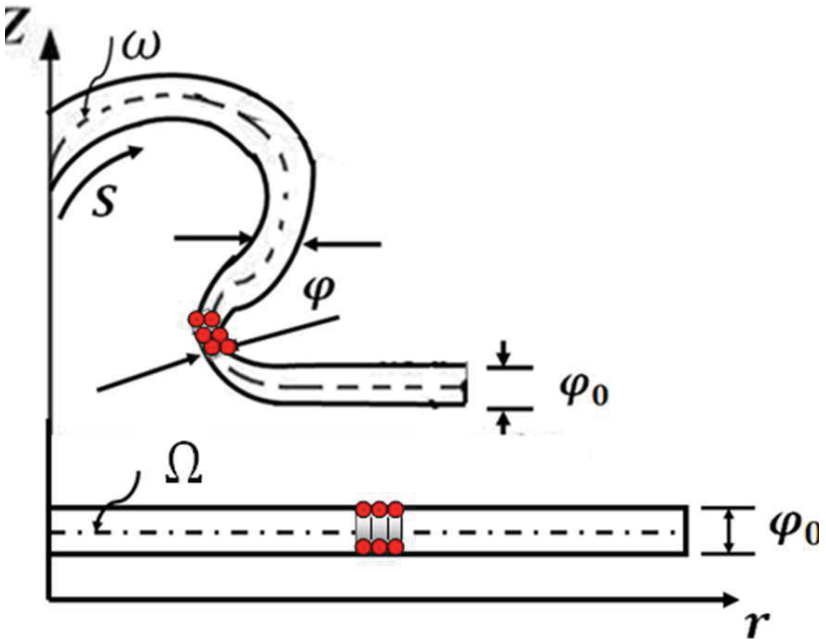


Fig. 5.2 Schematic representation of the deformation of lipid bilayer membrane surface. $\Omega$ is the mid-surface of the membrane and represents the reference configuration of an initially flat membrane whereas $\omega$ is mid-surface of the membrane in the current configuration membrane. The gray box shows the space occupied by a sample of lipid molecules during the deformation process.

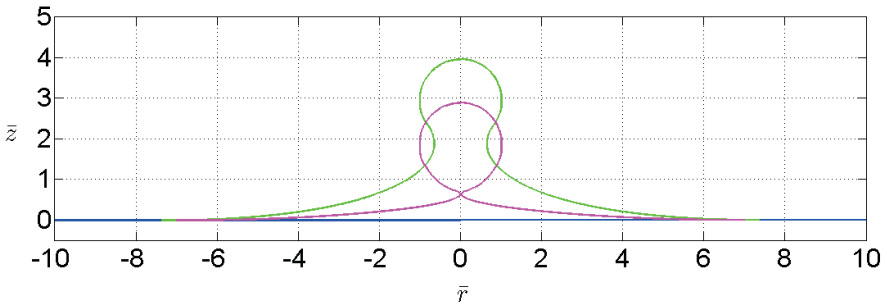


Fig. 5.3 Sequence of membrane shape-changes with the effect of thickness distension, as the protein diffusion proceeds with $(\gamma = 0.00104555)$, and weak membrane tension of $(f_\upsilon = 0.001)$.

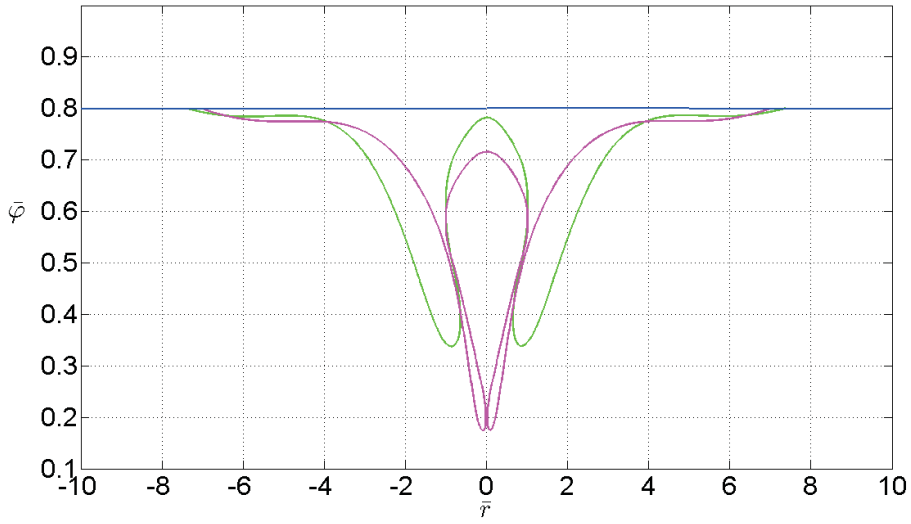


Fig. 5.4 Sequence of thickness distension induced by the deformation of the membrane as the protein diffusion proceeds with $(\gamma = 0.00104555)$, and weak membrane tension of $(f_\upsilon = 0.001)$.

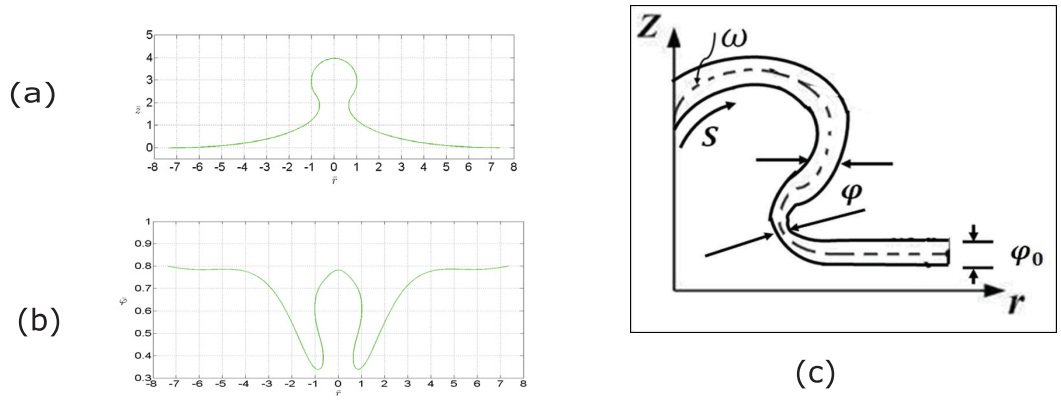


Fig. 5.5 (**a**) a bulged membrane shape , (**b**) the corresponding inhomogeneous thickness distension and (**c**) a schematic of the bud formation showing simultaneous change of the shape and thickness distension as the protein diffusion proceeds in correspondence of $(\gamma = 0.00104555)$, and weak membrane tension of $(f_\upsilon = 0.001)$.

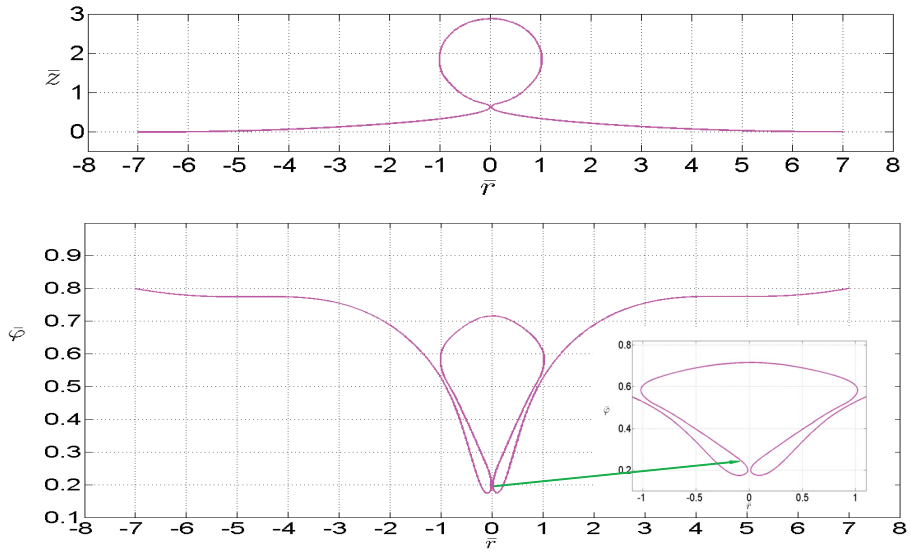


Fig. 5.6 A fully budded membrane shape $(up)$ and the corresponding inhomogeneous thickness distension $(down)$ as the protein diffusion proceeds in correspondence of $(\gamma = 0.00104555)$, and weak membrane tension of $(f_\upsilon = 0.001)$.

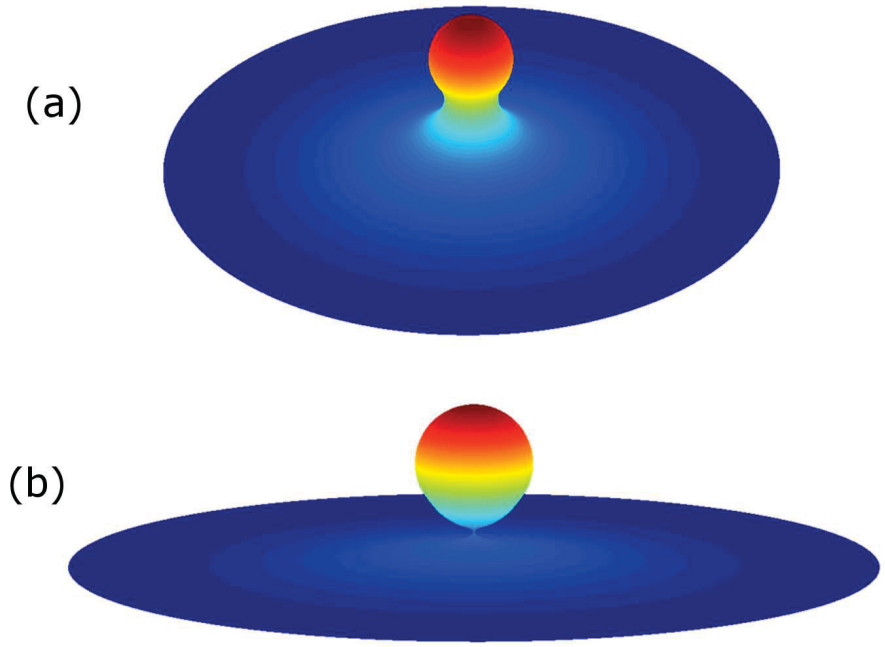


Fig. 5.7 Contour plot for a sequence of membrane shape-changes: $(\mathbf{a})$ for bulged, and $(\mathbf{b})$ fully budded membrane, as the protein diffusion proceeds with $(\gamma = 0.00104555)$, and weak membrane tension of $(f_\upsilon = 0.001)$.

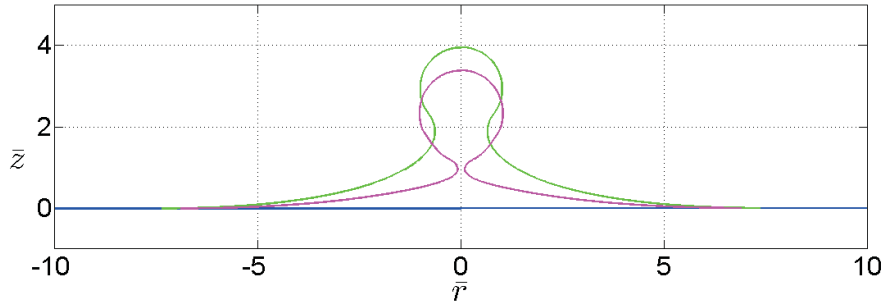


Fig. 5.8 Sequence of membrane shape-changes with the effect of thickness distension, as the protein diffusion proceeds with $(\gamma = 0.0)$, and weak membrane tension of $(f_\upsilon = 0.001)$.

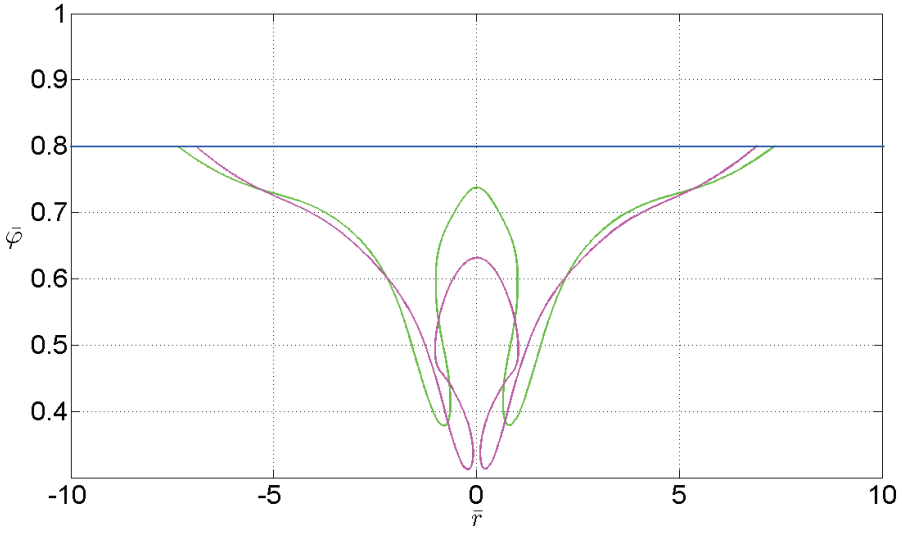


Fig. 5.9 Sequence of membrane thickness distension as the protein diffusion proceeds with $(\gamma = 0.0)$, and weak membrane tension of $(f_\upsilon = 0.001)$.

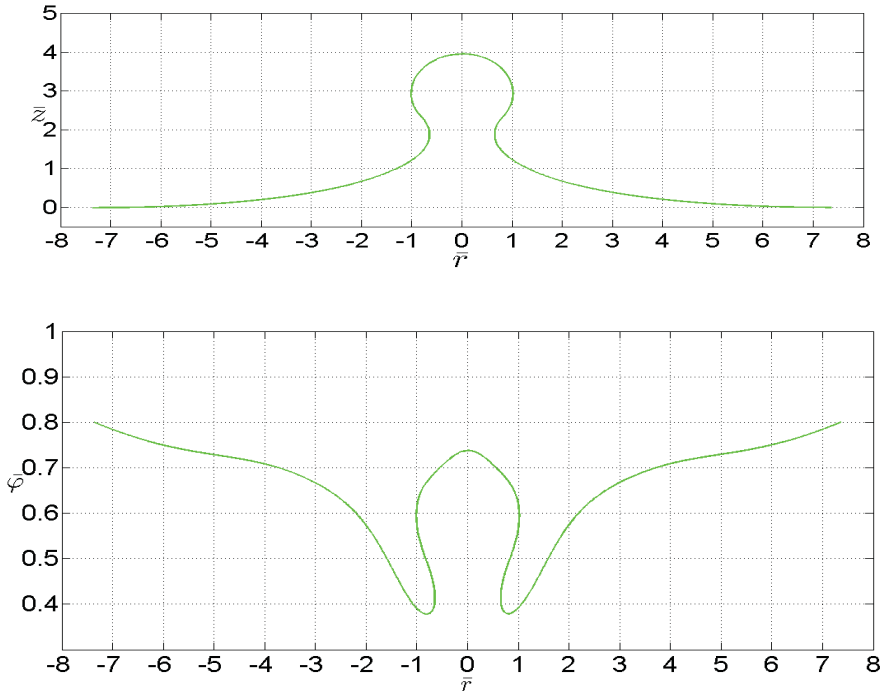


Fig. 5.10 A bulged membrane shape with its inhomogeneous thickness variation as the protein diffusion proceeds with $(\gamma = 0.0)$, and weak membrane tension of $(f_v = 0.001)$.

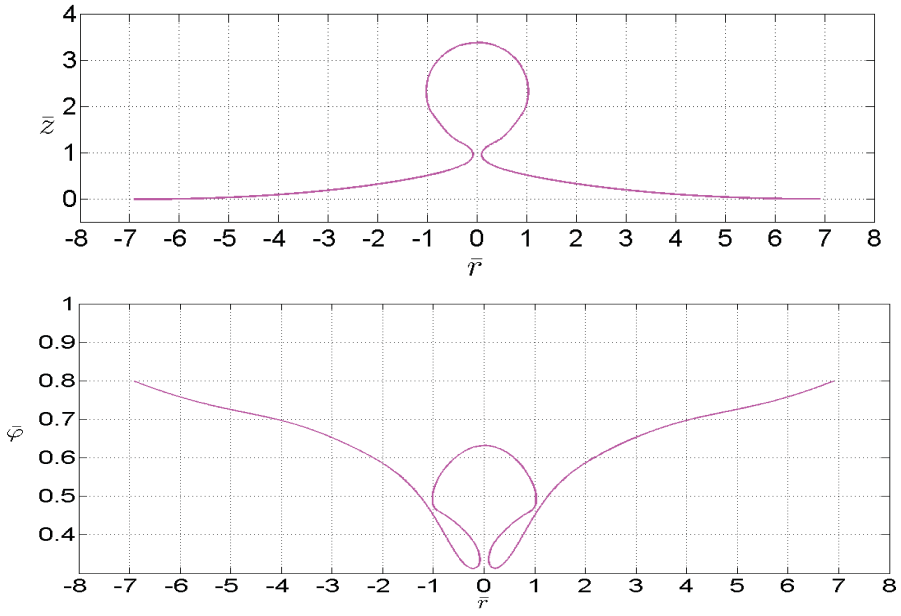


Fig. 5.11 A fully budded membrane shape with its inhomogeneous thickness variation as the protein diffusion proceeds with $(\gamma = 0.0)$, and weak membrane tension of $(f_v = 0.001)$.

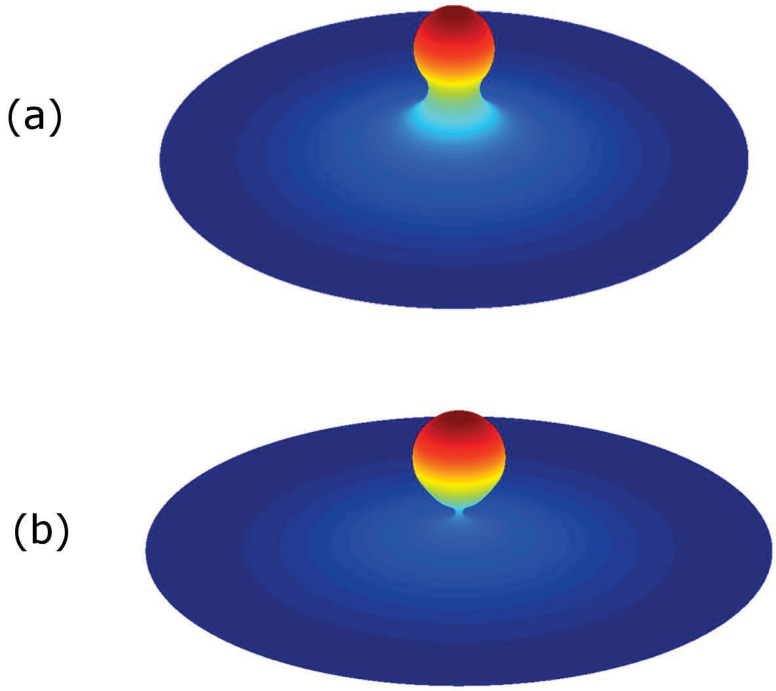


Fig. 5.12 Contour plot for a sequence of membrane shape-changes (**a**) for bulged and (**b**) fully budded membrane, as the protein diffusion proceeds with ($\gamma = 0.0$), and weak membrane tension of ($f_{\upsilon} = 0.001$).

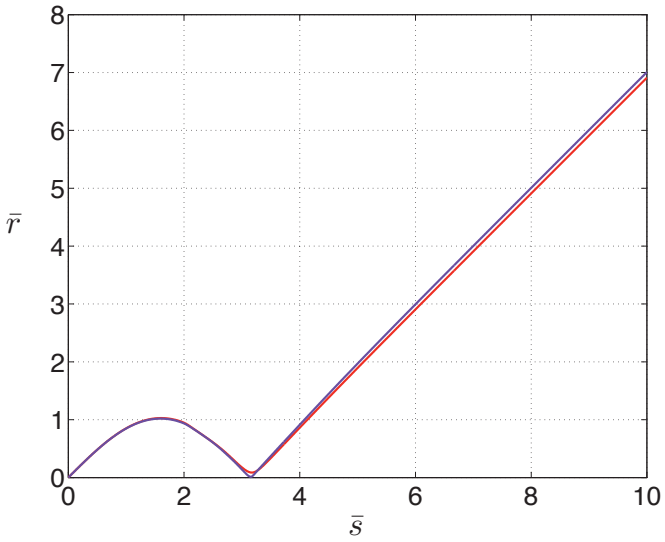


Fig. 5.13 Radial distance of a membrane point from the axis of symmetry of a fully budded membrane subjected to thickness distension (*down*) and combined with line tension effect (*up*).

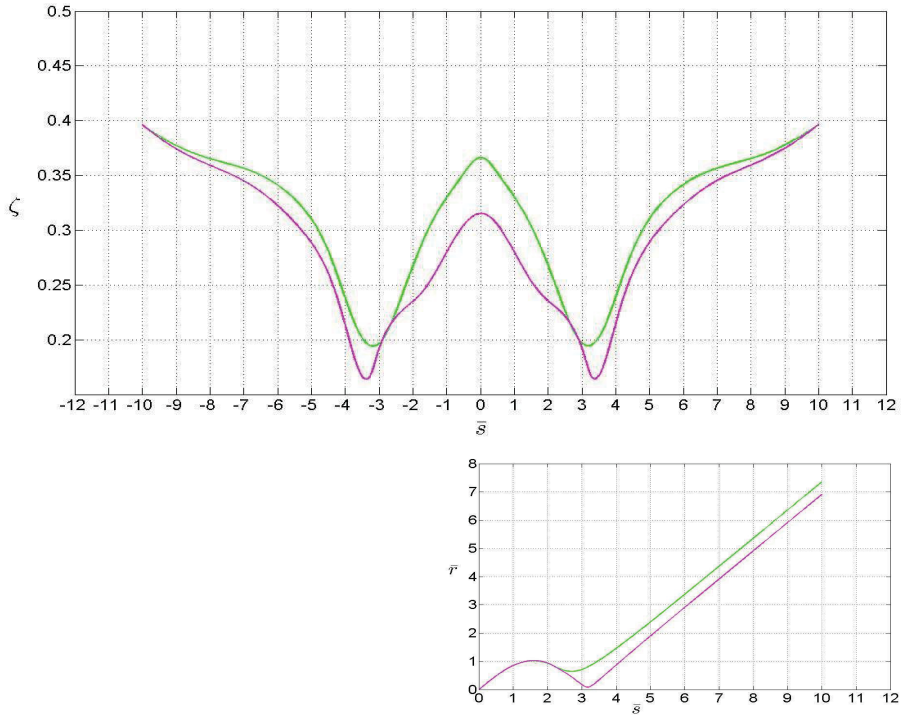


Fig. 5.14 Sequence of change of Landau potential free energy $(up)$ and radial distance of a membrane point from the axis of symmetry depicting necking location on the membrane $(down)$ as the protein diffuses proceeds in correspondence of $(\gamma = 0)$, and weak membrane tension of $(f_\upsilon = 0.001)$.

Finally, in all of our simulation results, we observe a smooth variation of thickness on the domain of interest and the formation of stable membrane bud. This elucidates the fact that the strong localization deformation which occurs in our analysis leads to the possible coexistence of a thicker region (the ordered phase ) and a thinner region (the disordered phase ).

## 5.5 Conclusions

We present a continuum-based model (centered on the Helfrich potential) describing the bud formation of a lipid bilayer subjected to thickness distension, surface diffusion of proteins and acting line tension. The proposed energy potential incorporates the mean and Gaussian curvatures of the surface, the corresponding spontaneous curvature, the surface gradient of dilation and the line tension energy on the membrane. In particular, the thickness distension on the membrane and the desired potential to simulate phase equilibria are incorporated into the augmented energy functional by relaxing the constraint of bulk incompressibility. The protein concentration level is coupled with the deformations of the membrane through the spontaneous curvature term appearing in the resulting shape equation. As such, the membrane budding is assumed to be induced by the surface diffusion of transmembrane proteins in which the protein distribution over the membrane is assumed to be non-uniform. The equilibrium shape equation of the bilayer membrane and the complete set of necessary boundary conditions are also derived using variational methods and work-energy principles. The resulting shape equation is solved numerically and its solutions demonstrate the strong influence of the thickness distension on budding formation in the bilayer membrane. In fact, the thickness distension plays a significant role in the process of bud formation which was analyzed as the interaction between the bilayer bending energy, thickness distension and the acting line tension on the domain of interest. In addition, the associated thickness distension of the membrane demonstrates a smooth transition from one phase to the other (including

necking domains) with 'minimum' thickness on the necking domain. Our results indicate that, even in the absence of acting line tension on the membrane, there is great potential for thickness distension to drive membrane budding. It is also found that the final deformed configuration of the membrane (in the form of a spherical bud) is an energetically favourable state and therefore the bud formation of the membrane is natural and stable.

We conclude that thickness distensions encountered in lipid bilayer membranes result in significant energetic consequences for bud formation and possibly necking and/or vesicle formations on the lipid membrane. Further, it is believed that the separation processes of vesicles from the mother lipid bilayer will most likely initiate on the necking domain in view of the fact that the necking area shows minimum thickness. Consequently, by providing essential quantitative information, our results can be extended to the study of important cellular functions associated with budding and vesicle formations in cellular processes.

# Chapter 6

# Conclusions and Future Work

## 6.1 Conclusions

In this work we have studied the mechanical response of both uniform and non-uniform bilayer membranes induced by cellular functions in the context of continuum mechanics. Much attention was given to the discussion of the deformation behaviour of lipid membranes subjected to some specified practically applicable boundary conditions and/or membrane-substrate interactions. In this regard, the mechanics of lipid bilayer membrane morphology with different membrane shapes were studied using a combination of analytical and numerical methods. These techniques are complementary approaches to solving the corresponding governing equations of the membrane and yield results which would probably have been overlooked if just one approach was chosen. Thus, using both analytical and numerical methods, a framework has been proposed for the prediction of the deformation profile of lipid membranes.

The first part of this study presented two analytical expressions for predicting the deformation profile of a uniform bilayer membrane morphology with different membrane shapes, and given boundary conditions. The first analytical solution is for predicting the deformation of a rectangular lipid membrane in the case of vanishing lateral pressure, subjected to various boundary forces acting on its edges. Here, emphasis is placed on the cases where the

rectangular membrane is subjected to applied boundary moments, since the corresponding deformation profiles are quantitatively equivalent to those induced by the lateral pressure gradient in the membrane conformation. The principle of superposed incremental deformation is effectively applied to reduce the highly non-linear shape equation of the lipid membrane to a single mathematically tractable PDE with minimum loss of generality. Hence, a complete analytical solution is obtained which predicts smooth membrane morphological transitions over the domain of interest and satisfies the imposed boundary conditions. Several examples, which demonstrate the evolution of the membrane shape in response to an applied bending moment for different values of the aspect ratio of the sides of the rectangular patch, have been presented. In all the examples, it has been found that for isotropic membranes, as the shape evolves in response to the bending moment, the surface pressure develops in the rectangular patch spatially in a homogeneous manner and intensifies as bending moment increases.

The second is a semi-analytical solution, which describes the morphological transitions of lipid membranes when interacting with solid elliptical cylindrical substrates (which may represent the action of, e.g., proteins) through an elliptical contact region. In this solution, the deformation mode of the membrane-substrate interaction is characterized by modified Mathieu functions and performed in the framework of a general curvilinear coordinate system. The actual deformation profiles are computed from infinite series of eigenfunctions for the desired elliptical domain. The semi-analytic solution method was used to study the effect of hydrophobicity on the evolution of the membrane shape subjected to the film/substrate interaction. In this regard, through the demonstration of many examples, we found that larger values of hydrophobicity create a depressed region in the membrane and this intensifies as the value of hydrophobicity increases. Consequently, the significant depression induced in the membrane indicates a dominant non-linear response and thus, we conclude that the linear solution developed for the linearzed shape equation is valid for only sufficiently small val-

ues of hydrophobicity. Furthermore, the semi-analytic solution successfully predicts smooth membrane morphological transitions over the domain of interest and overcomes one of the main challenges that one faces in the analysis of lipid membrane, which is removing the assumption of axisymmetry.

In part II of this work, we proposed a comprehensive continuum based model describing bud (vesicle) formation of lipid membranes induced by the surface diffusion of transmembrane proteins. Much attention was also given to the discussion of the role of line tension energy and/or thickness distension in the membrane budding, while our main objective was to provide a rigorous numerical analysis of the model. As such, the protein distribution over the membrane in consideration is assumed to be non-uniform. The proposed model is based on the free energy functional that involves the mean and Gaussian curvatures of the surface including the spontaneous curvature as well as the surface gradient of dilation and the acting line tension energy on the membrane. An energetic term, which regulates the thickness distension on the membrane and has the desired potential to simulate phase equilibria, is included in the free energy function of the membrane. In the analysis, the protein concentration level is coupled to the deformation of the membrane through the spontaneous curvature term appearing in the resulting equilibrium equation. In addition, coupling the thickness distension and line tension energy effect into the membrane model was challenging; nevertheless, our numerical results successfully predict the vesicle formation phenomenon on a flat lipid membrane surface, which was possible under the parametric representation of the membrane surface (not limited to the Monge representation) together with the presence of the acting line tension and/or thickness distension. In fact, in the absence of thickness distension, the acting line tension plays a significant role in the bud formation process which was analyzed as an interplay between the bilayer bending energy and the line tension on the domain of interest. This, in turn, suggests that the bud formation is potentially driven by the acting line tension on the membrane surface. Therefore, we conclude that a sufficient

amount of line tension energy at the boundary between protein concentrated domain and the surrounding bulk lipid plays a major role in controlling the bud formation process of the lipid bilayer membranes. Interestingly, in the absence of line tension from the model, our results also show that thickness distension has strong potential to drive membrane budding. Hence, we also conclude that a thickness distension encounter in biological lipid bilayer membrane is a significantly energetic consequence for bud formation and possibly necking in lipid bilayer membrane. It is also found that the final deformed configuration of the membrane (in the form of a spherical bud) is an energetically favourable state and therefore, the bud formation of the membrane is natural and stable. Finally, these numerical results can be further extended to the study of important cellular functions associated with budding, morphological aspect of cellular processes in particular, by providing necessary quantitative information for the bud formation of cellular membranes.

## 6.2 Future work

The results of the numerical study of bilayer membrane budding (Chapter 4 and 5) which is induced by the surface diffusion of the transmembrane proteins with the presence of either acting line tension energy on the membrane or thickness distension or with a combination of both methods have shown a new insight into the understanding of the mechanics of bud formation on a lipid bilayer membrane and furthermore, giving confidence on the validity of the proposed continuum based membrane model to predict the membrane's mechanical response.

A bilayer membrane structure is symmetric with respect to its mid-plane and since it is held together by weak non-bonded interaction forces, it is very susceptible to external forces, which give rise to deformations of the overall shape of the bilayer and to flow within the bilayer. In this regard, shear flows directed along the bilayer membrane surface by the

surrounding aqueous environment, may induce shear deformation in the bilayer, which is not addressed in this study.

A comprehensive continuum-based model for predicting the deformation behavior of a non-uniform bilayer membrane should include the shear deformation mode of the bilayer membrane. This also requires the need to include dynamic membrane properties such as surface shear viscosity and the intermonolayer friction of the bilayer membrane into the model. The presence of these dynamic membrane properties may affect the diffusion of transmembrane proteins over the composite membrane surface. Therefore, taking this into consideration, the investigation on the contribution of shear mode deformation on membrane budding, for example, is one new area to be explored.

To take the bilayer shear deformation mode into account may also be a challenge for the numerical simulation of bud formation process on the membrane. So far, the extension of the standard equilibrium membrane energy which accounts for protein concentration, thickness distension and acting line tension energy on the membrane worked well in the prediction of the bud formation on the lipid membrane. The constitutive equation for the associated concentration flux was based on a classical Fickean diffusion theory. If adopting and modifying a similar approach used in [34], i.e. describing the diffusion of membrane proteins by an expression which is defined in terms of the lipid bilayer thickness, protein shape geometry, viscosities of the membrane and the adjacent bulk fluid [77], the proposed continuum-membrane models in Chapters 4 and 5 could be easily extended to accommodate the effects of surface viscosity and the intermonolayer friction of the bilayer in membrane budding or in general other modes of deformation of the membrane.

# References


[1] Agrawal, A. and Steigmann, D. (2009a). Boundary-value problems in the theory of lipid membranes. *Contin. Mech. Thermodyn.*, 21:57–82.

[2] Agrawal, A. and Steigmann, D. (2009b). Modelling protein-mediated morphology in biomembranes. *Biomech. Model. Mechanobiol.*, 8:371–379.

[3] Agrawal, A. and Steigmann, D. (2011). A model for surface diffusion of transmembrane proteins on lipid bilayers. *Z. Angew. Math. Phys.*, 271(1):549–563.

[4] Aris, R. (1989). *Vectors, Tensors and the Basic Equations of Fluid Mechanics*. Dover, New York.

[5] Ayton, G., McWhirter, J., McMurtry, P., and Voth, G. (2008). Coupling field theory with continuum mechanics: A simulation of domain formation in giant unilamellar vesicles. *Biophys. J.*, 88:3855–3869.

[6] Baumgart, T., Hess, S., and Webb, W. (2003). Imaging coexisting uid domains in biomembrane models coupling curvature and line tension. *Nature*, 425:821–824.

[7] Belay, T., Kim, C., and Schiavone, P. (2016a). Bud formation of lipid membranes in response to the surface diffusion of transmembrane proteins and line tension. *Math. Mech. Solids*, (doi:10.1177/1081286516657684).

[8] Belay, T., Kim, C., and Schiavone, P. (2016b). Mechanics of a lipid bilayer subjected to thickness distension and membrane budding. *Math. Mech. Solids*, (doi: 10.1177/1081286516666136).

[9] Belay, T., Kim, C. I., and Schiavone, P. (2016c). Analytical solution of lipid membrane morphology subjected to boundary forces on the edges of rectangular membrane. *Continuum Mech. Thermodyn.*, 28:305–315.

[10] Belay, T., Kim, C. I., and Schiavone, P. (2016d). Interaction-induced morphological transitions of lipid membranes in contact with and elliptical cross section of a rigid substrate. *J. App. Mech. (ASME)*, 83(1):011001–011001–12. doi: 10.1115/1.4031485.

[11] Benedict, J. R., Gregoria, I., Vagelis, A. H., Martin, M., K., K., and Markus, D. (2007). Aggregation and vesiculation of membrane proteins by curvature-mediated interactions. *Nature*, 447(7143):461–464.

[12] Boucrot, E., Camdere, A., Liska, N., Evergren, E., MacMahon, H., and Kozlov, M. (2012). Membrane fission is promoted by insertion of amphipathic helices and restricted by crescent bar domains. *Cell*, 149:124–136.

[13] Bruinsma, R. and Pincus, P. (1996). Protein aggregation in membranes. *Curr. Opin. Solid State Mater. Sci.*, 1(3):401–406.

[14] Canham, P. (1970). The minimum energy of bending as a possible explanation of the biconcave shape of the red blood cell. *J. Theor. Biol.*, 26:61–81.

[15] Chernomrdik, L. and Kozlov, M. (2008). Mechanics of membrane fusion. *Nat. Struct. Mol. Biol.*, 15:675–683.

[16] Churchill, R. V. (1963). *Fourier series and boundary value problems*. McGraw-Hill, New York.

[17] dell'Isola, F., Gouin, H., and Seppecher, P. (1995). Radius and surface tension of microscopic bubbles by second gradient theory. *C.R. Acad. Sci.*, 320(Série IIb):211–216.

[18] dell'Isola, F. and Romano, A. (1987). On the derivation of thermomechanical balance equations for continuous systems with a non-material interface. *Int. J. Eng. Sci.*, 25:1459–1468.

[19] dell'Isola, F. and Seppecher, P. (1997). Edge contact forces and quasi-balanced power. *Meccanica*, 32(1):33–52.

[20] dell'Isola, F., Seppecher, P., and Madeo, A. (2012). How contact interactions may depend on the shape of cauchy cuts in n-th gradient contiua: approach "à la d'alembert". *Z. Angew. Math. Phys.*, 63(6):1119–1141.

[21] Deseri, L., Piccioni, M., and Zurlo, G. (2008). Derivation of a new free energy for biological membranes. *Continuum Mech. Thermodyn.*, 20:255–273.

[22] Deseri, L. and Zurlo, G. (2013). The stretching elasticity of biomembranes determines their line tension and bending rigidity. *Biomech. Model Mechanobiol.*, 12:1233–1242.

[23] Deserno, M., Muller, M., and Guven, J. (2007). Contact lines for fluid surface adhesion. *Phys. Rev. E*, 76(1):011605.

[24] Ebihara, L., Hall, J., MacDonald, R., McIntosh, T., and Simon, S. (1979). Effect of benzyl alchohol on lipid bilayers. a comparisons of bilayer systems. *Biophys. J.*, 28:185–196.

[25] Evans, E. (1974). Bending resistance and chemically induced moments membrane bilayers. *BioPhys. J. Vol.*, 14:923–931.

[26] Farsad, K. and De Camilli, P. (2003). Mechanisms of membrane deformation. *Curr. Opin. Cell Biol.*, 15:372–381.

[27] Feng, F. and Klug Williams, S. (2006). Finite element modelling of lipid bilayer membranes. *J. Comput. Phys.*, 220:394–408.

[28] Frolov, V., Chizmdzhev, Y., and Zimmerberg, J. (2006). Entropic traps in the kinetics of phase separation in multicomponent membranes stabilize nanodomains. *Biophys. J.*, 91:189–205.

[29] Frost, A., Unger, V., and Camilli, P. D. (2009). The bar domain superfamily: membrane-molding macromolecules. *Cell*, 137(2):191–196.

[30] Geoffrey, M. C. (2000). *The Cell: A Molecular Approach*. Sinauer Associates, Sunderland(MA).

[31] G.K., V. and Prinz, W. (2007). Sheets, ribbons and tubules - how organelles get their shape. *Nat. Rev. Mol. Cell Biol.*, 8:258–264.

[32] Goldstein, R. and Leibler, S. (1989). Structural phase transitions of interacting membranes. *Phys. Rev. A.*, 40(2):1025–1035.

[33] Gorter, E. and Grendel, F. (1925). On bimolecular layers of lipids on the chromocytes of the blood. *J. Exp. Med.*, 41:439–443.

[34] Guigas, G. and Weiss, M. (2015). Membrane protein mobility depends on the length of extra-membrane domains and on the protein concentration. *Soft Matter*, 11:33–37.

[35] Gutiérrez-Vega, J., Chávez-Cedra, S., and Rodríguez-Dagnino, R. (1999). Free oscillations in an elliptical membrane. *Rev. Mex. Fis.*, 45(6):613–622.

[36] Hamai, C., Yang, T., Kataoka, S., Cremer, P., and Musser, S. (2006). Effect of average phospholipid curvature on supported bilayer formation on glass by vesicle fusion. *Biophys. J.*, 90(4):1241–1248.

[37] Helfrich, W. (1973). Elastic properties of lipid bilayers: theory and possible experiments. *Z. Naturforsch.*, 28:693–703.

[38] Honerkamp-Smith, A., Cicuta, P., Collins, M., Veatch, S., and den Nijs, M., e. a. (2008). Line tensions, correlation lengths, and critical exponents in lipid membranes near critical points. *Biophys. J.*, 95:236–246.

[39] Jülicher, F. and Lipowsky, R. (1993). Domain-induced budding of vesicles. *Phys. Rev. Lett.*, 70:2964–2967.

[40] Jung, S., Choi, S., Kim, Y., and Jeon, T. (2012). Storable droplet interface lipid bilayers for cell-free ion channel studies. *Bioprocess Biosyst. Eng.*, 35:241–246.

[41] Kim, C. I. and Steigmann, D. (2014). Distension-induced gradient capillarity in lipid membranes. *Contin. Mech. Thermodyn. DOI 10.1007/s00161-014-0333-1*.

[42] Kim, K., Neu, J., and Oster, G. (1998). Curvature-mediated interactions between membrane proteins. *Biophys. J.*, 75:2274–2291.

[43] Kim, Y.-R., Jung, S., Ryu, H., Yoo, Y.-E., Kim, S. M., and Jeon, T.-J. (2012). Synthetic biomimetic membranes and their sensor applications. *Sensors*, 12:9530–9550.

[44] Klein, K., Reed, J., Tanaka, M., Nguyen, V., S., G., and Lingappa, J. (2011). Hiv gag-leucine zipper chimeras form abce1-containing intermediates and rnase-resistant immature capsids similar to those formed by wild-type hiv-1 gag. *J. of Virol.*, 85(14):7419–7435.

[45] Koiter, W. (1964). Couple-stresses in the theory of elasticity. *Proc. Knononklijke Ned. Akad. Wet. B*, 67:17–44.

[46] Komura, S., Shirotori, H., Olmsted, P., and Andelman, D. (2004). Lateral phase separation in mixtures of lipids and cholesterol. *Europhys. Lett.*, 67(2):321.

[47] Kozlov, M. (2010). Biophysics: Joint effort bends membrane. *Nature*, 463(7280):439.

[48] Kusumi, A., Tsunoyama, T., Hirosawa, K., Sasai, R., and Fujiwara, T. (2014). Tracking single molecules at work in living cells. *Nat. Chem. Biol.*, 10:524–532.

[49] Landau, L. and Lifschitz, E. (1986). *Theory of Elasticity, and 3rd ed. vol. 7 of the Course of Theoretical Physics*. Pergamon, Oxford, UK.

[50] Langer, J., Stoops, E., Béthune, J., and Wieland, F. (2007). Conformational changes of coat proteins during vesicle formation. *FEBS Lett.*, 581:2083–2088.

[51] Lee, M., Hamamoto, S., Futai, E., Ravazola, M., and Schekman, R. (2005). Sarlp n-terminal helix initiates membrane curvature and completes the fission of a copii vesicle. *Cell*, 122:605–617.

[52] Leibler, S. (1986). Curvature instability in membranes. *J. Phys.*, 46:507–516.

[53] Lenz, M., Morlot, S., and Roux, A. (2009). Mechanical requirements for membrane fission: Common facts from various examples. *FEBS. Lett.*, 583:3839–3846.

[54] Li, L., Vorobyov, I., and Allen, T. (2012). The role of membrane thickness in charged protein-lipid interaction. *Biochim. Biophys. Acta.*, 1818:135–145.

[55] Liposwsky, R. (1993). Domain-induced budding of fluid membranes. *Biophys. J.*, 64:1133–1138.

[56] Lodish, H., Berk, A., Matsudaira, P., Kaiser, C. A., Krieger, M., Scott, M., Zipursky, L., and Darnell, J. (2004). *Molecular Cell Biology*. W. H. Freeman and Co., New York, NY, fifth edition.

[57] Maleki, M., Seguin, B., and Fried, E. (2013). Kinematics, material symmetry, and energy densities for lipid bilayers with spontaneous curvature. *Biomech. Model Mechanobiol.*, 12(5):997–1017.

[58] Maria, D. L. and Carlos, G. D. (2003). Membrane and cytoskeleton dynamics during axonal elongation and stabilization. *Int. Rev. Cytol.*, 227:183–219.

[59] McLachlan, N. (1947). *Theory and application of Mathieu functions*. Oxford, UK.

[60] McMahon, H. and Gallop, J. (2005). Membrane curvature and mechanisms of dynamic cell membrane re-modelling. *Nature*, 428:590–596.

[61] Mindlin, R. and Tiersten, H. (1962). Effects of couple-stress in linear elasticity. *Arch. Ration. Mech. Anal.*, 11:415–448.

[62] Moon, P. and D.E., S. (1971). *Field theory handbook: including coordinate systems, differential equations and their solutions 2nd ed.* Springer-Verlag, New York.

[63] Nigel, U. (2005). Refined structure of the nicotinic acetyl-choline receptor at resolution. *J. Mol. Biol.*, 346(4):967–989.

[64] Owicki, J. and McConnel, H. (1979). Theory of protein-lipid and protein-protein interactions in bilayer membranes. *Proc. Natl. Acad. Sci. USA*, 76:4750–4754.

[65] Perry, M. and Gilbert, A. (1979). Yolk transport in the ovarian follicle of the hen (gallus domesticus): Lipoprotein-like particles at the periphery of the oocyte in the rapid growth phase. *J. Cell Sci.*, 39:257–272.

[66] Peter, B., Kent, H., Mills, I., Vallis, Y., Butler, P., Evans, P., and MacMahon, H. (2004). Domains as sensor of membrane curvature: the amphiphysin bar structure. *Science*, 303:495–499.

[67] Phillips, R., K. J. and Theriot, J. (2009). *Physical Biology of the cell*. Garland Science.

[68] Poulos, J., Jeon, T., and Schmidt, J. (2010). Automatable production of shippable bilayer chips by pin tool deposition for an ion channel measurement platform. *Biotechnol. J.*, 5:511–514.

[69] Preston, S., Jensen, O., and Richardson, G. (2007). Buckling of an axisymmetric vesicle under compression: the effects of resistance to shear. *J. Mech. Appl. Math.*, 61:1–24.

[70] Rangamani, P., Agrawal, A., Mandadapu, K. K., Oster, G., and Steigmann, D. (2012). Interaction between surface shape and intra-surface viscous flow on lipid membrane. *Biomech. Model Mechanobiol.*, 12(4):833–845.

[71] Razani, B. and Lisanti, M. P. (2001). Caveolins and caveolae molecular and functional relationships. *Exp. Cell Res.*, 271(1):36–44.

[72] Reister, E. and Seifert, U. (2005). Lateral diffusion of a protein on a fluctuating membrane. *Europhys. Lett.*, 71:859–865.

[73] Robertson, J. D. (1959). The ultrastructure of cell membranes and their derivatives. *Biochem. Soc. Symp.*, 16:3–43.

[74] Ross, R. and Virga, E. (1999). Adhesive borders of lipid membranes. *Proc. R. Soc. Lond. A*, 455:4145–4168.

[75] Rothman, J. (2002). The machinery and principles of vesicle transport in the cell. *Nat. Med.*, 8:1059–1062.

[76] Sackmann, E. (1995). Physical basis of self-organization and functions of membranes: physics of vesicles. in: Lipowsky r., sackmann e. (eds.) the structure and dynamics of membranes. *Elsevier Amsterdam*, pages (Hoff A (Ed): Handbook of Biological Physics, 1.).

[77] Saffman, P., , and Delbrück, M. (1975). Brownian motion in biological membranes. *Proc. Natl. Acad. Sci. USA*, 72:3111–3113.

[78] Sato, K. (2006). Bending of an elliptical plate on elastic foundation and under the combined action of lateral load and in-plane force. *III European Conference on Computational Mechanics Solids, Structures and Coupled Problems in Engineering*, page 49.

[79] Schley, D., Whittaker, R., and Neuman, B. (2013). Arenavirus budding resulting from viral-protein-associated cell membrane curvature. *J. R. Soc. Interface.*, 10: 20130403.

[80] Schmidt, N.W, e. a. (2011). Criterion for amino acid composition of defensins and antimicrobial peptides based on geometry of membrane destabilization. *J. Am. Chem. Soc.*, 133(17):6720–6727.

[81] Schultz, S. G. and Yu-Tu., L. (1970). Thickness changes in lipid bilayer membranes. *Biochim. Biophys. Acta.*, 196:354–357.

[82] Schwerzmann, K., Cruz-Oriver, L., Eggman, R., Sanger, A., and ER., W. (1986). Molecular architecture of the inner membrane of mitochondria from rat liver: a combined biochemical and stereological study. *J. Cell Biol.*, 102:97–103.

[83] Scriven, L. (1960). Buckling of an axisymmetric vesicle under compression: the effects of resistance to shear. *J. Mech. Appl. Math.*, 12:98–108.

[84] Seifert, U. (1997). Configurations of fluid membranes and vesicles. *Adv. Phys.*, 46(1):13–137.

[85] Shampine, L.F., G. I. and Thompson, S. (2003). *Solving ODEs with Matlab*. Cambridge Univ. Press, New York.

[86] Sheetz, M. P. (2001). Cell control by membrane-cytoskeleton adhesion. *Nat. Rev. Mol. Cell Biol.*, 2(5):392–396.

[87] Skar-Gislinge, N., Simonsen, J., Mortensen, K., Feindenhans'l, R., Sligar, S., Møller, B., Bjønholm, T., and Arleth, L. (2010). Elliptical structure of phospholipid bilayer nanodics encapsulated by scaffold proteins: Casting the roles of the lipids and the protein. *J. AM. CHEM. SOC VOL.*, 132(39):13713–13722.

[88] Song, J. and Waugh, R. E. (1990). Bilayer membrane bending stiffness by tether formation form mixed pc-ps lipid vesicles. *J. Biomech. Engr.*, 112:235–240.

[89] Stachowiak, J., Schmid, E., Ryan, C., Ann, H., Sasak, D., Sherman, M., Geissler, P., Fletcher, D., and Hayden, C. (2012). Membrane bending by protein-protein crowding. *Nat. Cell Biol.*, 14:944–949.

[90] Steigmann, D. (1999a). Fluid films with curvature elasticity. *Arch. Ration. Mech. Anal.*, 150:127–152.

[91] Steigmann, D. (1999b). On the relationship between the cosserat and kirchhoff-love theories of elastic shells. *Math. Mech. Solids*, 4:275–288.

[92] Steigmann, D. (2003). Irreducible function bases for simple fluids and liquid crystal films. *Z. Angew. Math. Phys.*, 54:462–477.

[93] Steigmann, D. (2013). A model for lipid membranes with tilt and distension based on three-dimensional liquid crystal theory. *Int. J. Non-Linear Mech.*, 56:61–70.

[94] Steigmann, D., Baesu, E., R.E., R., Belak, J., and McElfresh, M. (2003). On the variational theory of cell-membrane equilibria. *Interface Free Boundaries*, 5:357–366.

[95] Stoker, J. (1969). *Differential Geometry. In: Courant, R., Bers, L., Stoker, J.J. (eds.) Vol. XX in Pure and Applied Mathematics*. Wiley, New York.

[96] Sukharev, S. I., Sigurdson, W. J., Kung, C., and Sachs, F. (1999). Energetic and spatial parameters for gating of the bacterial large conductance mechanosensitive channel, mscl. *J. Gen. Physiol.*, 113:525–539.

[97] Sweitzer, S. and Hinshaw, J. (1998). Dynamin undergoes a gtp-dependent conformational change causing vesiculation. *Cell*, 93:1021–1029.

[98] Tanford, C. (1991). *The Hydrophobic Effect: Formation of Micels and Biological Membranes*. Krieger Publishing Company, Malabar, FL.

[99] Tero, R. (2012). Substrate effects on the foundation process, structure and physicochemical properties of supported lipid bilayers. *Materials*, 5:2658–2680.

[100] Toupin, R. (1964). Theories of elasticity with couple stress. *Arch. Ration. Mech. Anal.*, 17:85–112.

[101] Virga, E. (1994). *Variational Theories for Liquid Crystals*. Chapman & Hall, London, UK.

[102] Waterman-Storer, C., Worthylake, R., Liu, B., Burridge, K., and E.D., S. (1999). Microtubule growth activatesrac1 to promote lamellipodial protrusion in fibroblasts. *Nat. Cell Biol.*, 1(1):45–50.

[103] Yanagisawa, M., Imai, M., and Taniguchi, T. (2008). Shape deformation of ternary vesicles coupled with phase separation. *Phys. Rev. Lett.*, 100:148102.

[104] Zimmerberg, J. and Kozlov, M. (2005). How proteins produce cellular membrane curvature. *Nat. Rev. Mol. Cell Biol.*, 7(1):9–19.